ESR DATING OF PLEISTOCENE DEPOSITS

ESR DATING OF PLEISTOCENE DEPOSITS

by

STEVE ZYMELA, B.Sc.

A Thesis

Submitted to the School of Graduate Studies

in Partial Fulfilment of the Requirements

for the Degree

Master of Science

McMaster University

March 1986

MASTER OF SCIENCE (1986) McMASTER UNIVERSITY
(Geology) Hamilton, Ontario

TITLE: ESR Dating Of Pleistocene Deposits

AUTHOR: Steve Zymela, B.Sc. (University of Western Ontario, London, Ontario)

SUPERVISOR: Professor Henry P. Schwarcz

NUMBER OF PAGES: x, 118

ABSTRACT

Near Medicine Hat, Alberta, Pleistocene deposits are exposed on numerous bluffs along the South Saskatchewan River. The Quaternary beds are very fossiliferous, yielding a large number of mammal bones and teeth. The enamel (calcium hydroxyapatite) portion of teeth within the sediments, is used to date the deposits with the electron spin resonance (ESR) dating method. The ESR age is strongly dependent on the dose rate which in turn depends on the uranium accumulation in the tooth fragments. Two U uptake models are used based on an early and a continuous, linear accumulation of uranium.

At young, well dated sites the ESR ages are in relatively good agreement with independent estimates. For slightly older samples (approx. 100 ka), the linear U uptake model comes closer to the estimated age at one site, but at another site, the early U uptake model agrees more favourably with the estimated age. Based on the ESR ages, several older sites can be assigned to interglacial stages 7, 9 and 13, however, these ages are much younger than those determined by faunal and stratigraphic correlation (>0.5 Ma). Samples with extremely high U contents in dentine and enamel gave unreliable ESR results. These samples may have experienced a late stage of U accumulation.

ACKNOWLEDGEMENTS

I wish to thank my supervisor Dr. Henry P. Schwarcz for suggesting this research project. The numerous discussions with him throughout the course of this thesis proved to be very helpful and encouraging. I would like to thank Dr. Rainer Grün for reviewing this thesis, for his many useful comments and for permitting me the use of some of his figures. I would also like to thank Dr. Archie Stalker of the Geological Survey of Canada for field work funding and for his help in collecting samples. Dr. C.S. (Rufus) Churcher of the University of Toronto provided several samples from his own collecton for which I am most grateful.

Thanks are also in order to the following people:

- Dr. Ann Wintle for some useful suggestions,
- Ian Thompson for technical advice on ESR spectrometry,
- Chris Lopresti at the Gamma Irradiation Facility for irraation of all samples.
- Martin Knyf for his technical advice,
- Diane Ivanauskas for ESR measurements of some samples,
- Ota Mudroch for help with XRF,
- Jack Whorwood for photopraphing the figures,
- Allison Cormie for preparing a few samples and her technical advice, and
- Chris Hale for some useful comments.

TABLE OF CONTENTS

LIST OF FIGURES

LIST OF TABLES

CHAPTER 1

INTRODUCTION

1.1 SCOPE AND OBJECTIVE

Dating by electron spin resonance (ESR) is based upon the ability of minerals to accumulate trapped electrons during geologic time. The trapped electrons result from ionization caused by natural radiation from the decay of radioactive elements within and/or surrounding the minerals and from cosmic rays. Detection of the unpaired, trapped electrons is made possible with ESR spectroscopy. With time, the natural radiation causes a steady increase of the trapped electron population. The ESR signal, which is proportional to the population of free electrons, will therefore also increase.

The ESR age of the sample can be deduced from the following simplified formula,

$$\text{Age} = \text{Accumulated Dose} / \text{Annual Dose}. \qquad (1.1)$$

The accumulated dose (AD) which the sample attained since the time of formation is evaluated by ESR spectroscopy. The annual dose that the sample received is determined from the analysis of U, Th and K of the sample and its surroundings.

The objective of this thesis is to apply ESR dating to Quaternary deposits. The feasibility of the method depends on the following conditions:

1) The sample to be dated must have formed during the depositional period.
2) The sample must not have undergone subsequent re-crystallization or other alteration.
3) The sample must yield an ESR signal that accurately reflects the accumulated dose.
4) The various traps in the crystal lattice to be used for dating, must not be saturated with electrons.
5) The traps must have remained stable with time.
6) Electrons, once trapped, must not have spontaneously leached out of the traps.
7) All the parameters that contribute to the annual dose must be known.

The Quaternary deposits near Medicine Hat, Alberta, were chosen because they contain units which are very fossiliferous. The bone and teeth fragments in these units were laid down with the sediment and are therefore possible candidates for ESR dating. The enamel portion of teeth was chosen for dating because it consists almost completely of crystalline calcium phosphate (96-97%; Driessens, 1980) with a crystallographic organization resembling calcium hydroxyapatite, $Ca_{10}(PO_4)_6(OH)_2$ (Weatherall and Robinson, 1973). ESR dating of apatite has been applied by Zeller et al. (1967), and their conclusions indicate that it is a suitable mineral for ESR dating. Bones, ivory tusks and the dentine/cementum

portion of teeth were not used. They contain organic components up to 25% (Driessens, 1980), are less dense and more porous than enamel, and are therefore more susceptible to alteration after deposition.

1.2 QUATERNARY GEOLOGY OF SOUTHERN ALBERTA

Quaternary sediments in the Prairies of southern Alberta and Saskatchewan (Fig. 1.1) have been extensively described by A. M. Stalker (eg. Stalker 1963, 1969, 1972, and 1976). C. S. Churcher has studied and identified bones in the same areas (eg. Stalker and Churcher, 1972 and 1982). Quaternary deposits in the Foothills of southwestern Alberta, where both Laurentide and Cordilleran tills overlie each other, are described by Alley and Harris (1974) and Stalker and Harrison (1977). The sediments around Cypress Hills, southern Alberta, one of the few areas in Canada that escaped glaciation during the Quaternary, are described by Westgate (1972). The most recent Quaternary composite stratigraphic section for the southwestern Canadian Prairies is given by Stalker and Churcher (1982).

1.2.1 PROBLEMS ENCOUNTERED IN QUATERNARY STRATIGRAPHY

The Quaternary composite section of southern Alberta (Table 1.2; Stalker and Churcher, 1982) relates specific

FIG. 1.1. Map of Alberta and Saskatchewan showing location of sample sites. More precise locations of the Medicine Hat sites are shown in Fig. 3.1. The approximate coordinates for the other sites are:

B - 49°55'N111°30'W

E - 50°57'40"N110°1'W

R - 52°15'5"N106°35'25"W

W - 50°40'25"N107°51'50"W

B = BOW ISLAND SITE; E = EMPRESS SITE
M = MEDICINE HAT SITES; R = RIDDELL SITE
W = WELLSCH VALLEY SITE

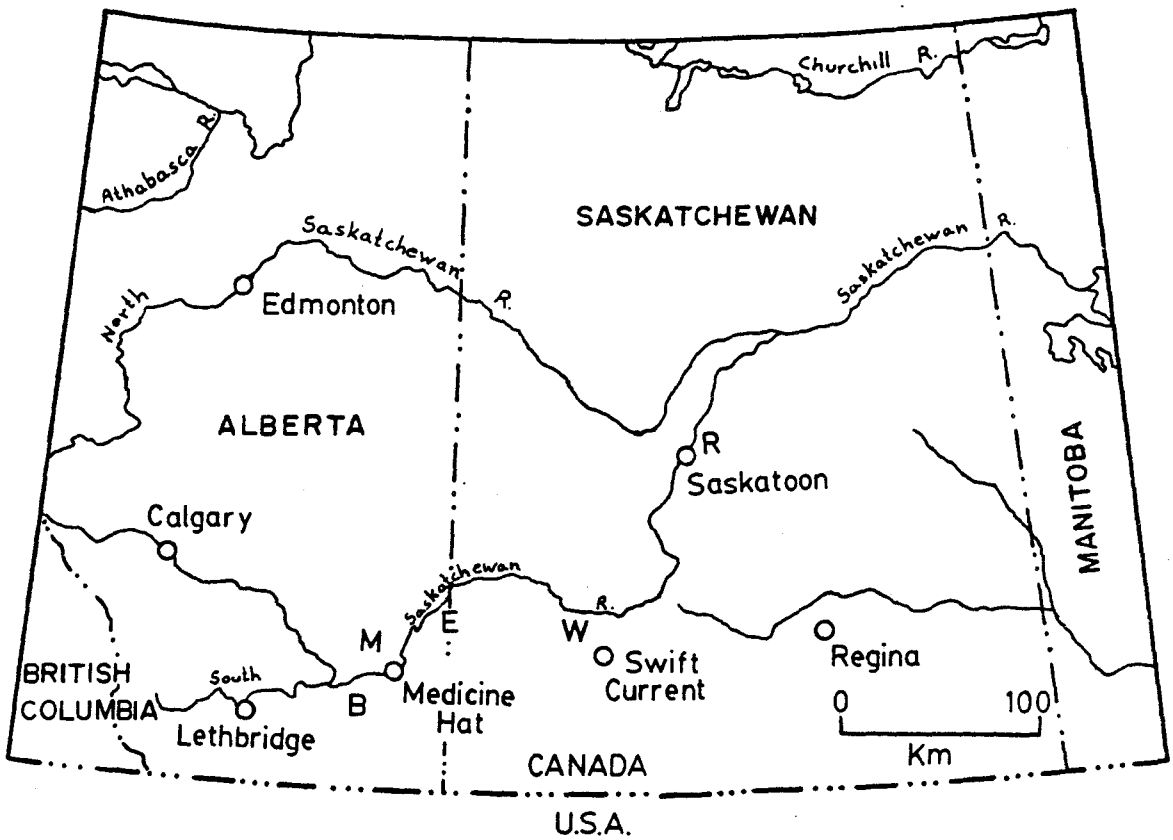

interglacial periods with vertebrate faunal assemblages. The section is based on the assumption that there were only four major continental glaciations during Pleistocene time: the Wisconsin, Illinoian, Kansan and Nebraskan. This has led to a number of problems in interpretation. First, in the Medicine Hat area, names given to glacial and stadial units beyond the range of carbon-14 dating have been obtained from the identification of vertebrate fossils. These names do not necessarily correlate directly with the nomenclature used by glacial geologists, and are generally older (Stalker, 1969).

The second problem is that the four continental glacial stage names have been used too loosely in the past. Too often, at any given locality the youngest Pleistocene glacial cycle has been labelled the Wisconsin, the first interglacial cycle the Sangamon, the second glacial cycle Illinoian and so on. This sort of "counting from the top" naming process has lead to a considerable overlap of the glacial and interglacial time spans (Fig. 1.2).

Lastly, Shackleton and Opdyke's (1973 and 1976) oxygen isotope records of deep sea cores, indicate that rather than 4, there have been over 20 glaciations during the Pleistocene (Gibbons et al., 1984). Figure 1.3 shows that interval "A" representing the time period from 0 to 0.9 Ma, had 10 major glacial cycles. Intervals "B" and "C" spanning the time

FIG. 1.2. Usage of pre-Wisconsin stage terms. The chronology for the Iowa and Nebraska sequences are based on fission track dating of volcanic glass shards. The chronology for the Gulf of Mexico and South Atlantic sequences are based on paleomagnetic dating. (After Boellstorf, 1978).

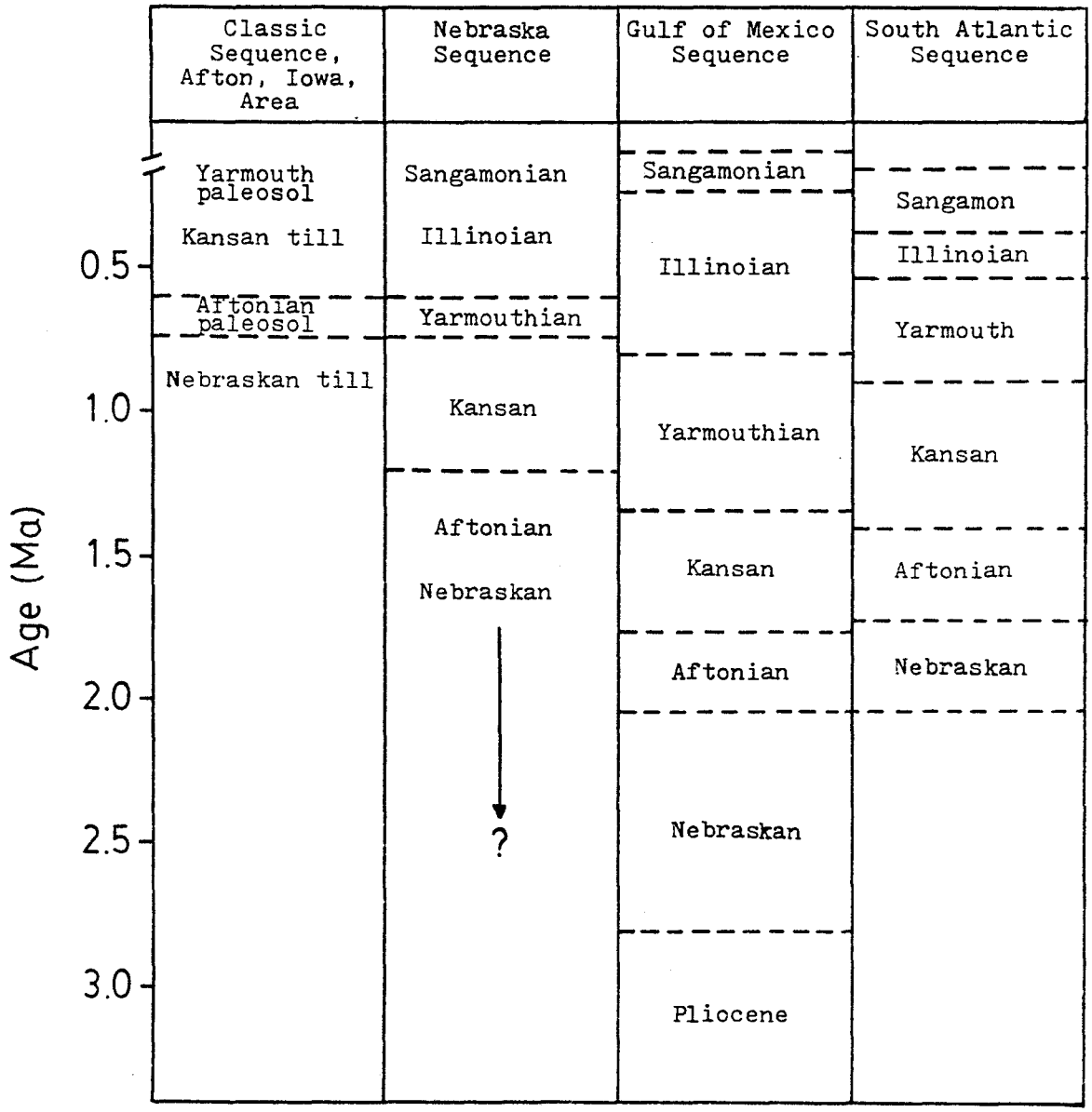
Classic Sequence, Afton, Iowa, Area
Nebraska Sequence
Gulf of Mexico Sequence
South Atlantic Sequence
Age (Ma)
0.5
1.0
1.5
2.0
2.5
3.0
Yarmouth paleosol
Kansan till
Aftonian paleosol
Nebraskan till
Sangamonian
Illinoian
Yarmouthian
Kansan
Aftonian
Nebraskan
?
Sangamonian
Illinoian
Yarmouthian
Kansan
Aftonian
Nebraskan
Pliocene
Sangamon
Illinoian
Yarmouth
Kansan
Aftonian
Nebraskan

FIG. 1.3. Oxygen isotope record for entire Pleistocene core V28-239 (Shackleton and Opdyke, 1976). Based on the duration and amplitude of the glacial/interglacial cycles, the Pleistocene record can be subdivided into 3 intervals, "A", "B", and "C". X denotes a glacial stage. (From Gibbons et al., 1984)

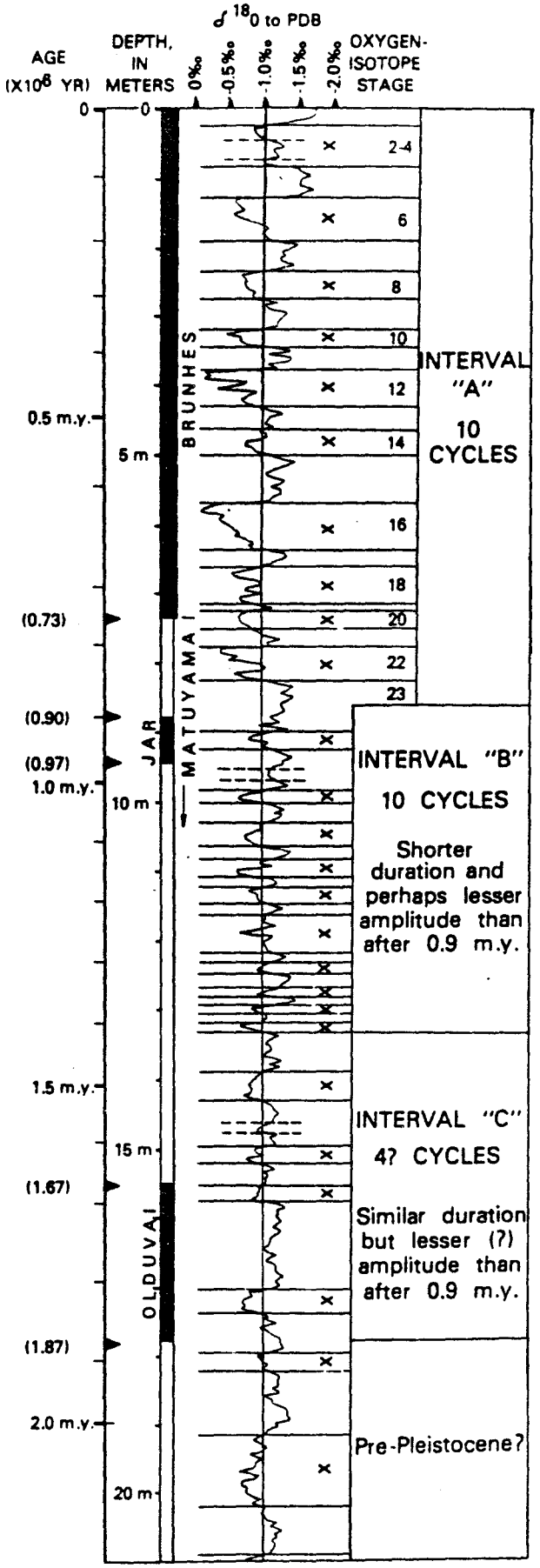
δ 18O to PDB
AGE (X10^6 YR)
DEPTH, IN METERS
0‰
-0.5‰
-1.0‰
-1.5‰
-2.0‰
OXYGEN-ISOTOPE STAGE
0
0.5 m.y.
1.0 m.y.
1.5 m.y.
2.0 m.y.
5 m
10 m
15 m
20 m
(0.73)
(0.90)
(0.97)
(1.67)
(1.87)
BRUNHES
MATUYAMA
JAR
OLDUVAI
2-4
6
8
10
12
14
16
18
20
22
23
INTERVAL "A"
10 CYCLES
INTERVAL "B"
10 CYCLES
Shorter duration and perhaps lesser amplitude than after 0.9 m.y.
INTERVAL "C"
4? CYCLES
Similar duration but lesser (?) amplitude than after 0.9 m.y.
Pre-Pleistocene?

period 0.9 to 1.87 Ma, had 14 glacial cycles but of shorter duration and lesser amplitude. Furthermore, reef terraces in Barbados, dated by Bender et al. (1979), suggest that there were at least 7 interglacial cycles during the past 640,000 years. Their results agree favourably with the oxygen isotope stages as defined by Shackleton and Opdyke (1973). Each interglacial isotope stage back to 640,000 years is represented by at least one Barbados reef tract.

The record of glaciation as defined by the presence of a till unit is a selective one because glacial advances will generally obliterate tills deposited by less extensive previous glacial advances. This process of obliteration of a till unit when overlapped by a later, more extensive glacial advance is termed "obliterative overlap". Gibbons et al. (1984) applied a probability analysis model to study the impact of obliterative overlap on the completeness of a glacial record. Their probability model considers the following 3 assumptions:

1) The distribution of relative distances of glacial advances is random over time.
2) Tills of a given succession are restricted to the same glacial pathway.
3) The only till units to survive obliterative overlap are those deposited at greater distances than any subsequent till deposit.

A close examination of Fig. 1.3 suggests that only the 10 glaciations during the past 0.9 Ma need to be considered because older glacial cycles were of lesser amplitude and therefore would have been susceptible to obliteration by the first major glaciation of interval "A". On the basis of the probability model, if 10 glacial episodes took place, the number of surviving tills and the probability of their survival is given in Table 1.1.

No. of surviving tills	Probability of survival
1	10%
2	28%
3	32%
4	20%
>5	10%

TABLE 1.1. The probability of the survival of till deposits after 10 glacial episodes. (Gibbons et al., 1984)

There is a 90% chance that after 10 glacial episodes only 1 to 4 tills will survive. The predicted probabilities are close to the observed 1 to 4 and more commonly 2 to 3 till units represented in the deposits of a given glacial

valley or ice-sheet lobe. The numerical mismatch between the typical 2 to 3 till units of the global Pleistocene and the number of major Pleistocene glacial-interglacial oscillations (probably 10 but perhaps as many as 24), matches the expected outcome of the process of obliterative overlap, functioning in a random manner over time (Gibbons et al., 1984).

1.2.2 THE MEDICINE HAT AREA

Medicine Hat is situated on the South Saskatchewan River in southern Alberta (Fig. 1.1). A complex system of buried valleys, ranging in age from possibly pre-Quaternary to pre "Classical Wisconsin", criss-crosses the area near Medicine Hat. The buried valleys are filled with material deposited by successive glaciers, lakes, aggrading rivers and wind (Stalker, 1969). The deposits are now exposed on numerous bluffs along the modern South Saskatchewan River. Stalker (1969) noted that the stratigraphy is highly variable, not only from bluff to bluff, but even within any single, long exposure. A strong glaciation will generally have had a drastic effect on the features left by earlier glaciers. This has led to an intermittent and very incomplete sedimentary record. The interpretation is therefore difficult, for it involves dealing with scattered remnants of sediment, commonly of unknown age or correlating between different types

of features (Stalker and Harrison, 1977).

Near Medicine Hat, the Quaternary beds are very fossiliferous, yielding a large number of mammal bones. In certain areas, up to eight till sheets are present, alternating with several bone bearing beds (Stalker, 1972). However, even with such well exposed sequences, there has still been difficulty in relating the glacial (till) deposits here to sequences found elsewhere in North America. Stalker (1972) has even found it difficult to correlete these deposits with others found upstream along the Oldman River.

All the tills in the area were deposited by Laurentide glaciers and are identifiable as such by the presence of Shield Stone (stones derived from the Canadian Shield to the east and northeast). Cordilleran tills are confined to the area west of Lethbridge, Alberta (Stalker and Harrison, 1977). Since no single exposure exhibits a complete record, the composite stratigraphic section of the southwestern Prairies (Table 1.2; Stalker and Churcher, 1982) is based on information obtained from 12 separate sections near Medicine Hat and one from the Wellsch Valley site, 40 km north of Swift Current, Saskatchewan (Fig. 1.1). For want of a better alternative, Stalker and Churcher (1982) used the mid-continental chronology, which is based on the assumption that there were only 4 major glaciations during Pleistocene time.

TABLE 1.2. Pleistocene composite stratigraphic section of the southwestern Canadian Prairies (modified from Stalker and Churcher, 1982). C = ^{14}C, F = fauna, FT = fission-track, M = paleomagnetism, and US = uranium-series.

UNIT NUMBER	TYPE OF DEPOSIT	ORIGIN OF DEPOSIT	# OF SPECIES IN FOSSILIF. UNIT	TIME SUBDIVISION	ESTIMATED AGES (years)
XXX	silt & sand	river slip-off slopes and floodplains	2	Postglacial	1,100 (C) 6,600 (C) 8,100 (C)
XXIX	sand & gravel	river terraces	5		9,500 (US) 11,200 (C)
XXVIII	sand & gravel	deltas & river channels	2		14,000 (F)
XXVII	till	directly from glacier		Young Wisconsin	
XXVI	sand & gravel	stream floodplains and shallow ponds	6		20,000 (F) 73,000 (US)
XXV	till	directly from glacier			
XXIV	silt	stream floodplains		Mid Wisconsin	
XXIII	organic silt	river floodplains (permafrost conditions)			24,000 (C) 28,600 (C) 430,000 (FT)
XXII	clay & silt	lakes, river floodplains	14		38,000 (C) 45,000 (F)
XXI	sand & gravel	lag material			
XX	sand	river deposition		Older Wisconsin	
XIX	till	directly from glacier			
XVIII	till	directly from glacier			
XVII	clay & silt	stream & lake deposition	3		>38,000 (C) 65,000 (F)
XVI	sand & gravel	stream & lake deposition			
XV	till	directly from glacier			
XIV	sand & gravel	stream floodplains and braided stream channels			

(continued)

UNIT NUMBER	TYPE OF DEPOSIT	ORIGIN OF DEPOSIT	# OF SPECIES IN FOSSILIF. UNIT	TIME SUBDIVISION	ESTIMATED AGES (years)
					>71,000 (US)
XIII	sand & gravel	stream floodplains and braided stream channels	31	Sangamon	72,000 (US) 100,000 (F)
XII	silt & sand	stream floodplains and braided stream channels			
XI	gravel	stream lag from till			
X	till	directly from glacier		Illinoian	
IX	sand & gravel	river floodplains and channels			
VIII	till	directly from glacier			
VIIb	silt & sand	preglacial lake deposition	3	Yarmouthian	195,000 (US) 420,000 (F)
VIIa	clay & silt	preglacial lake deposition			
VI	clay, sand & gravel beds	river floodplains		Late Kansan	
V	gravel, minor clay	river floodplains and channels	11		>200,000 (US) 600,000 (F)
IV	sand & gravel	flash floods, slope wash & steams		Nebraskan	
					2 reversals (P)
III	silt & sand with pebble bands	flash floods, slope wash & streams	17		690,000 (FT) 1,750,000 (F)
II	gravel	flash floods, slope wash & streams			
I	bedrock		4	Cretaceous	

The section at Wellsch Valley consists of one bone bearing unit, resting unconformably on bedrock or gravel deposits and is overlain by at least 4 till units. The bones here are more mineralized than bones from any of the horizons at Medicine Hat. The fauna of this unit, probably greater than 1.5 Ma, also indicates an age older than any at Medicine Hat (Stalker and Churcher, 1972). The base of this section (ie. units II - IV in Table 1.2) is therefore placed at the bottom of the composite statigraphic record. The age of the four or so tills above the bone bearing unit cannot be estimated, nor can they be correlated with tills found elsewhere in the Prairies.

The numerous bluffs near Medicine Hat each contain from 1 to 4 bone bearing horizons. Based on the faunal assemblage, 8 different bone bearing units can be distinguished (Stalker and Churcher, 1982). The oldest unit (V) contains a fauna of mid to late "Kansan" age and is placed above the Wellsch Valley units in the composite stratigraphic record. The remaining fossiliferous units are interbedded with tills and other sediments and comprise the rest of the stratigraphic record up to the present (Table 1.2).

Although the composite record extends intermittently back to approximately 2 Ma, it only records a small part of Quaternary time. The gap of more than one million years

between deposition of units IV and V alone encompasses more time than is recorded by all the other Quaternary deposits shown (Stalker and Churcher, 1982).

1.2.3 INDEPENDENT CHRONOLOGICAL CONTROL

Radiocarbon dating has been carried out on bones, wood, and buried soils within the various units. The oldest unit datable by carbon-14 is unit XXII, and yields an age of 38,000 years near its base (Stalker, 1976). The age estimates of the units beyond the range of radiocarbon dating are almost entirely based on the chronology obtained from the vertebrate fauna. In certain sections, there is some difficulty in determining the age of the fauna because of intermingling of taxa that are usually found separated in time (Stalker and Churcher, 1972). Although the faunal assemblage can in most cases be satisfactorily correlated with faunas found elsewhere on the continent, assignment of absolute ages to the various faunas is more difficult, due to uncertainties in the boundary dates of land mammal faunal stages (eg. compare: Flint, 1971, Fig.21-2 and Table 29D; Harington, 1984, Fig. 1).

Ages of till deposits are estimated, and are based on their position with respect to beds containing a well-defined faunal assemblage. For example, the lowest till deposit

(unit VIII) is assigned an "Illinoian" age, and is based on its position above beds containing "Yarmouthian" vertebrate fossils and below beds containing a well-developed "Sangamon" vertebrate fauna (Stalker, 1976).

Paleomagnetic work was carried out on a number of interglacial sediments (Foster and Stalker, 1976; Barendregt and Stalker, 1978). Unit III at Wellsch Valley was the only site where magnetically reversed sediments were observed.

Fission track dating on a vitric tuff bed 4 m above the fossiliferous horizon of unit III at Wellsch Valley was attempted by Westgate et al. (1978). Ages of 0.63 ± 0.06 and 0.69 ± 0.11 Ma were obtained. The dates should be regarded as minimum estimates, given the susceptibility of tracks in glass to annealing. Westgate et al. (1978) also obtained a fission track date of 0.43 Ma on a vitric ash, 7 m above a bone bearing horizon in unit XII near Medicine Hat. Radiocarbon dates of $37,900 \pm 1,000$ and $38,700 \pm 1,100$ a from 1 m above the same horizon were reported by Stalker (1976). However, the magnitude of the ages suggests that they are probably infinite radiocarbon dates.

^{230}Th and ^{231}Pa dating of bones from a number of sites near Medicine Hat was attempted by Szabo et al. (1973). In general, there is a large discrepancy between the uranium

series dates and the age estimates derived by other means (ie. faunal correlation; see Table 1.2). The discrepancies could arise from:

1) incorrect identification of the faunas;
2) incorrect correlation of the faunas with faunas elsewhere;
3) incorrect age estimates or age restrictions for the reference faunas;
4) incorrect stratigraphic correlation of units between various bluffs;
5) incorrect results from isotope dating, and
6) inclusion of bones reworked from earlier deposits which would result in older dates.

Since there was no alternative means of checking the ages of the various units, causes for the discrepancies were indeterminable.

CHAPTER 2

PRINCIPLES OF ESR DATING

2.1 ELECTRON TRAPPING

Radioactive elements within minerals and in the surrounding environment emit alpha-, beta-, and gamma-particles as a result of their decay. This radiation as well as cosmic rays, can ionize atoms or molecules within the mineral. The ionization process leading to trapping of electrons is shown in Fig. 2.1. The ionized electrons will diffuse within the crystal (in its conduction band) until they are trapped at charge defect centers (electron or hole traps) in the crystal lattice structure or until they recombine with electron holes. Trapped electrons in tooth enamel are associated with CO_3^{3-} radicals within the inorganic hydroxyapatite matrix (Cevc et al., 1972; Sato, 1979). The paramagnetic CO_3^{3-} center forms due to capture of an electron by the CO_3^{2-} radical which replaces PO_4^{3-} in the apatite structure (Gilinskaya et al., 1971).

2.2 PHYSICAL BASIS OF ESR

An unpaired trapped electron is characterized by its intrinsic angular momentum and associated magnetic moment. The magnetic moment ($\vec{\mu}_S$) is related to the angular momentum (spin $\vec{s}$) by the following equation:

$$\vec{\mu}_S = -g\mu_B\vec{s}/\hbar \qquad (2.1)$$

FIG. 2.1. Illustration of the trapping process.

E_a = activation energy, ie. trap depth.

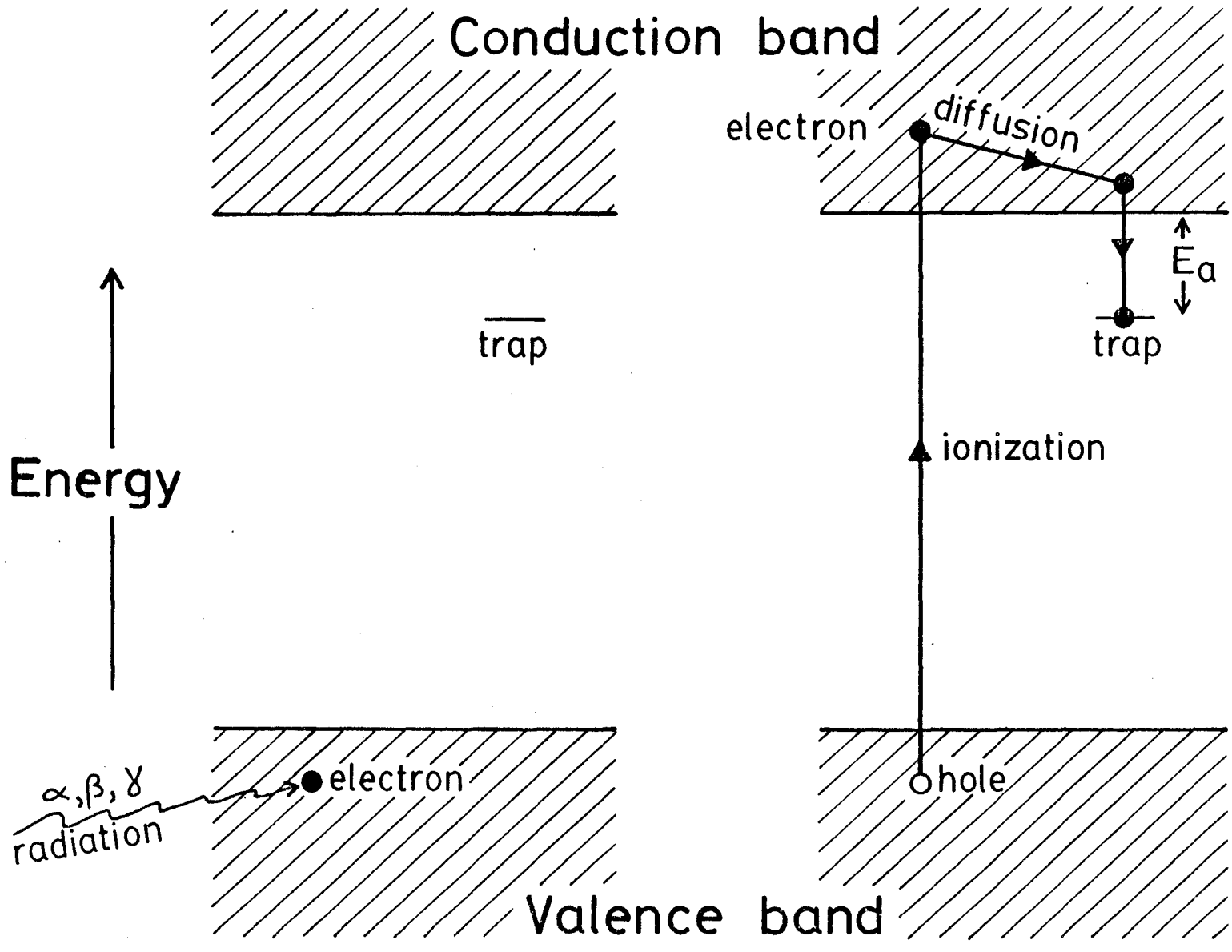
Conduction band
electron
diffusion
E_a
trap
trap
Energy
ionization
α, β, γ
radiation
electron
hole
Valence band

where g is the Landé-factor or the "electron free-spin g value" (g = 2.0023 for a free electron), μ_B is the Bohr magneton, and $\hbar = h/2\pi$ (h is Planck's constant).

When unpaired electrons are placed in an external static magnetic field, the direction of the electron spin vector may be either the same or opposite to the magnetic field vector. Only these two states with spin quantum number (M_S) +1/2 and -1/2 are allowed according to the laws of quantum mechanics (Fig. 2.2). The two states are energetically different (Fig. 2.3). The splitting of the initial energy level (E_0) into two discrete energy levels E_+ and E_- by an external magnetic field is known as the Zeeman effect. The energy difference (ΔE) between these two levels is,

$$\Delta E = g\mu_B H \qquad (2.2)$$

where H is the external magnetic field strength (Gauss).

If an external electromagnetic wave (microwave) of frequency ν is applied to the electrons, flipping of spins from one direction to another will occur if the condition $h\nu = \Delta E$ is met. The microwave is absorbed due to the transition from one state to another. This absorption of microwave energy is called electron spin resonance (ESR).

FIG. 2.2. Electron spin orientation in an external magnetic field (ω = resonance frequency = $2\pi\nu$).

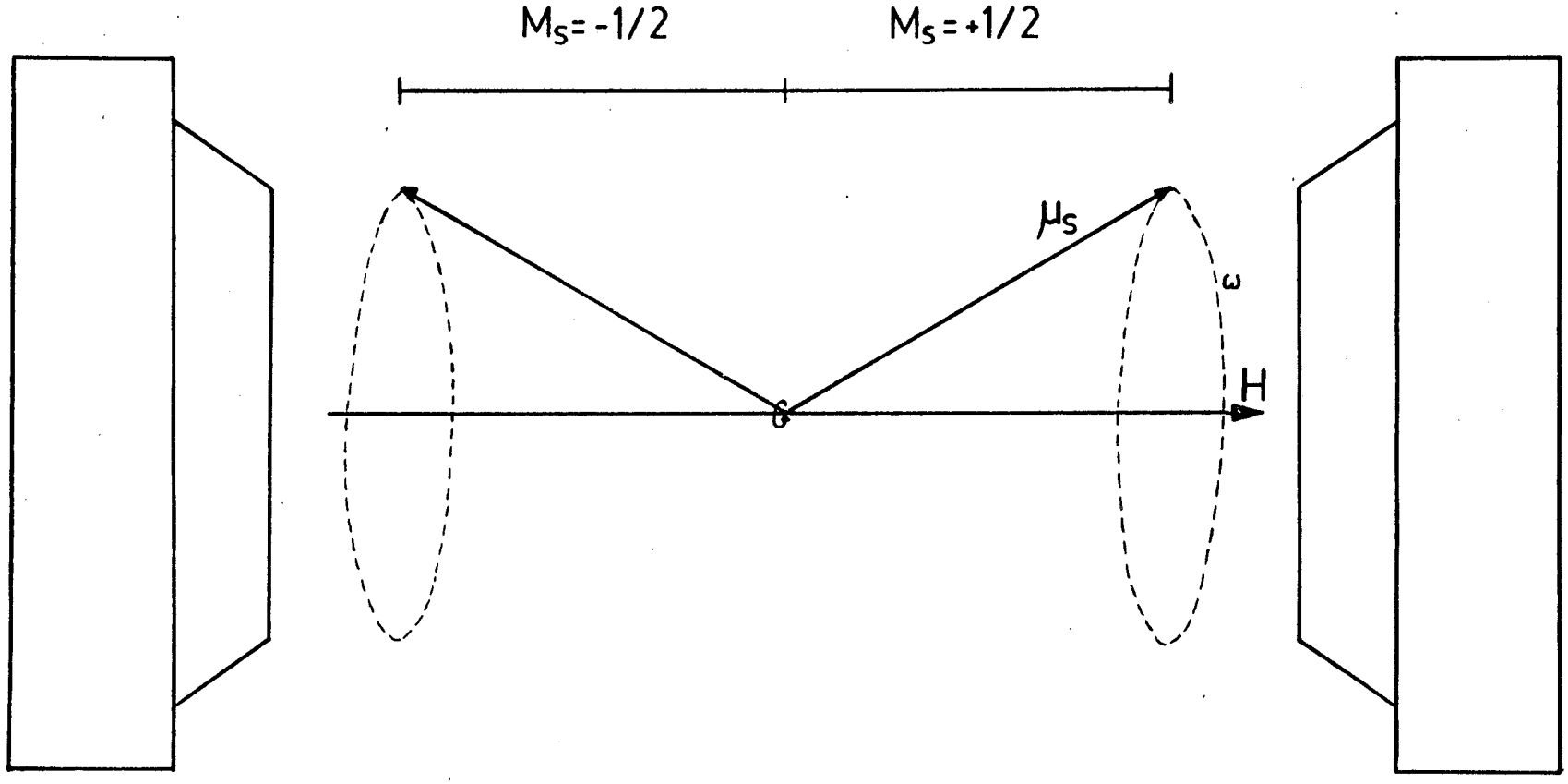
$M_S = -1/2$
$M_S = +1/2$
μ_S
ω
H

FIG. 2.3. Zeeman splitting into two energy levels for free electrons (s = 1/2) by an external magnetic field.

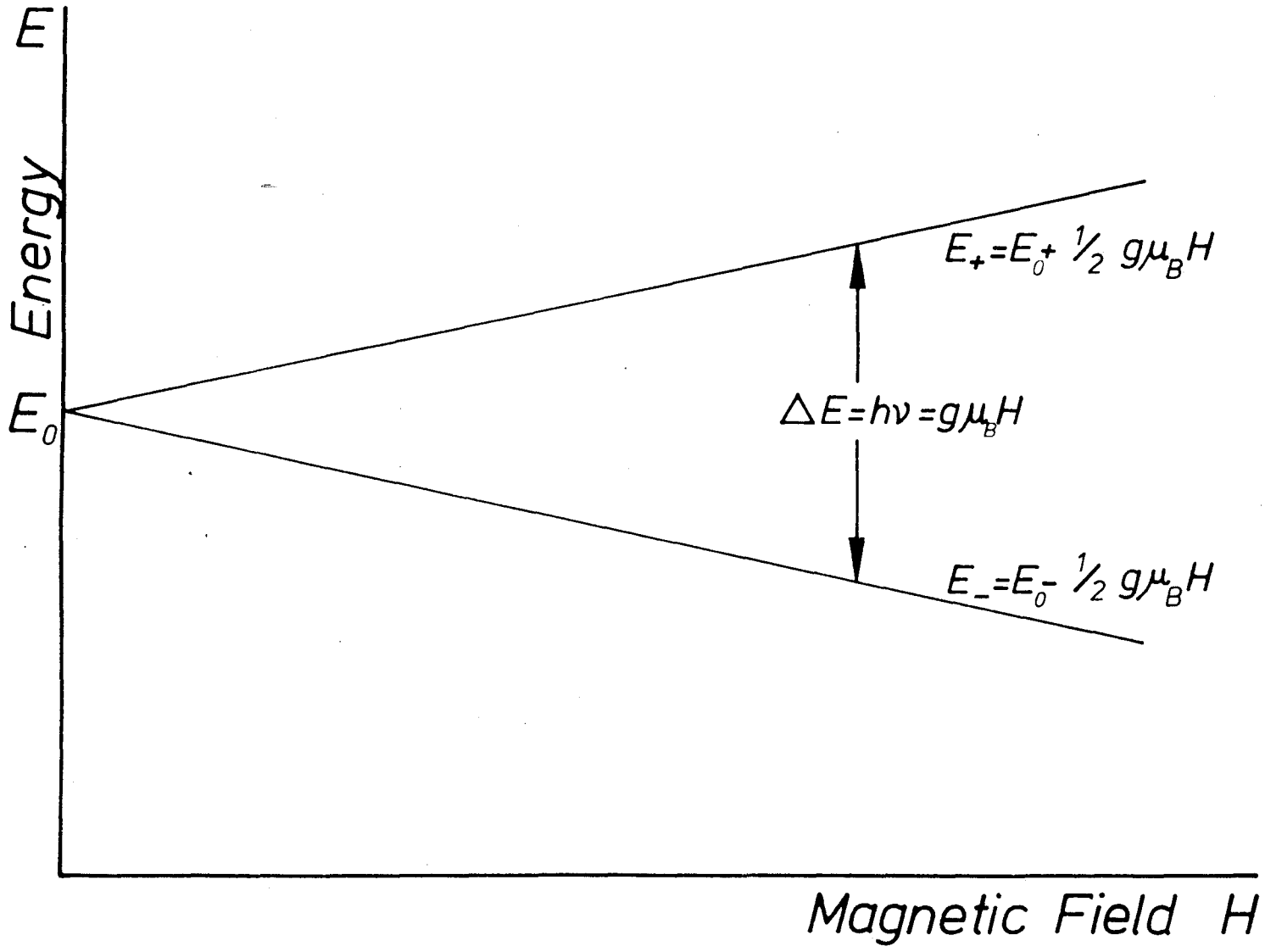
E
Energy
E_0
$E_+ = E_0 + \frac{1}{2} g\mu_B H$
$\Delta E = h\nu = g\mu_B H$
$E_- = E_0 - \frac{1}{2} g\mu_B H$
Magnetic Field H

2.3 ESR SPECTROMETER

A Bruker ER100D ESR spectrometer with a TE4101 cavity, of the Chemistry Department at McMaster University was used for all the samples analysed. An ESR spectrometer is principally built of three components (Fig. 2.4):

1) An electromagnet and its associated power supply.
2) A klystron that generates microwaves and is attached by a waveguide to the resonant cavity suspended between the magnetic polepieces.
3) Electronic circuitry for signal detection, processing and recording.

A powdered sample is placed in a glass tube which is inserted into the resonant cavity. The klystron generates microwave radiation which is conducted to the resonant cavity by means of a waveguide. The normal microwave frequency (ν) used is near 9.5 GHz (X-band) at a magnetic field H= 3,500 G. Since the frequency used is dependent on the geometry of the waveguide and resonant cavity, ν is kept constant while H is varied. Resonance occurs when $H = h\nu/g\mu_B$ (ie. $h\nu = \Delta E = g\mu_B H$). Microwave energy is absorbed and an absorption signal (Fig. 2.5, top) is picked up by a detector. The signal is processed by additional electronic circuitry and is transmitted to an X-Y recorder which plots the first derivative of the ESR signal (I) against magnetic field strength (H). (Fig.

FIG. 2.4. A block diagram of an ESR spectrometer.

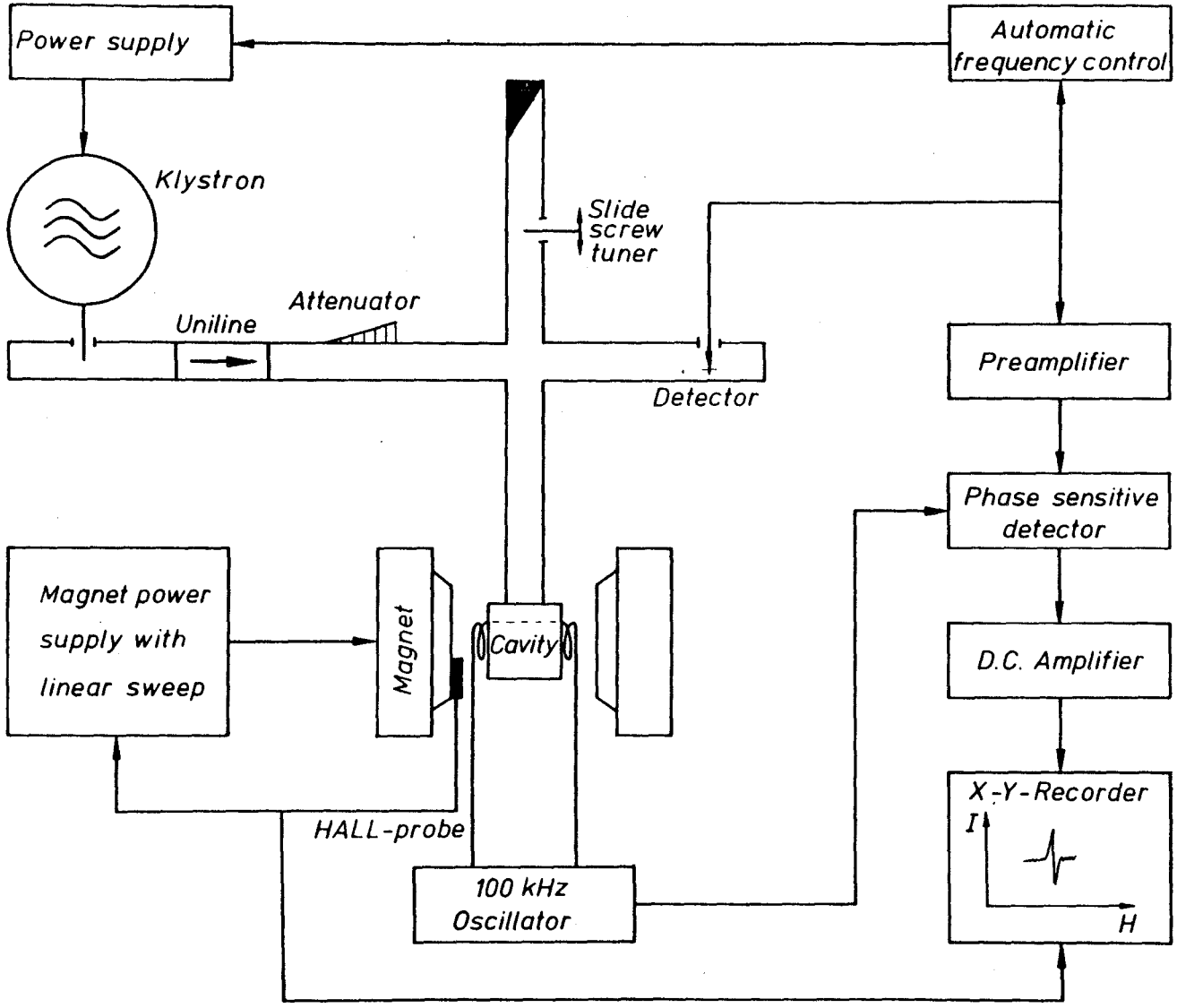
Power supply
Automatic frequency control
Klystron
Slide screw tuner
Attenuator
Uniline
Preamplifier
Detector
Phase sensitive detector
Magnet power supply with linear sweep
Magnet
Cavity
D.C. Amplifier
X-Y-Recorder
I
H
HALL-probe
100 kHz Oscillator

FIG. 2.5. ESR absorption line and its first derivative (ESR signal) obtained by a magnetic field modulation (H_m).

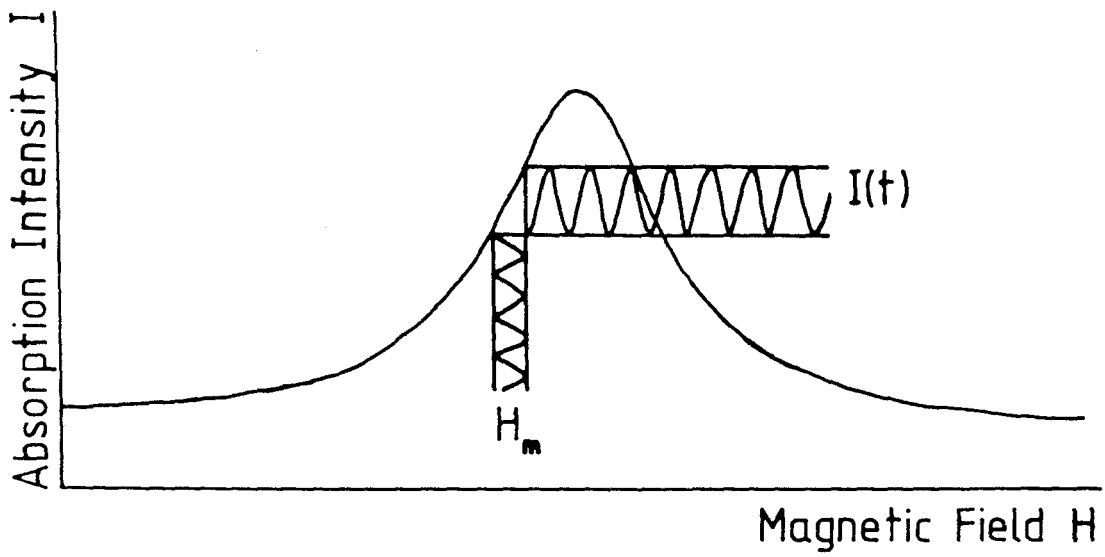
Absorption Intensity I
I(t)
H_m
Magnetic Field H

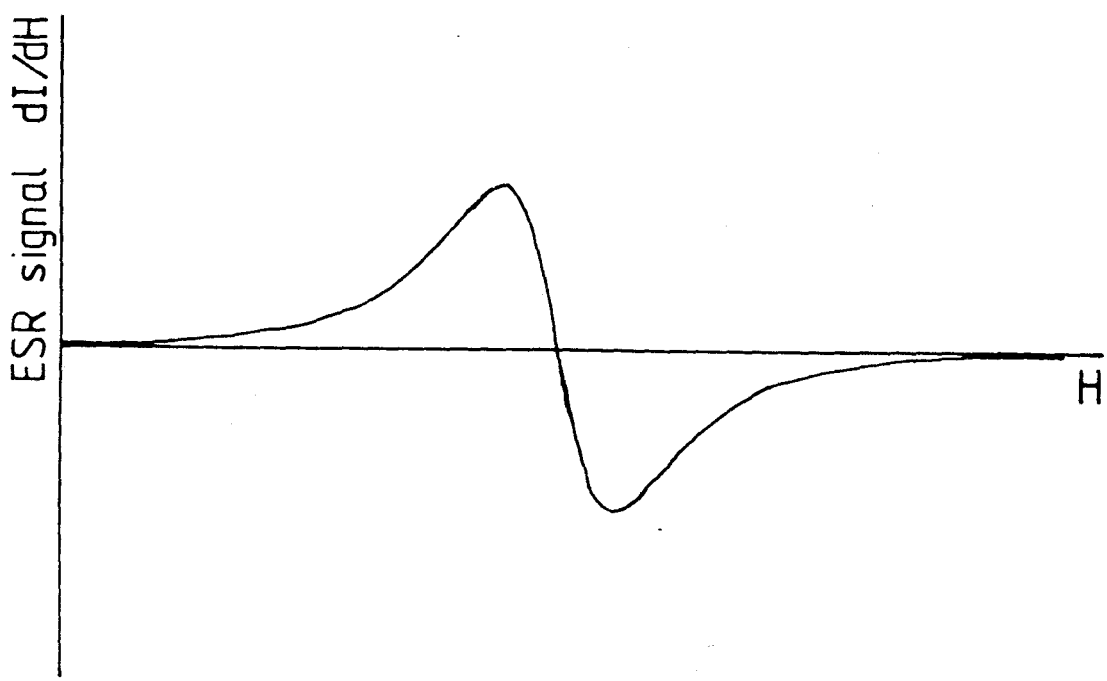
ESR signal dI/dH
H

2.5, bottom). The intensity of the ESR signal is proportional to the total number of trapped electrons of a particular g-value.

2.4 ESR DATING - GENERAL METHOD

ESR dating of geological materials was first suggested by Zeller et al. (1967). This was followed by McMorris (1969) and then more vigorously by Ikeya (1975, 1978, etc). Presently there are over 30 laboratories engaged in ESR dating. The most recent papers covering the major aspects of ESR dating in Quaternary geology are by Hennig and Grün (1983) and Ikeya (1985).

The ESR signal intensity of a natural mineral (Fig. 2.6) is proportional to the total number of unpaired electrons that have accumulated in electron traps since time of formation of the sample. The trapped electron population in turn is proportional to the radiation dose (or accumulated dose - AD) that the sample has received over this time period. If the effective annual dose emitted from radioactive elements within (internal dose rate - IDR) and surrounding (external dose rate - EDR) the sample can be determined, then the age of the sample is deduced by the following simplified equation,

$$\text{Age (a)} = \text{AD (rad)}/[\text{EDR} + \text{IDR (rad/a)}]. \qquad (2.3)$$

FIG. 2.6. ESR signal of tooth enamel. The signal intensity at g = 2.0015 is used for ESR dating.

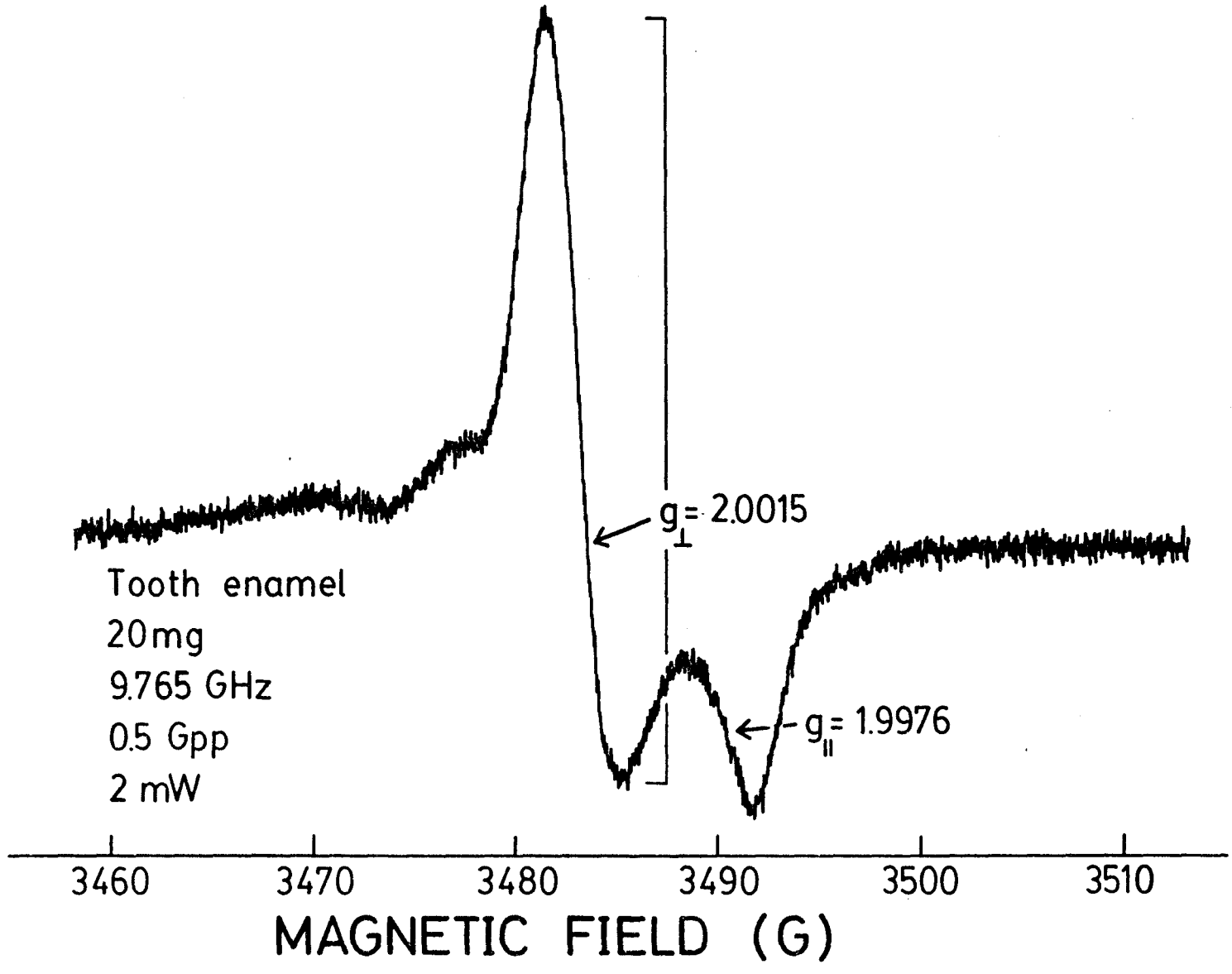
$g_{\perp}$= 2.0015
$g_{\parallel}$= 1.9976
Tooth enamel
20mg
9.765 GHz
0.5 Gpp
2 mW
3460
3470
3480
3490
3500
3510
MAGNETIC FIELD (G)

The accumulated dose (AD) that a sample received during geologic time is determined by the additive dose method (Fig. 2.7). Several equal, homogeneous aliquots of a sample are exposed to successive increasing doses of gamma irradiation and their corresponding increasing ESR signal is recorded. The AD is determined by extrapolating a linear fit through the data points to zero ESR intensity.

AD determination of extremely old samples or samples exposed to a high annual dose may be difficult, since such samples can display saturation effects. The effect is one where a major fraction of the electron traps are filled with electrons and additional gamma iradiation results in a non-linear increase of the ESR signal. This non-linearity will continue until all the traps are filled and maximum ESR intensity (I_{max}) is attained (Fig. 2.8a). Apers et al. (1981) proposed a model that could lead to reliable values of AD if saturation effects are observed. The model is based on plotting the ESR intensity in terms of $-\ln(1 - I/I_{max})$ instead of I. Such an approach can lead to reasonable linear graphs with good correlation coefficients (Fig. 2.8b).

As noted above, the annual dose in most cases, consists of two parts, the external or environmental dose rate (EDR) and the internal dose rate (IDR). The EDR can be determined by three methods:

FIG. 2.7. Determination of the accumulated dose (AD) by the additive dose method.

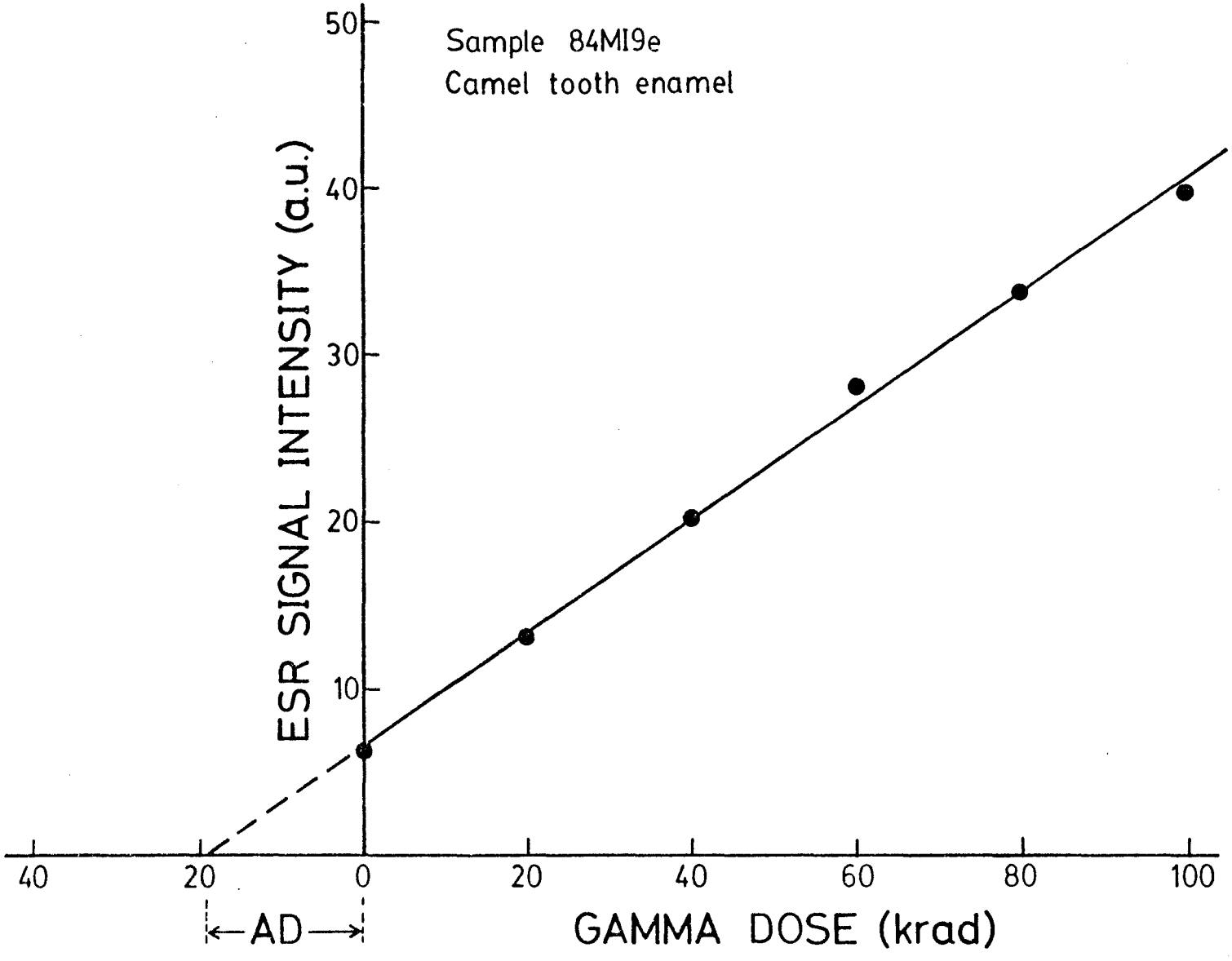
Sample 84MI9e
Camel tooth enamel
ESR SIGNAL INTENSITY (a.u.)
50
40
30
20
10
40
20
0
20
40
60
80
100
AD
GAMMA DOSE (krad)

FIG. 2.8. An alternative method of AD evaluation if saturation effects are observed upon additional exposure to gamma doses. I_{max} = maximum ESR signal intensity attained under extremely high gamma dose exposures. In Fig. 2.8a, a = linear extrapolation from points up to 50 krads, b = exponential fit (from Hennig and Grün, 1983).

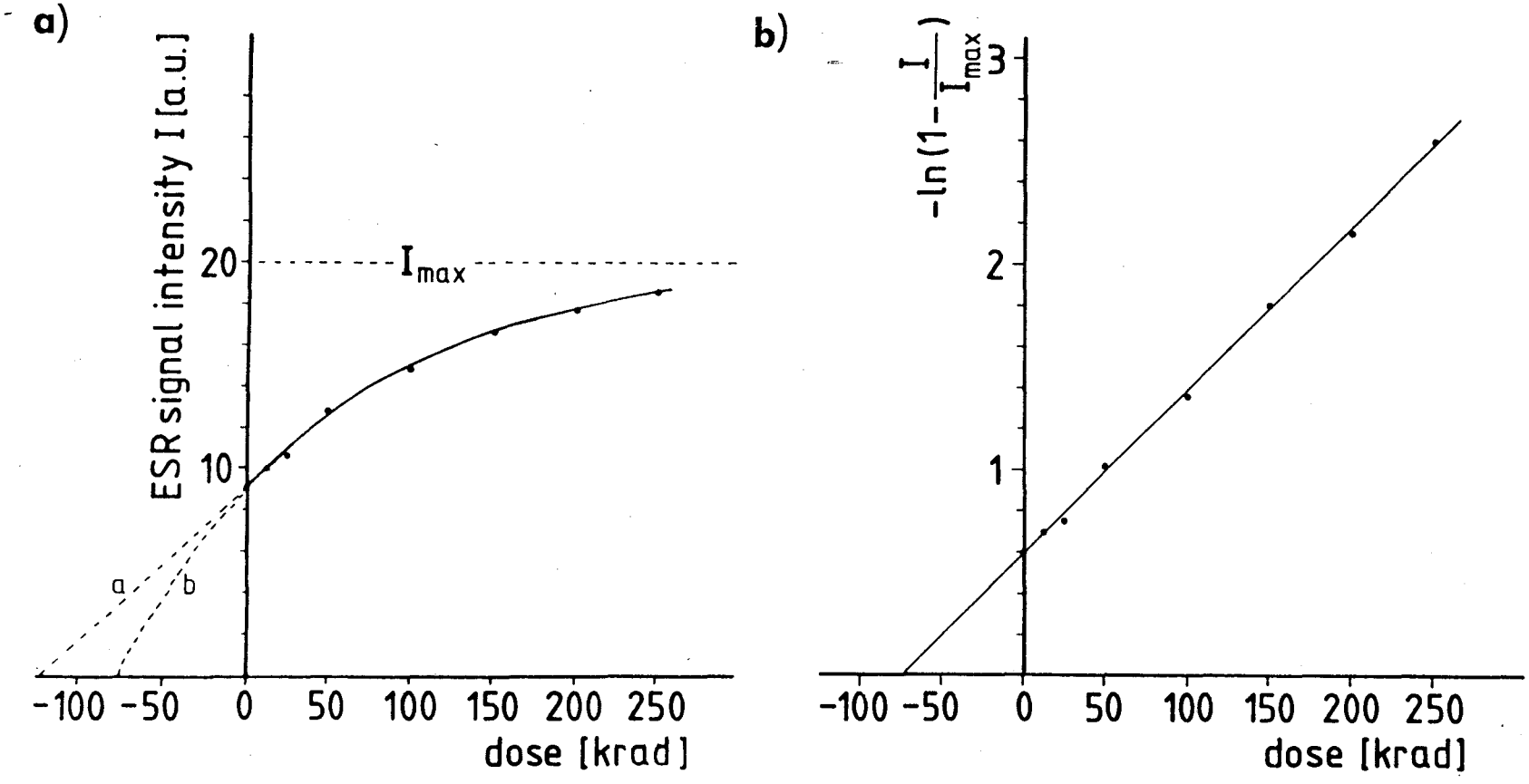
a)
ESR signal intensity I [a.u.]
20
10
I_{max}
a
b
-100 -50 0 50 100 150 200 250
dose [krad]
b)
$-\ln(1-\frac{I}{I_{max}})$
3
2
1
-100 -50 0 50 100 150 200 250
dose [krad]

1) Chemical analysis of the surrounding sediment for U, Th and K.

2) Gamma ray spectroscopy at the sampling site.

3) TL dosimetry, - burying a TL dosimeter at the same location as the sample for a period of one year.

The IDR can be determined by analysing the sample for U and its daughter isotopes. Th and K are generally found in negligible concentrations within tooth enamel.

CHAPTER 3

ANALYTICAL PROCEDURE

3.1 SAMPLE PREPARATION

Fossil teeth were collected from five sites in southern Alberta and Saskatchewan. (Fig. 1.1). The Medicine Hat Site (Fig. 3.1), consists of 7 separate exposures along the South Saskatchewan River and one (Frisch Site) occurs in an outlier of Quaternary sediments, several kilometers distant from the river. Additional samples came from the collection of Dr. C. S. Churcher, University of Toronto.

All the samples are fragments of tooth from large land mammals, predominantly horse, elephant, camel and bison. The tooth fragments are composed mainly of enamel; most have varying amounts of dentine/cementum attached. The sediment surrounding the sample was collected for U, Th and K analysis so that an environmental dose rate (EDR) could be determined.

The samples were cleaned with water to remove any remaining sediment. The thickness of the enamel was measured and the geometry of the samples noted for future beta dose rate calculations. The dentine/cementum was chiseled away from the enamel and any remaining dentine/cementum as well as the outer 100 micrometers of enamel was removed with a high speed, dental drill. The cleaned enamel was ground with a mortar and pestle until it passed through a 0.5 mm sieve. The dentine/cementum and some of the enamel were saved for U

FIG. 3.1. Map of Medicine Hat district showing location of sites along the South Saskatchewan River where fossil samples were collected.

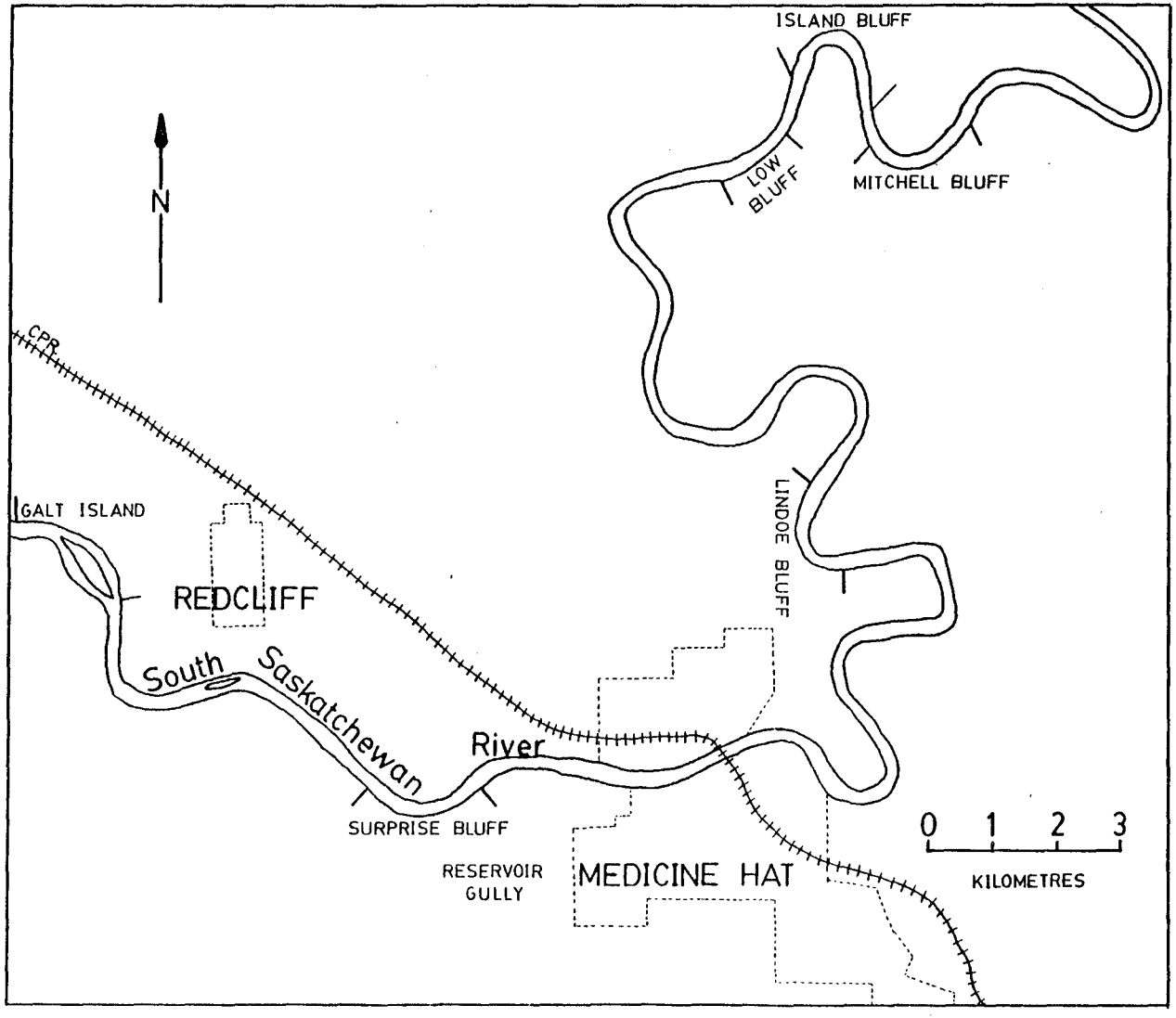
ISLAND BLUFF
LOW BLUFF
MITCHELL BLUFF
N
CPR
GALT ISLAND
REDCLIFF
LINDOE BLUFF
South Saskatchewan River
SURPRISE BLUFF
RESERVOIR GULLY
MEDICINE HAT
0 1 2 3
KILOMETRES

analysis so that the dentine and enamel dose rate contribution could be determined.

3.2 SPECTROMETRY PROCEDURE

All enamel samples analysed on the ESR spectrometer were transferred into a 4 mm pyrex tube sealed at one end. The tube was marked at a determined height to ensure that all the samples would be positioned at the same location in the cavity. Each sample was run 3 times and the signal intensity at g = 2.0015 (Fig. 2.6) was recorded and averaged. After numerous runs, the data revealed that one run per aliquot of sample was sufficient to yield an AD with a good correlation coefficient. For tooth enamel the best instrumental settings were found to be:

Microwave power	2 mW
Modulation amplitude	0.5 Gpp
Sweep width	100 G
Sweep time	200 s
Time constant	10 to 50 ms.

3.3 ARTIFICIAL IRRADIATION

Six aliquots, each 20 mg in weight were taken from the cleaned, crushed enamel. Five aliquots were exposed to successively increasing doses of artificial gamma rays from a

^{60}Co source. All irradiations were performed at the Gamma Irradiation Facility, McMaster Nuclear Reactor. The samples were irradiated in 4 mm diameter glass tubing with 1 mm thick walls. The tubes were aligned so that all samples were the same distance from the irradiation source (ie. there was no shielding by other samples). One enamel sample was also irradiated in glass tubing with 2 mm wall thickness to determine if any irradiating rays with lower energies would be attenuated by the additional thickness of glass and to test whether the "buildup" of secondary beta rays was sufficient in the 4 mm tubes. The difference in the AD of the sample irradiated in tubes with 1 mm and 2 mm thick walls was negligible.

A test of the possible effect of dose rate on the determination of AD is shown in Fig. 3.2. The agreement between AD's becomes progressively poorer as lower dose rates are approached. A possibility for this phenomena is that sample irradiation at lower dose rates took place further away from the ^{60}Co source, closer to the backwall of the irradiation chamber. In this area, scattered gamma rays of lower energies may become more prominant, resulting in inconsistent irradiation of the sample. Since higher dose rates gave consistent AD's, all samples were irradiated at a dose rate of 10 or 20 krad/hr. Other experiments with lithium fluoride (Tochilin and Goldstein, 1966) demonstrated that a dose rate as high as 10^{10} rads per second can be used.

Fig. 3.2. Dependence of AD on the gamma dose rate of the artificial irradiation from a ^{60}Co source. The 3 different symbols represent 3 separate tests.

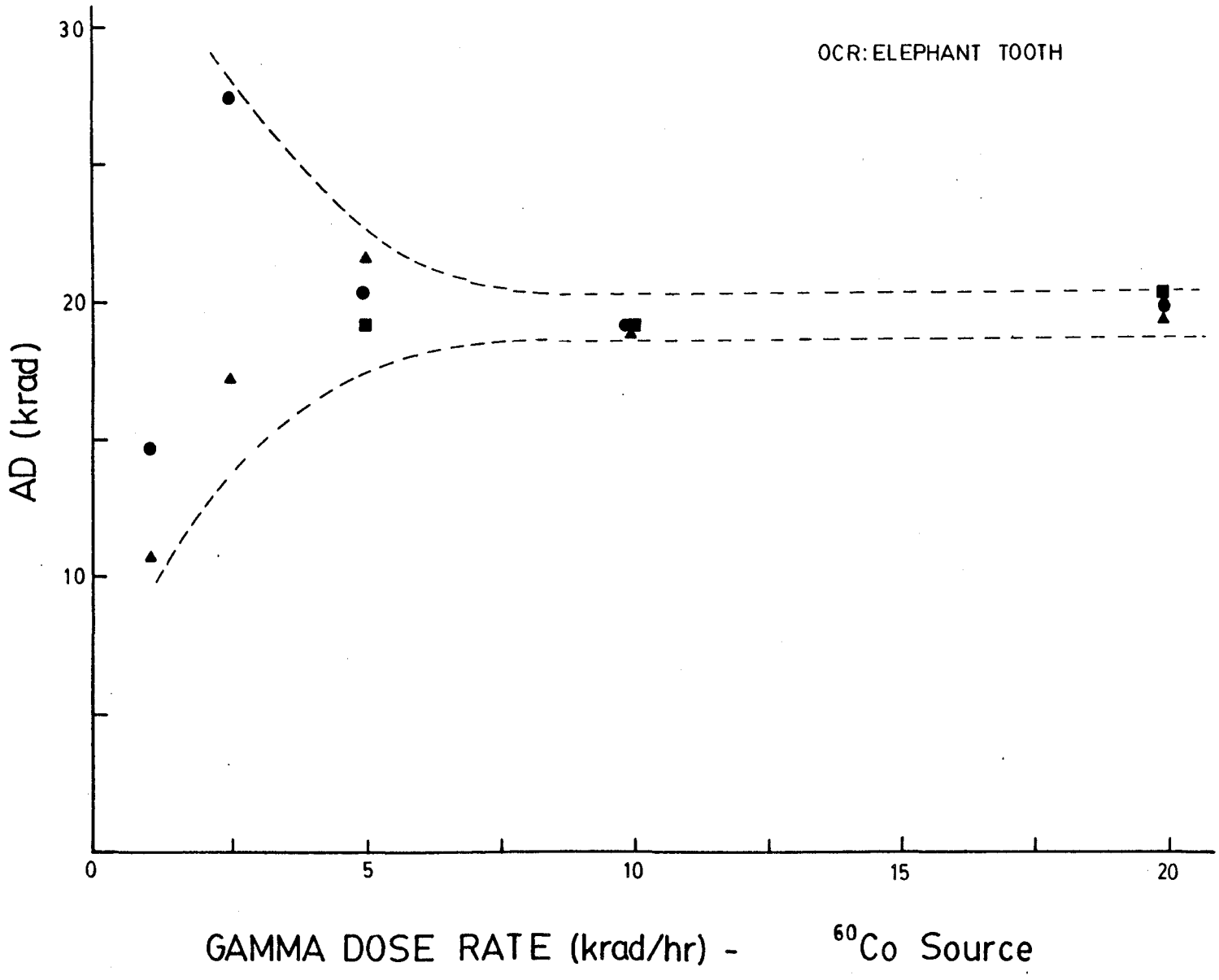
OCR: ELEPHANT TOOTH
AD (krad)
30
20
10
0
5
10
15
20
GAMMA DOSE RATE (krad/hr) - ^{60}Co Source

CHAPTER 4

DETERMINATION OF AD

4.1 SATURATION

Five aliquots of each sample were irradiated at doses of 20, 40, 60, 80 and 100 krad respectively. In all cases the ESR signal intensity increased linearly over the 100 krad dose range. Two samples with AD's of 2.2 and 120 krad were intentionally irradiated to a dose of 500 krad to test for saturation (Figs. 4.1 and 4.2). Signs of saturation appeared at a dose (artificial + AD) of 150 and 370 krad respectively.

Fig. 4.3a demonstrates that as saturation is approached, ESR signal intensity is no longer linearly proportional to the dose the sample received. Onset of saturation is characterized by a decrease in the slope of the ESR intensity (ie. a decrease in the sensitivity of the sample to irradiation). The lower sensitivity will result in an overestimate of the AD (Fig. 4.3a & b).

A comparison of normalized ESR sensitivity with the AD of 35 enamel samples is shown in Fig. 4.4. At higher AD's there is a decrease of the ESR sensitivity. The decrease in sensitivity is attributed to saturation; the trend being similar to the saturation conditions encountered in samples 84LN3 and 84RG3 (Fig. 4.1 and 4.2). However, the sensitivity of all visibly altered samples is low regardless of their AD (Fig. 4.4). Therefore in some cases (ie. when alteration has

FIG. 4.1. Bison tooth irradiated at high gamma dose levels to test for saturation.

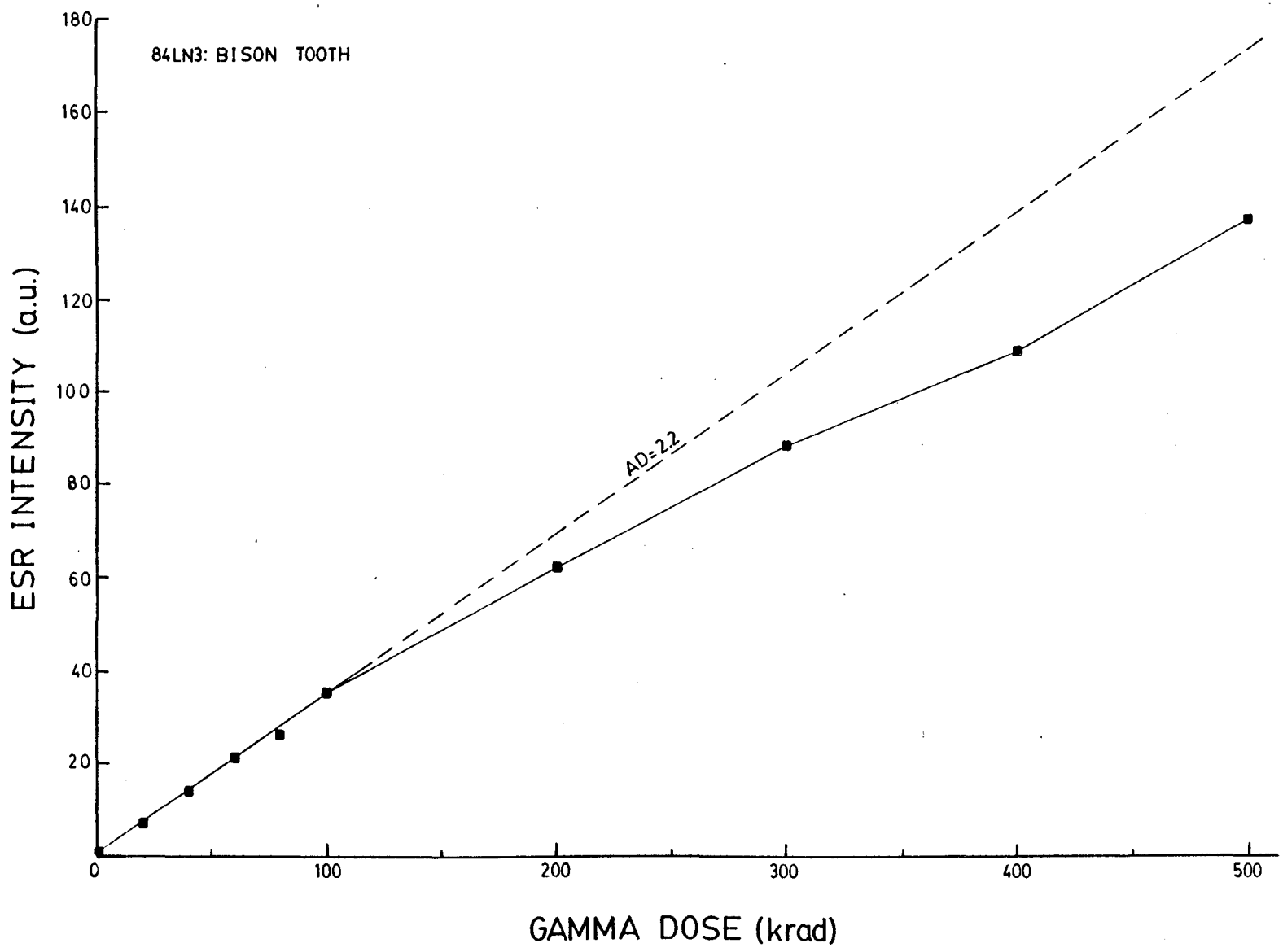
84LN3: BISON TOOTH
ESR INTENSITY (a.u.)
GAMMA DOSE (krad)
AD=2.2
0
20
40
60
80
100
120
140
160
180
0
100
200
300
400
500

FIG. 4.2. Horse tooth irradiated at high gamma dose levels to test for saturation.

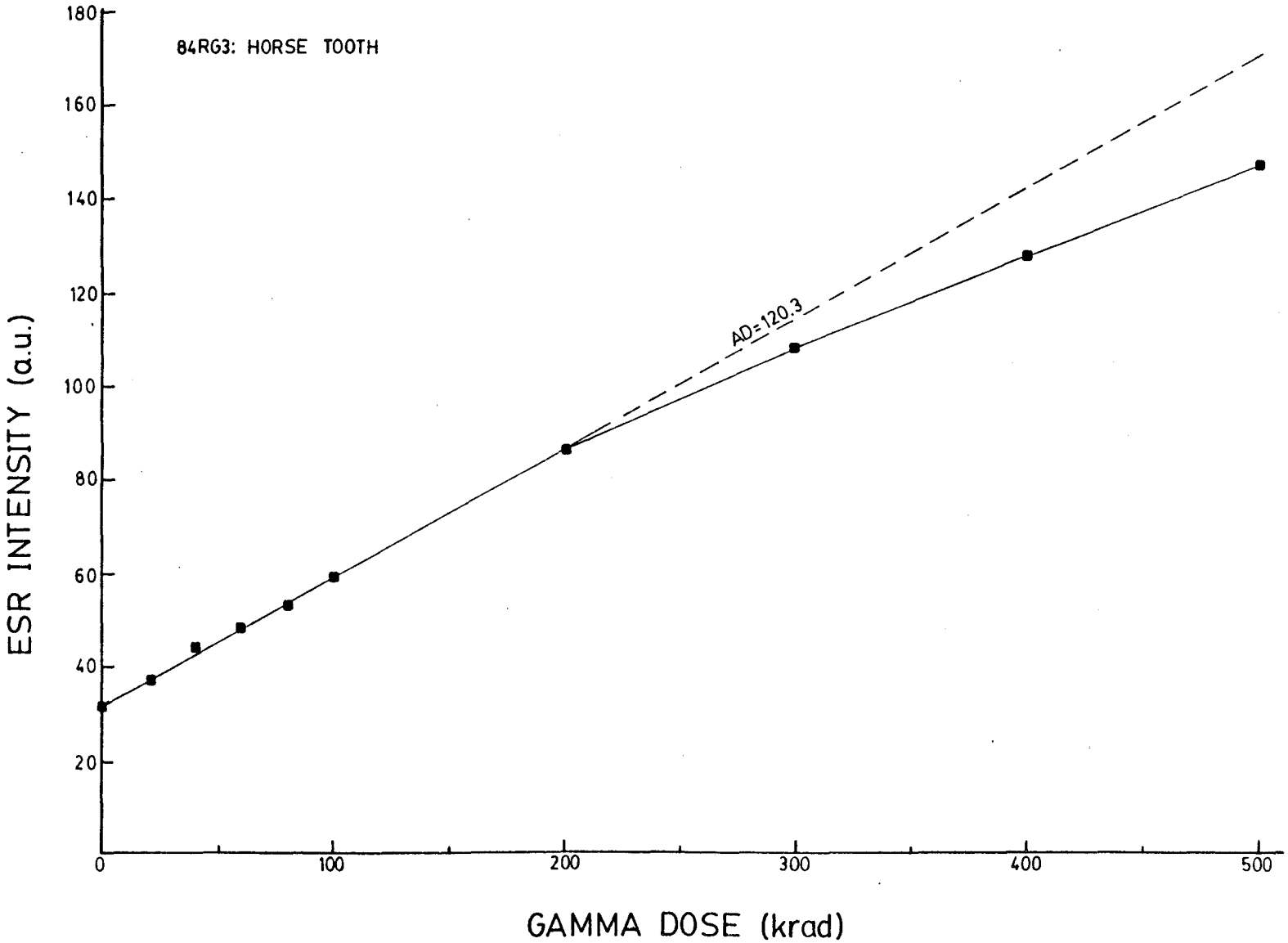
84RG3: HORSE TOOTH
AD=120.3
ESR INTENSITY (a.u.)
GAMMA DOSE (krad)
180
160
140
120
100
80
60
40
20
0
100
200
300
400
500

FIG. 4.3. The effects of saturation on ESR signal growth and the AD.

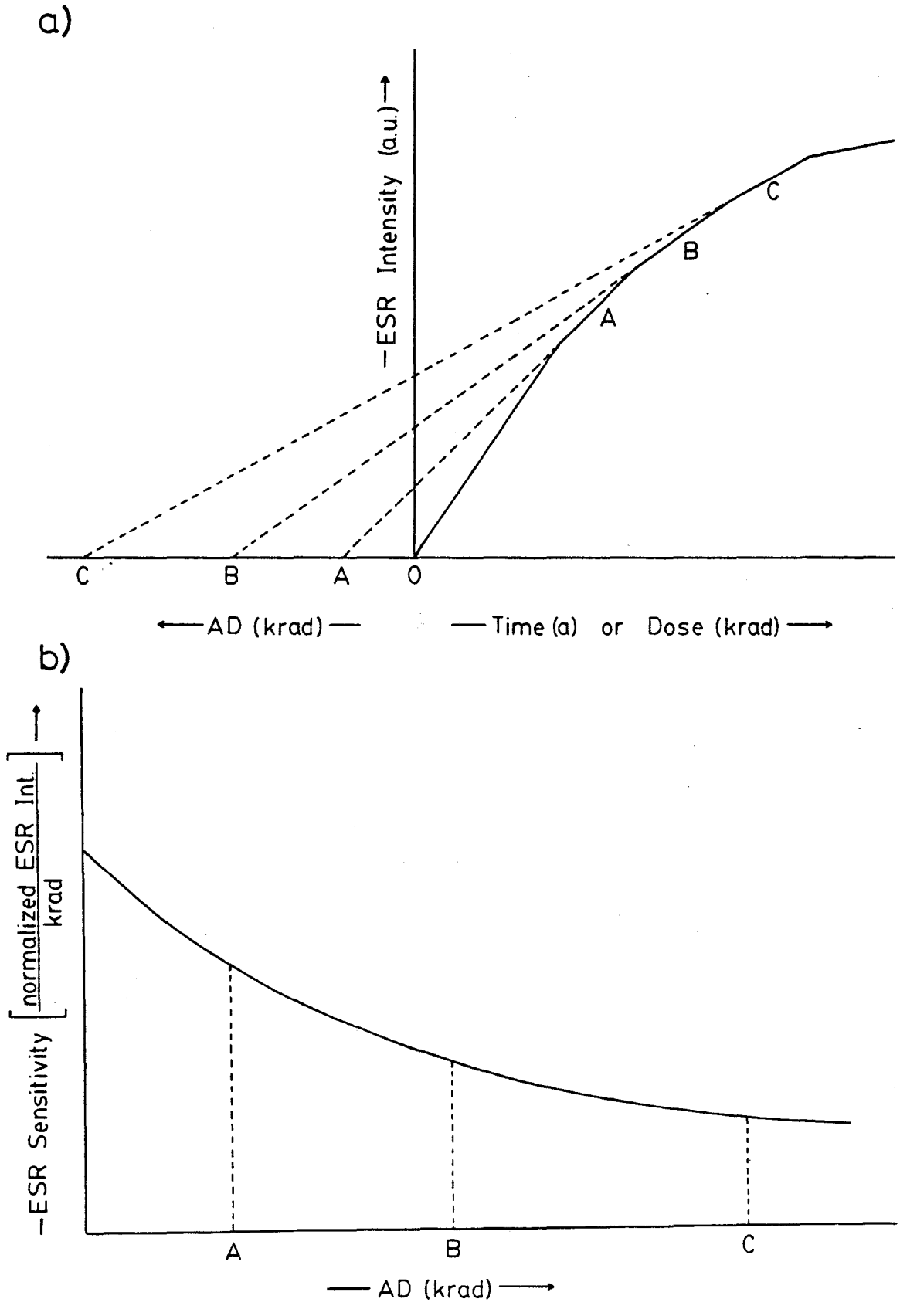
a)
−ESR Intensity (a.u.)
C
B
A
0
C
B
A
←AD (krad)—
—Time (a) or Dose (krad)→
b)
−ESR Sensitivity [normalized ESR Int. / krad]
A
B
C
—AD (krad)→

FIG. 4.4. Variation of ESR sensitivity with increasing AD.

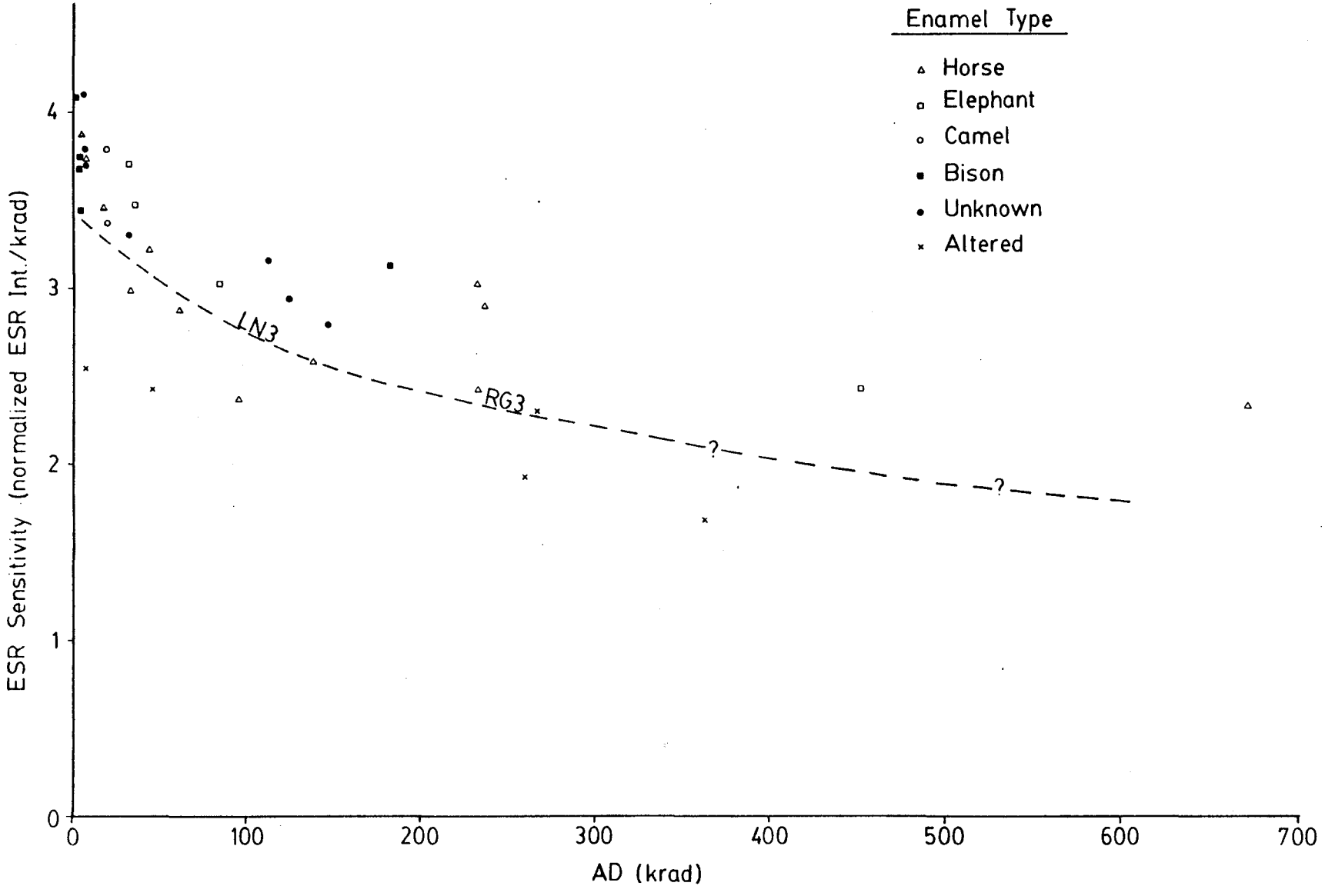
Enamel Type
Horse
Elephant
Camel
Bison
Unknown
Altered
LN3
RG3
?
?
ESR Sensitivity (normalized ESR Int./krad)
AD (krad)
0
1
2
3
4
0
100
200
300
400
500
600
700

occurred but is not visible) the decrease in sensitivity could be attributed to "aging" of the samples (ie. paramagnetic CO_3^{3-} centers and/or CO_3^{2-} ions are either removed or CO_3^{2-} are bound with other radicals). It is advisable to perform saturation tests on samples with AD's greater than 50 krad. If saturation conditions are revealed, then the AD must be determined by the method described by Apers et al. (1981).

4.2 SAMPLE WEIGHT AND GRAIN SIZE

From the powdered enamel, at least 0.4 g is removed for U analysis. Since most of the samples are small, only a small portion will be left for ESR analysis. A test was therefore performed to find the minimum weight required for a reliable AD determination. The results displayed in Fig. 4.5 show that a sample weight as low as 10 mg can be used. The deviation of the 5 mg sample is attributed to an increase in the weighing error. This is supported by a decrease in the 5 mg AD correlation coefficient.

To determine if the grain size of powdered enamel has any effect on the AD, a sample was subdivided into 4 grain size fractions (Fig. 4.6). The AD does not appear to be dependent on enamel grain size. Also, the similar AD's of the fine and coarse fraction indicates that grinding has no influence on the ESR signal. The 0.150 - 0.250 mm fraction

FIG. 4.5. The AD of an elephant tooth determined at different weights.

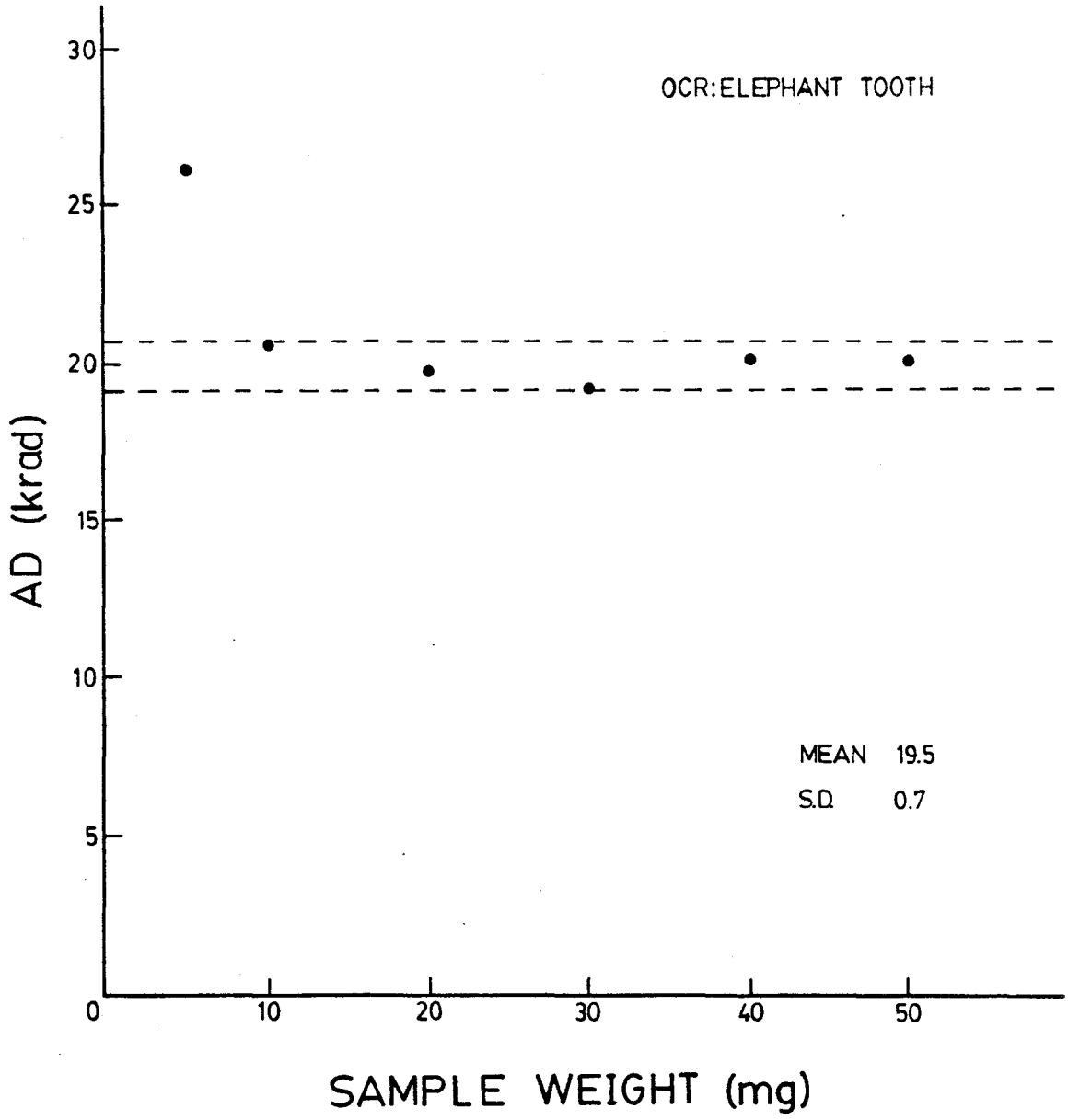
OCR:ELEPHANT TOOTH
MEAN 19.5
S.D. 0.7
AD (krad)
SAMPLE WEIGHT (mg)
0
5
10
15
20
25
30
0
10
20
30
40
50

FIG. 4.6. Dependence of AD on enamel grain size.

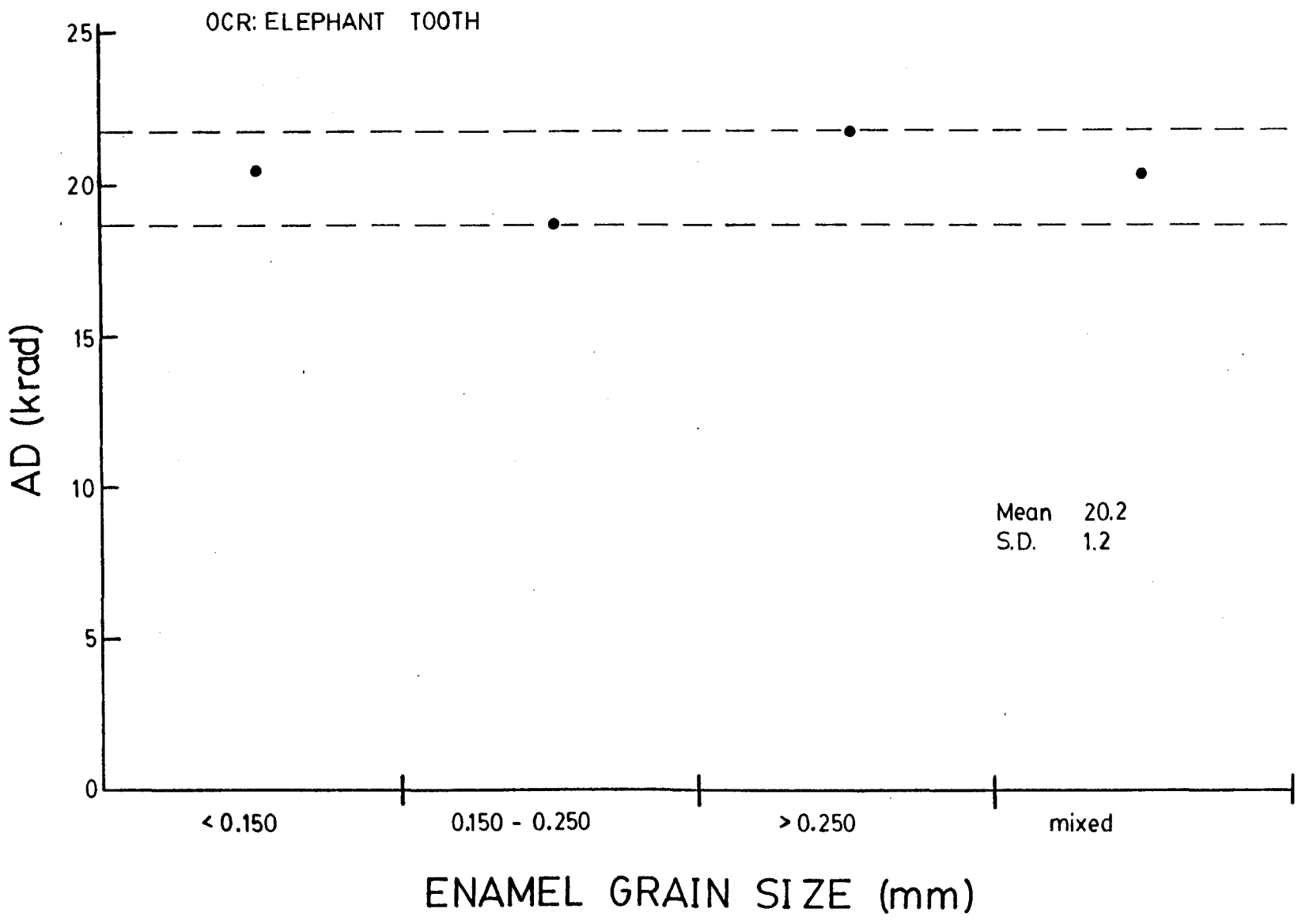
OCR: ELEPHANT TOOTH
25
20
15
10
5
0
AD (krad)
Mean 20.2
S.D. 1.2
< 0.150
0.150 - 0.250
> 0.250
mixed
ENAMEL GRAIN SIZE (mm)

is the easiest to work with and was therefore used for all the analysis. The <0.150 mm fraction leaves a fine powder in the sample tube after the enamel is removed. To prevent contamination the sample tube should be cleaned between each analysis if this size fraction is used. The >0.250 mm fraction was not used because the coarse grains tend to "bridge" when the sample is transfered into the analysing tube.

4.3 MODULATION AMPLITUDE AND MICROWAVE POWER

Due to the low signal-to-noise ratio of the ESR signal, it is transformed into an amplitude modulation signal, rather than being directly amplified. This is achieved by modulating the magnetic field H by a small additional magnetic field H_m generated by a 100 kHz oscillator (Fig.2.4). To prevent masking of any part of the signal and to get the highest resolution, a low modulation should be used (ie. the amplitude of the additional magnetic field H_m should not exceed the linewidth of the ESR absorption signal (Fig. 2.5).

In order to determine the appropriate modulation setting for tooth enamel, the modulation amplitude was varied from 0.2 to 5 Gpp (Gauss peak to peak). Over this amplitude range, the modulation had no influence on the AD (Fig. 4.7). However, certain enamel samples display an additional signal

FIG. 4.7. Dependence of AD on modulation amplitude.

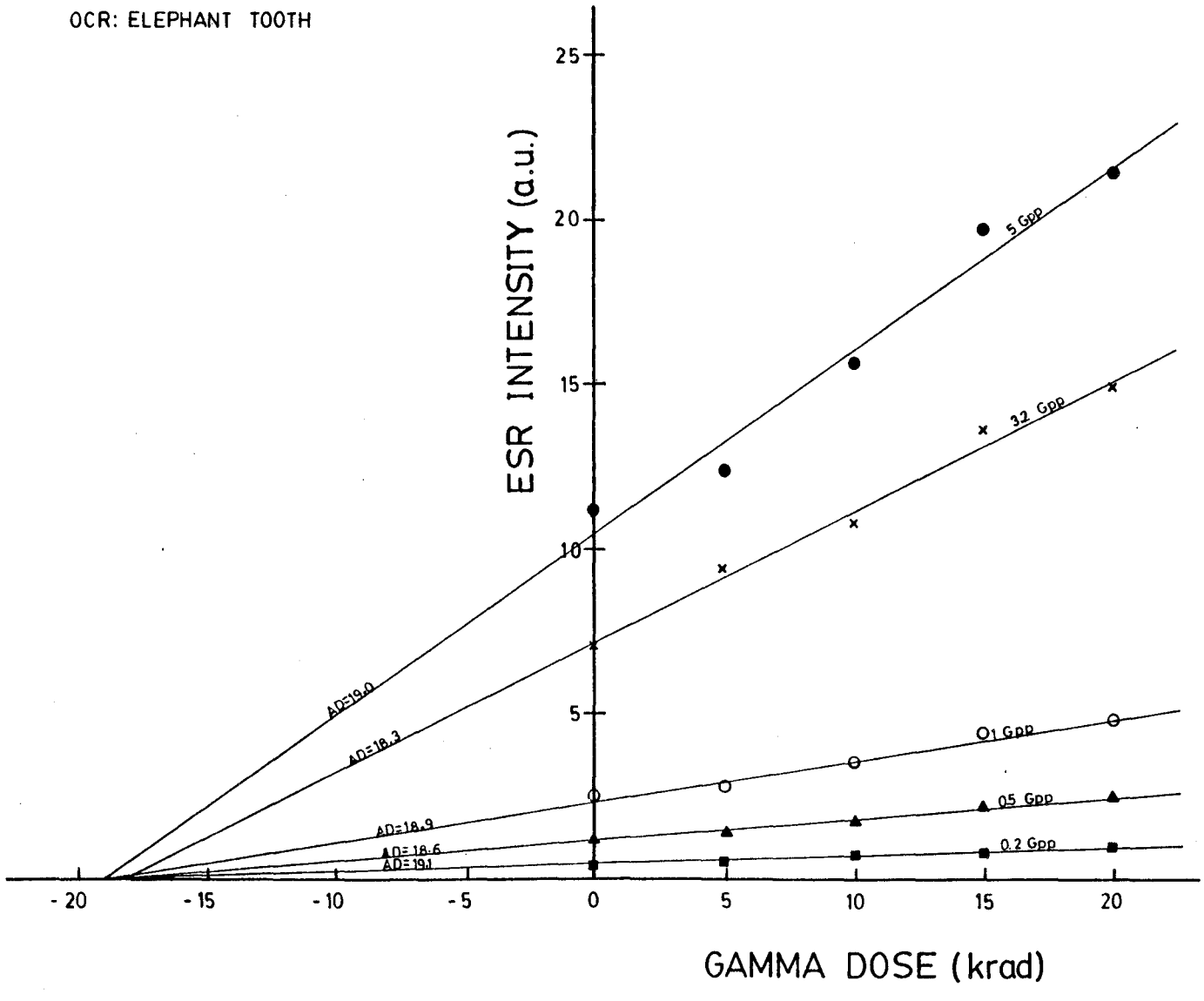
OCR: ELEPHANT TOOTH
ESR INTENSITY (a.u.)
25
20
15
10
5
- 20
- 15
- 10
- 5
0
5
10
15
20
GAMMA DOSE (krad)
5 Gpp
3.2 Gpp
1 Gpp
0.5 Gpp
0.2 Gpp
AD=19.0
AD=18.3
AD=18.9
AD=18.6
AD=19.1

that interferes with the trapped electron signal at g = 2.0015. This additional peak (Fig. 4.8) is attributed to alanine radicals (Ikeya, 1981) and can be detected in tooth enamel at lower modulation amplitudes (eg. 0.5 Gpp).

Hennig and Grün (1983) found that the AD of certain speleothem samples can be dependent on the microwave power generated by the klystron. The AD of an enamel sample determined at variable microwave powers, reveals that AD is not influenced by microwave power (Fig. 4.9). Other experiments (Grün, 1985) showed saturation effects of enamel at a microwave power of about 6 mW and hence, it is advisable to use a lower microwave power of 2 mW or less.

4.4 SIGNAL FADING AND BLEACHING

Anomalous fading (ie. other than thermal) has been observed in TL investigations of certain minerals (Wintle, 1977). To test for abnormal fading, Grün and Invernati (1985) irradiated a recent elephant tooth with a gamma dose of 10 krad. One year after irradiation the enamel sample was prepared for AD determination. The derived AD of 10.5 krad indicates that anomalous fading can be neglected.

At Empress, Alberta, a majority of samples were found lying on the surface, exposed to sunlight. The AD of two

FIG. 4.8. ESR signal of a natural and 20 krad irradiated enamel sample. A modulation of 0.5 Gpp is used to differentiate the alanine signal from the free electron signal ($g_{\perp}$).

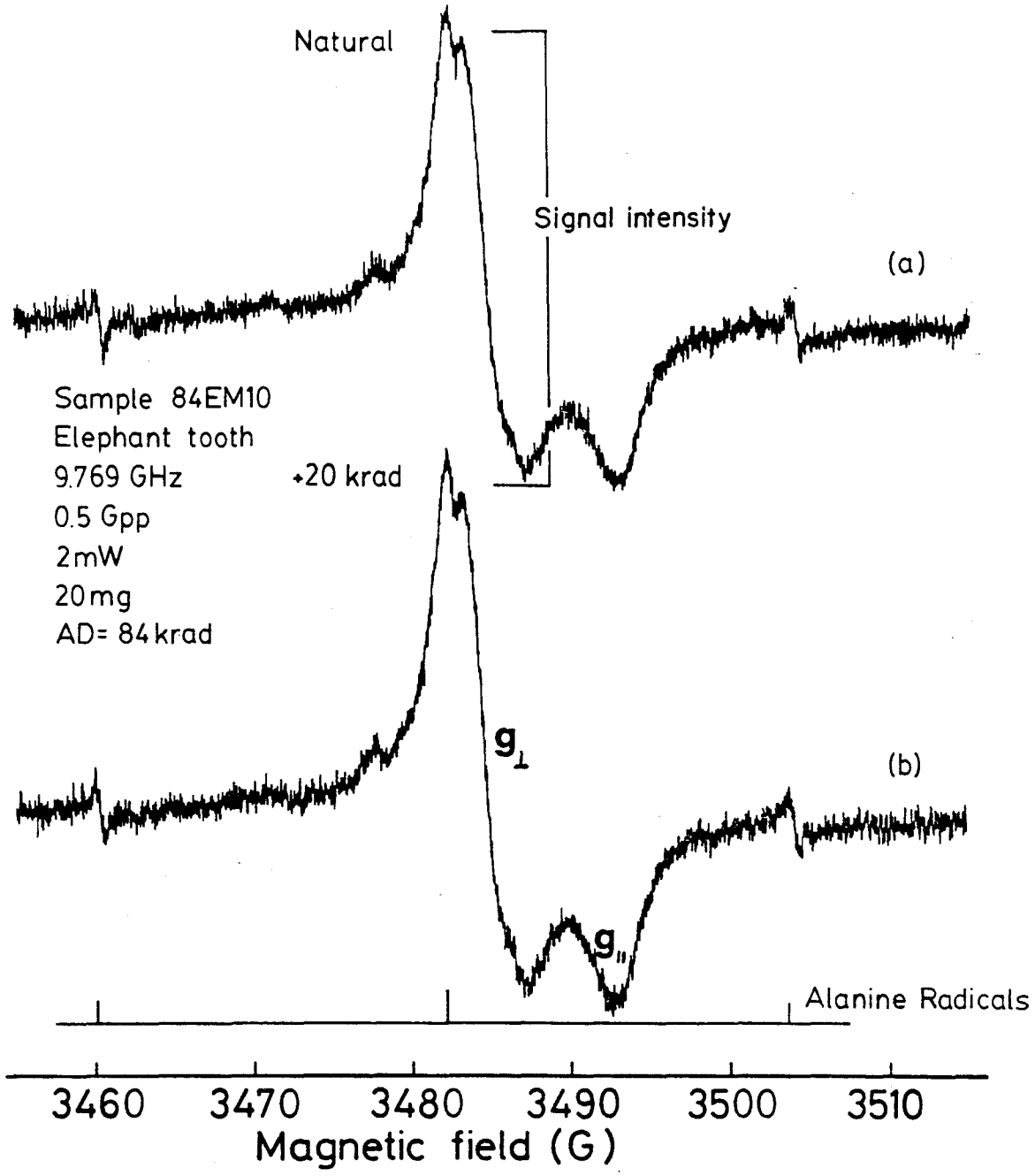
Natural
Signal intensity
(a)
Sample 84EM10
Elephant tooth
9.769 GHz
0.5 Gpp
2mW
20mg
AD= 84krad
+20 krad
$g_\perp$
(b)
$g_{\parallel}$
Alanine Radicals
3460
3470
3480
3490
3500
3510
Magnetic field (G)

FIG. 4.9. Dependence of AD on microwave power.

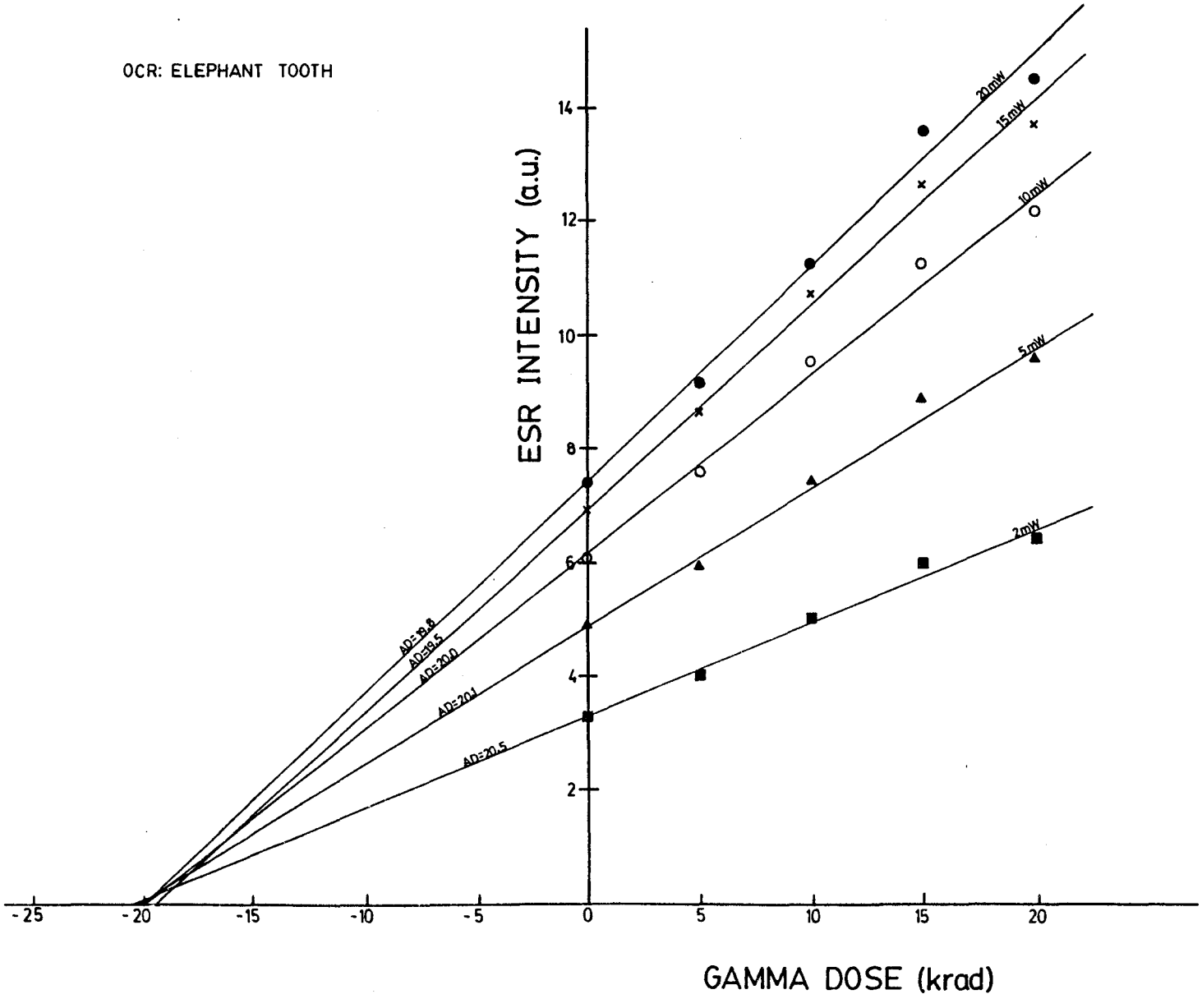
OCR: ELEPHANT TOOTH
ESR INTENSITY (a.u.)
GAMMA DOSE (krad)
20mW
15mW
10mW
5mW
2mW
AD=19.8
AD=19.5
AD=20.0
AD=20.1
AD=20.5
14
12
10
8
6
4
2
-25
-20
-15
-10
-5
0
5
10
15
20

exposed samples (84EM5: AD = 4.51 krad; 84EM8: AD = 6.68 krad) do not show any marked difference from a buried sample (84EM4a: AD = 5.22 krad). This indicates that for enamel, the ESR signal at g = 2.0015 is not affected by bleaching and therefore sample preparation and analysis may be carried out under normal light conditions.

4.5 EFFECT OF FLUORINE AND CARBONATE CONTENT

With time, fluorine ions are taken up by hydroxyapatite, displacing the OH^- radical in the molecule. The process is dependent upon the removal of part of the organic component so that the apatite molecule is accessible to groundwater (Molleson, 1981). Ikeya (1985) believes that an increase of fluorine content in bone will result in a lower AD determination. Gilinskaya et al. (1971), Cevc et al. (1972) and Sato (1979) concluded that the ESR signal (g = 2.0015 in this study) of tooth enamel is due to paramagnetic CO_3^{3-} centers at PO_4^{3-} sites in the apatite structure. Since fluorine uptake involves exchange with OH^- radicals, it is not clear how this would effect the AD.

The relationship between ESR sensitivity and CO_3/PO_4 ratio in tooth enamel is shown in Fig. 4.10. If the ESR signal is associated with CO_3^{3-} centers, then samples with lower CO_3/PO_4 ratios are expected to saturate at lower doses.

FIG. 4.10. Dependence of ESR sensitivity on the CO_3/PO_4 ratio of tooth enamel.

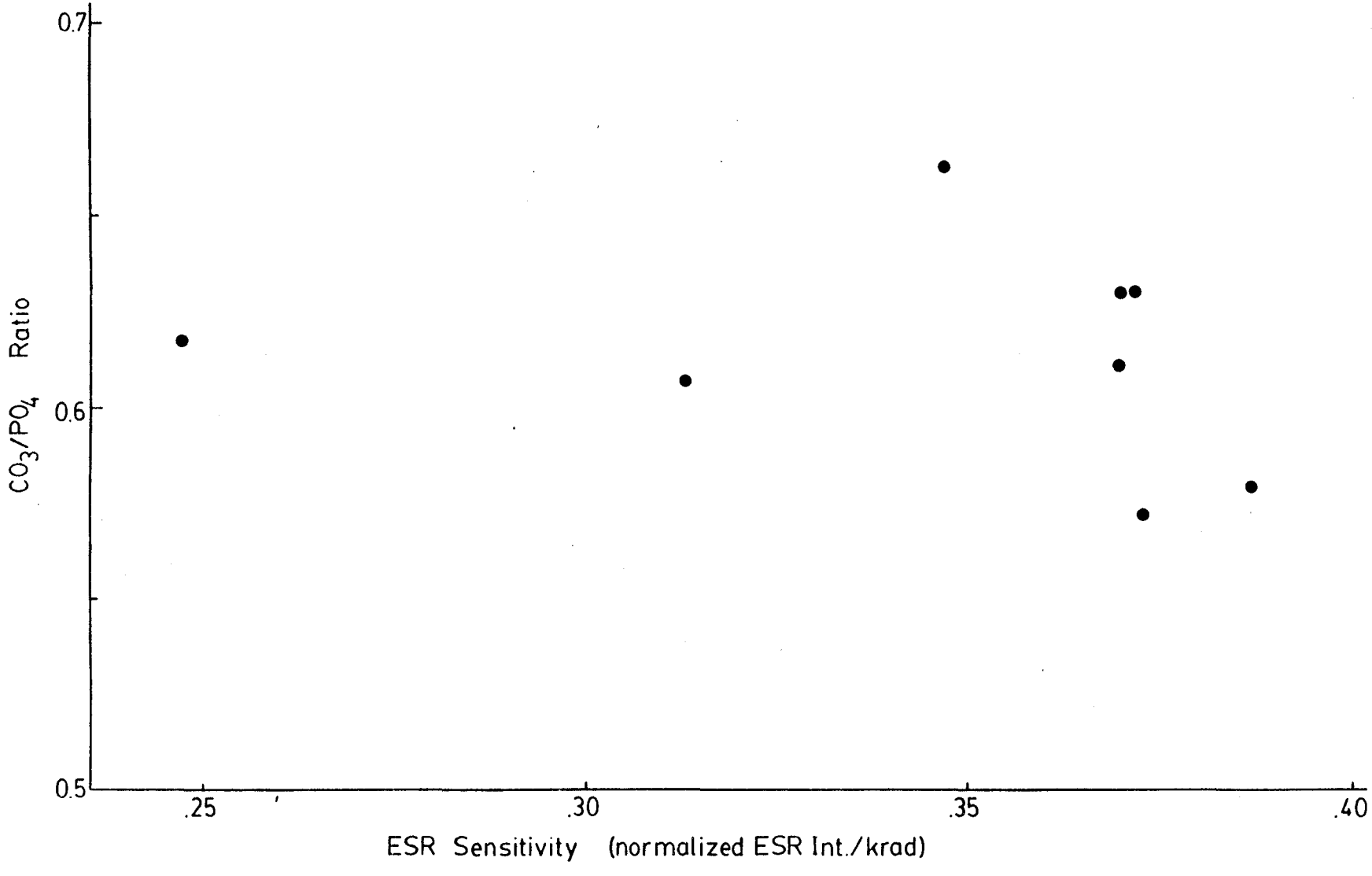
0.7
0.6
0.5
CO_3/PO_4 Ratio
.25
.30
.35
.40
ESR Sensitivity (normalized ESR Int./krad)

However, a decrease in ESR sensitivity with a corresponding decrease in CO_3/PO_4 in enamel is not observed (Fig. 4.10). Since CO_3 in hydroxyapatite can replace both PO_4^{3-} and OH^-, it is not certain whether the CO_3 groups at OH^- sites are paramagnetic. The comparison between CO_3(total)/PO_4 ratio and ESR sensitivity is therefore not a good test for determining the paramagnetic nature of CO_3^{3-} centers.

4.6 STABILITY OF ELECTRON TRAPS

The mean-life (τ) of trapped electrons exposed to a temperature T (^oK) is give by,

$$\tau = s^{-1}\exp(E_a/kT) \qquad (4.1)$$

where k is the Boltzman's constant (8.617×10^{-5} eV/^oK), E_a (eV) is the activation energy required to release the electrons from their traps (ie. trap depth, see Fig. 2.1), and s (sec^{-1}) is the frequency factor which expresses the attempts of the trapped charges to escape.

The mean-life can be determined by isothermal annealing experiments, where several aliquots of enamel are heated at different temperatures. For each annealing temperature, the ESR intensity (I) is recorded with increasing time (t) (Fig. 4.11a). At $I_{1/2}$ the half-life ($t_{1/2}$) is determined. The mean-life (τ) of trapped electrons at a temperature T is given by the expression,

FIG. 4.11. a) Determination of mean-life (τ) by isothermal annealing experiments.

b) Arrhenius plot of mean-life obtained by isothermal annealing experiments. Linear extrapolation of the experimental mean-lives gives the estimated mean-life at environmental temperatures.

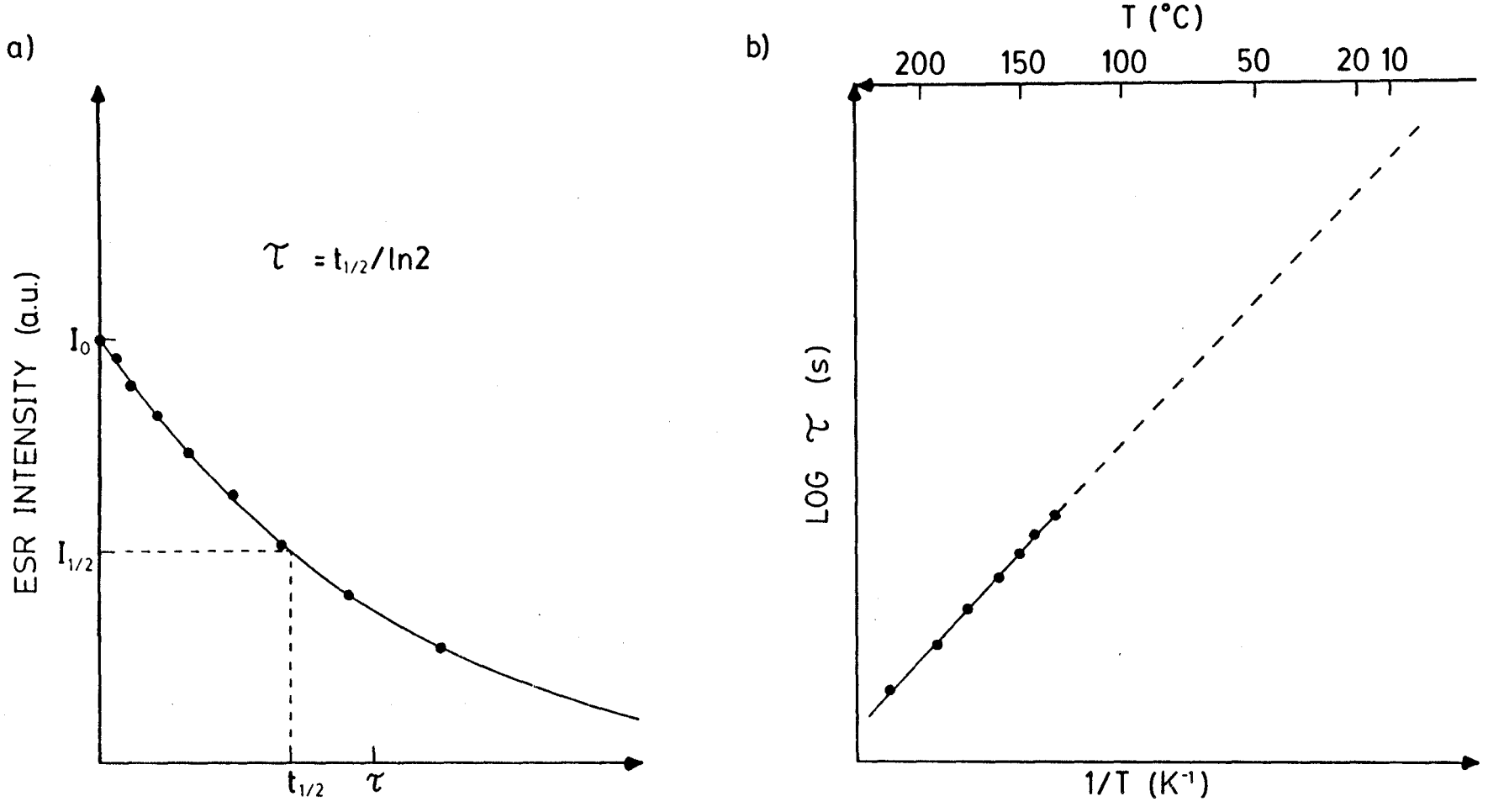
a)
ESR INTENSITY (a.u.)
$\tau = t_{1/2}/\ln 2$
I_0
$I_{1/2}$
$t_{1/2}$
τ
b)
T (°C)
200
150
100
50
20
10
LOG τ (s)
1/T (K^{-1})

$$\tau(T) = t_{1/2}/\ln 2. \qquad (4.2)$$

An Arrhenius plot of log (τ) vs 1/T should then yield a linear relation (Fig. 4.11b). The mean-life of the sample at normal environmental temperatures can then be calculated by extrapolation.

For enamel, the mean-life is difficult to determine because the signal is very stable at low temperatures (Hennig and Grün, 1983), eg. holding a sample for two weeks at 140 °C has very little effect on signal intensity. An accurate determination of the mean-life would therefore involve very long laboratory time intervals. A second problem is that at elevated temperatures, the ESR signal begins to change its form (split), which can lead to inaccurate measurements of the signal intensity.

Isothermal annealing experiments on apatite (bone) by Ikeya (1985) resulted in a mean-life estimate of 10 Ma. Well within this estimate, is a 3 Ma ESR age estimate on a fossil tooth which agrees favourably with the expected geological age (Grün, unpublished). It appears that for Pleistocene age fossil teeth exposed to normal environmental temperatures, the trapped electrons can be considered stable.

CHAPTER 5

DETERMINATION OF THE ANNUAL DOSE

5.1 DOSE RATE

The dose rate is defined as dose per unit time. In ESR dating, the term annual dose is used and is measured in rads (or millirads, mrad) per year. The radiation dose a sample receives over geologic time originates from alpha, beta and gamma particles emitted by the radionuclides of U and Th decay chains and by ^{40}K present in the surrounding environment and in the sample. If the samples were lying on or near the surface for extensive time periods, then gamma ray contribution by cosmic radiation must also be considered.

The uranium content of enamel and dentine/cementum was determined by delayed neutron activation analysis (DNAA). The surrounding matrix was also analysed for U and Th by DNAA and for K by XRF. Table 5.1 (Hennig and Grün, 1983) is used to convert the concentration levels of the radioactive elements to alpha, beta and gamma dose rate values. Similar radiation dose rate data was determined by Bell (1976, 1977 and 1979). New dose rate values calculated by Nambi and Aitken (pers. comm., 1985) do not show great deviations (<5%) from Table 5.1.

Determination of the annual dose for tooth enamel usually consists of 3 separate dose rate calculations; the environmental (EDR), the dentine (DDR) and the internal (enamel,

TABLE 5.1. Dose rates (in mrad/a) for 1 ppm of uranium series, 1 ppm of thorium series, 1% of potassium and 100 ppm of rubidium. (From Hennig and Grün, 1983).

Radioisotope or Decay Chain from-to (abund.)	α-energies (MeV)	α-dose rates (mrad/a)	β-energies (MeV)	β-dose rate (mrad/a)	γ-energies (MeV)	γ-dose rate (mrad/a)
^{238}U-^{206}Pb (0.9928)	42.866	267.60	2.2939	14.39	1.8634	11.64
^{234}U-^{206}Pb (0.9928)	38.681	241.48	1.4108	8.81	1.8041	11.26
^{230}Th-^{206}Pb (0.9928)	33.922	211.77	1.4108	8.81	1.7891	11.17
^{226}Ra-^{206}Pb (0.9928)	29.264	182.69	1.3938	8.73	1.7885	11.16
^{222}Rn-^{206}Pb (0.9928)	24.489	152.88	1.3956	8.70	1.7795	11.11
^{235}U-^{207}Pb (0.0072)	41.776	12.16	1.2011	0.35	0.5740	0.17
^{231}Pa-^{207}Pb (0.0072)	37.386	10.89	1.075	0.31	0.4104	0.12
Both U-Decay Series (1.0)		279.76		14.67		11.81
^{230}Th-^{208}Pb	35.398	73.74	1.4061	2.89	2.427	4.98
Potassium (^{40}K = 0.01167)						
1% K_2O			0.603 (0.89)	68.93	1.461 (0.11)	20.69
1% K				83.03		24.92
100 ppm Rubidium				4.64		

IDR) contribution. The effective penetration range of alpha, beta and gamma particles, approximately 25 micrometers, 2 mm and 30 cm respectively (for sample density of 2.7 g/cm^3) (Aitken, 1974), must also be considered in the dose rate calculations.

5.2 ENVIRONMENTAL DOSE RATE (EDR)

The environmental dose rate (EDR) is determined from the U, Th and K content of the surrounding matrix. Since the effective range of gamma rays is considerably greater than the thickness of the samples, gamma ray attenuation by the sample can be neglected. Beta particle contribution to EDR is dependent on sample geometry and is discussed in detail in chapter 5.5. Since the outer 100 micrometers of enamel is shaved away, alpha particle contribution from the surrounding matrix can be neglected.

The $^{234}U/^{238}U$ and $^{230}Th/^{234}U$ activity ratios of sediments from 3 different sites (of different ages) are all near 1.0, indicating the U-decay chain is in equilibrium. Beta and gamma dose rates for the entire U chain (Table 5.1) are therefore used.

At ground level, cosmic rays contribute 30 mrad/a to the dose rate and at a depth of 2 m it decreases to a level of 15

mrad/a. The cosmic ray dose rate (CDR) at a depth x (cm) can be calculated by the equation of Yokoyama et al. (1982),

$$CDR = 5.2 \exp(-x\rho/20) + 12.1 \exp(-x\rho/160) + 12.5 \exp(-x\rho/2500) \quad (5.1)$$

where ρ is the density (g/cm^3) of the matrix. Since all samples were buried at depths of several meters, cosmic ray contribution was considered negligible. Contribution from rubidium, radiocarbon and other radioactive elements is also negligible when compared to the dose rate originating from U, Th, K and their daughter products.

5.3 DENTINE DOSE RATE (DDR)

Most of the tooth fragments were buried with dentine/cementum still attached to the enamel. Dentine in living animals contains virtually no uranium. The fossilized dentine however, contains 4.2 to 1820 ppm U. Charalambous and Papastefanou (1977) found that the radioactivity in fossil bones is only due to the radionuclides of the uranium series. Radionuclides of the thorium series and ^{40}K are absent and can therefore be neglected.

The number of gamma rays emanating from U within the dentine, compared to that from the surrounding environment (ie. 30 cm effective radius) is very small. Its effect on enamel can therefore be considered negligible. Since the outermost 100 micrometers of enamel is shaved away, alpha

particles from dentine/cementum do not contribute to the dose rate. Only beta particles, which have an average effective range of approximately 2 mm, must be considered when determining the dentine's contribution (DDR) to the dose rate. The overall beta contribution is dependent on sample geometry and is discussed in chapter 5.5.

5.4 INTERNAL DOSE RATE (IDR)

Uranium concentration levels in the enamel range from 0.3 to 28.8 ppm. The internal dose rate (IDR) is dependent entirely on alpha and beta particles emitted by radionuclides of the U-decay chains. As for dentine, the gamma ray contribution can be neglected. The alpha efficiency or k-factor (ie. the effectiveness of alpha dose to beta or gamma dose) is known to vary for different minerals. Grün and Invernati (1985) experimentally determined the k-factor for enamel to be 0.15. DeCanniere et al. (1986) also obtained an alpha efficiency factor of 0.15 ± 0.02 for mammoth tooth enamel. This value was used for all dose rate calculations.

For internal beta rays, a beta correction factor (G_I) is required, since some of the particles will penetrate through into the dentine and sediment. The correction factor is obtained from the following relationship,

$$G_I = 1 - G_E \qquad (5.2)$$

where G_E is the beta ray attenuation correction factor for external radiation (sediment and dentine). The derivation of G_E is discussed in chapter 5.5.

5.5 BETA DOSE ATTENUATION

Contribution to the dose rate by beta rays is strongly dependent on the sample geometry (ie. the spatial distribution of dentine with respect to the enamel) and the thickness of the enamel. Buried tooth fragments are usually found in one of the following three situations (Fig. 5.1):

1) A separate fragment of enamel, detached from dentine.
2) A tooth fragment with dentine/cementum attached to one side of the enamel.
3) A tooth fragment with dentine/cementum attached on both sides of the enamel.

Consideration of the sample geometry is essential for precise dose rate calculations. Usually the geometry of a sample is such that the U concentration is different on either side of an enamel layer. It is therefore advisable to consider each side of the enamel separately and then sum the beta contributions to the total dose rate.

FIG. 5.1. Tooth fragments within a sediment can be found in three different configurations.

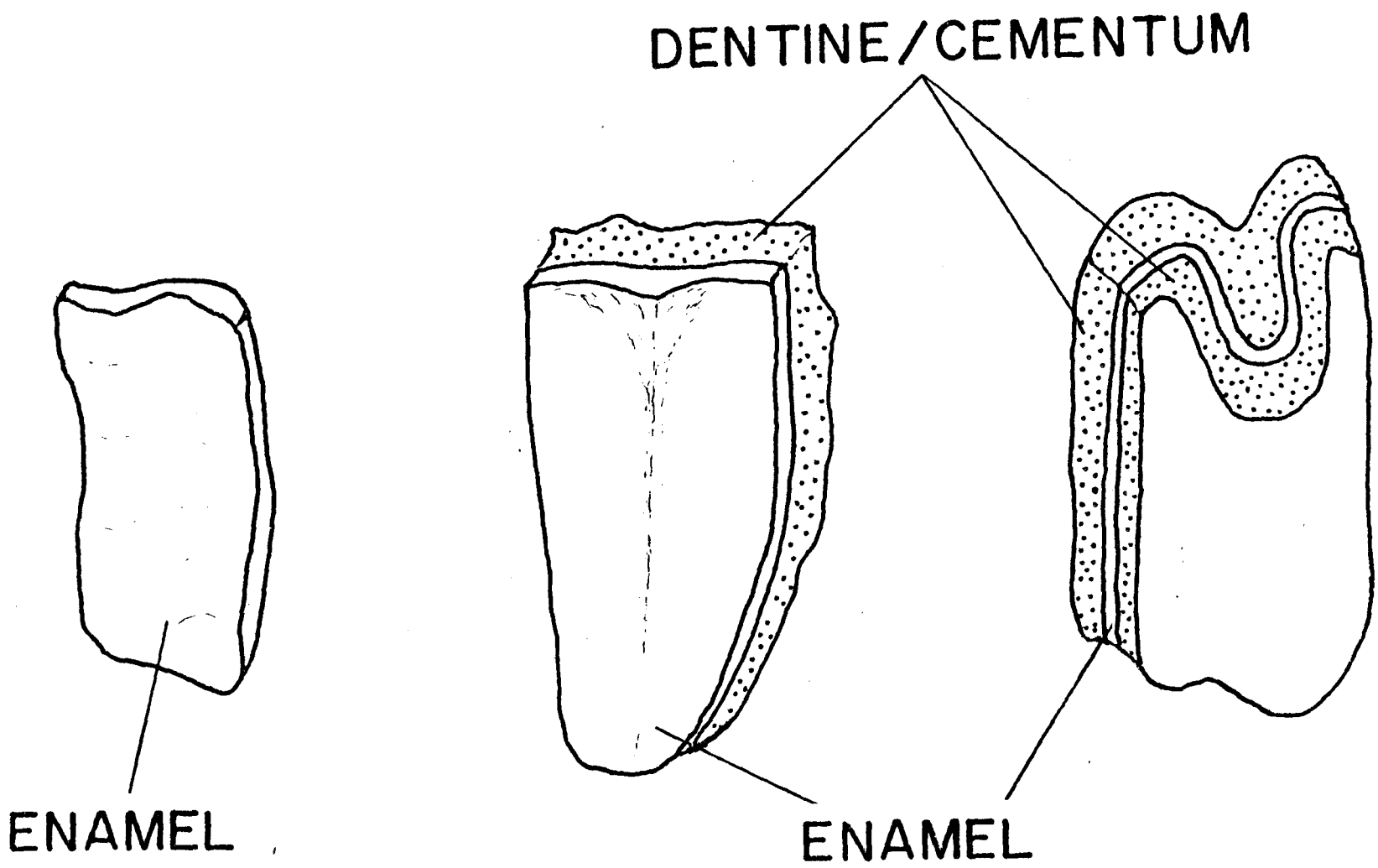

SEDIMENT

Yokoyama et al. (1982) and Grün (1986) proposed a simplified model for determining the beta ray attenuation factor for external radiation. Such a model has to be applied because the range of the beta particles from the sediment and/or dentine is comparable to the thickness of the shell or enamel analysed. The effective beta range P (cm) of a beta particle with maximum energy E_{max} (MeV) penetrating into a sample of density ρ (g/cm^3) is,

$$P = 0.0825((1 + 22.4E_{max}^2)^{-0.5} - 1)/\rho \quad . \qquad (5.3)$$

For external beta rays, the attenuation correction factor G_E, is the fraction of the total beta dose that is received by an enamel sample of thickness d (cm). It can be calculated using the following equation (for 2π geometry),

$$G_E = 0.5\ (1 - \exp(\mu d))/(\mu d) \qquad (5.4)$$

where μ is the attenuation coefficient per cm ($\mu = 3.3P$). The beta correction factor for an enamel sample where a thickness x (cm) has been removed from the total thickness d is (Aitken et al., 1985; Grün, 1986),

$$G_E(d-x) = [0.5/(\mu(d-x))][\exp(-\mu x) - \exp(-\mu d)]. \qquad (5.5)$$

The integral beta dose D received by an enamel layer subjected to a beta source of infinite matrix dose D_o is,

$$D = G_E \times D_o. \qquad (5.6)$$

Within a given decay chain there are several beta emitters (ie. beta decays). Each beta emitter can have several

transitions with a definite frequency f of occurence. When observing a large number of transitions, the beta particles have an energy distribution ranging from zero up to some maximum value (E_{max}) (Martin and Blichert-Toft, 1970). A beta transition to a particular energy level is characterized by E_{max} and the average energy (E_{av}) of the emitted beta particles.

For each beta emitter within a decay chain, the beta correction factor G_{EB} is,

$$G_{EB} = \sum_{T=1}^{n} G_{E(T)} \cdot f_T \cdot E_{av(T)} / \sum_{T=1}^{n} E_{av(T)} \qquad (5.7)$$

where n represents the total number of transitions. For the entire decay chain, the beta correction factor G_{EC} is,

$$G_{EC} = \sum_{b=1}^{N} G_{EB(b)} \cdot f_b \cdot E_{av(b)} / \sum_{b=1}^{N} E_{av(b)} \qquad (5.8)$$

where N represents the total number of beta emitters. The integral beta doses obtained by the above method are shown in Fig. 5.2. For U and Th decay chains, the results agree favourably with the experimental attenuation curves of Aitken et al. (1985). For K, there are at present no experimental attenuation curves to compare with.

The beta ray contribution from sediment can be derived directly from Fig. 5.2, assuming the decay chains are in equilibrium. Dentine/cementum however, accumulates uranium after deposition. Hence the ^{238}U decay chain in dentine will display $^{230}Th/^{234}U$ disequilibrium. Fig. 5.3 shows that the

FIG. 5.2. Integral beta doses in samples (2π geometry) for ^{40}K, ^{238}U, ^{235}U and ^{232}Th decay chains. (Grün, 1986).

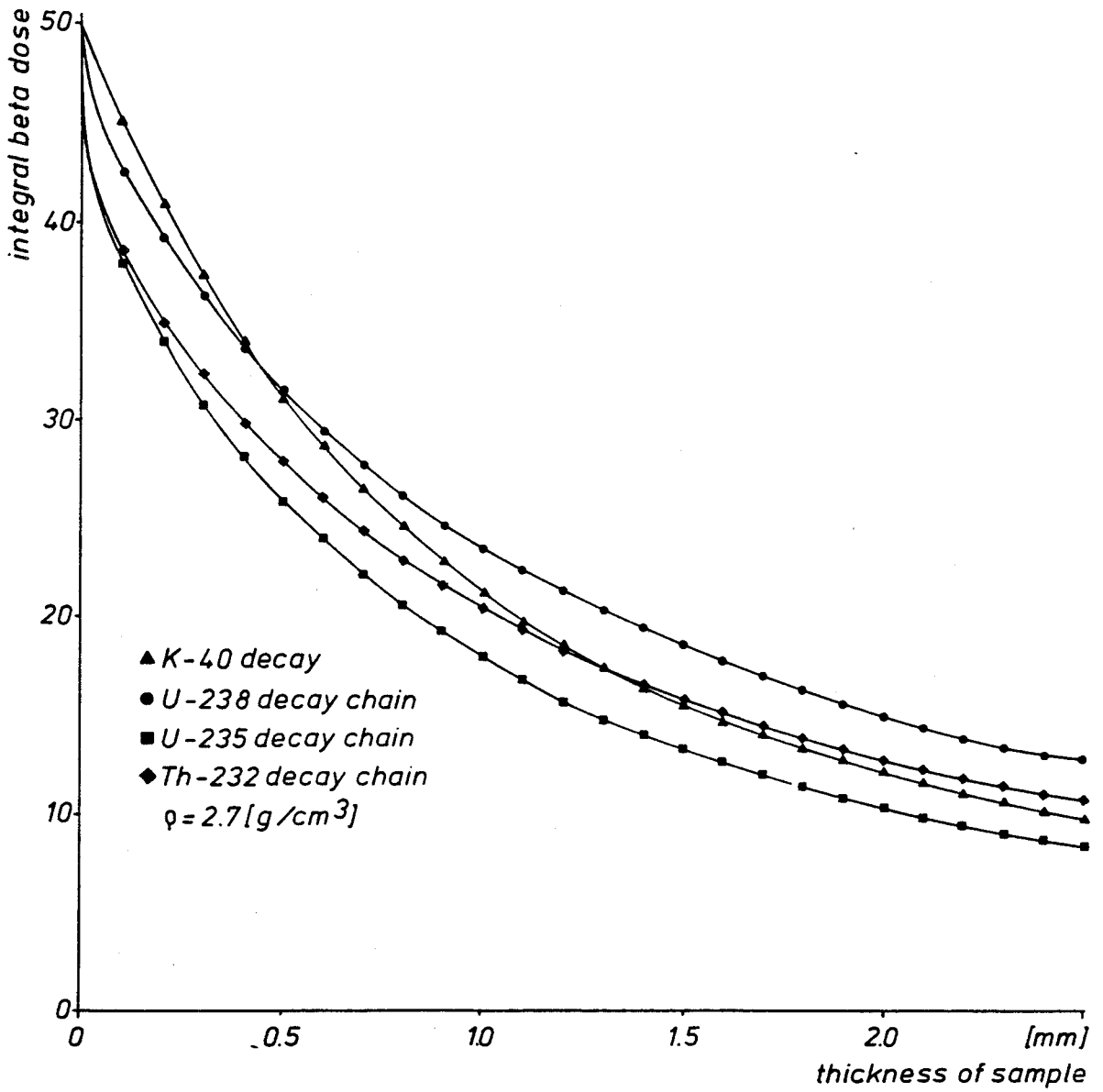
integral beta dose
50
40
30
20
10
0
0
0.5
1.0
1.5
2.0
[mm]
thickness of sample
▲ K-40 decay
● U-238 decay chain
■ U-235 decay chain
◆ Th-232 decay chain
ρ = 2.7 [g/cm3]

FIG. 5.3. Integral beta doses in samples (2π geometry) for beta decays between ^{238}U - ^{230}Th & ^{230}Th - ^{206}Pb. (Grün, 1986).

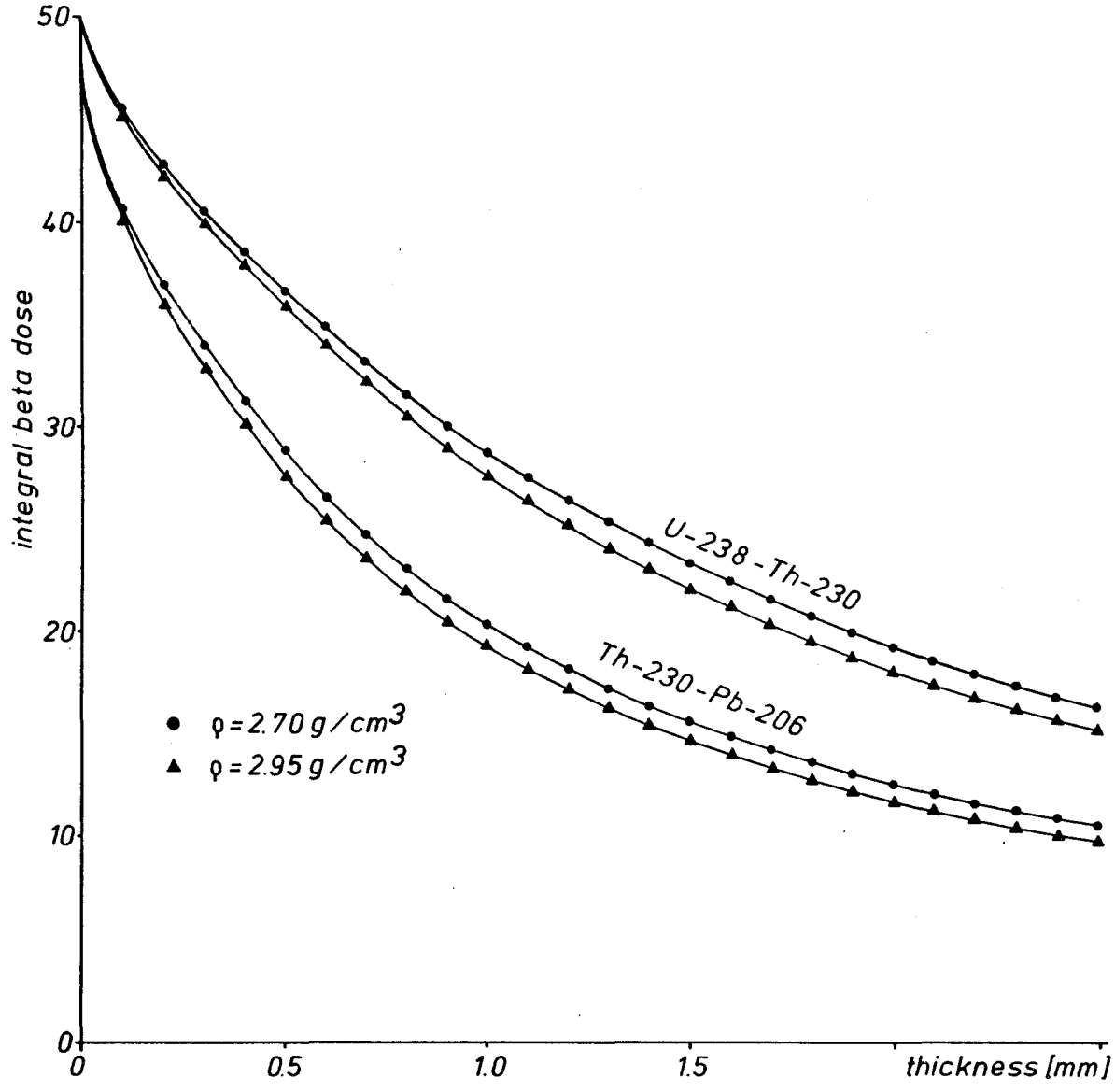
50
40
30
20
10
0
integral beta dose
0
0.5
1.0
1.5
thickness [mm]
U-238 - Th-230
Th-230 - Pb-206
● ρ = 2.70 g/cm3
▲ ρ = 2.95 g/cm3

integral beta doses produced by beta emitters from ^{238}U to ^{230}Th are significantly greater than those from ^{230}Th to ^{206}Pb (Grün, 1986). The $^{230}Th/^{234}U$ disequilibrium and corresponding different beta correction factors have to be considered for more precise beta dose rate calculations.

The integral beta doses received by a sample from the ^{232}Th, ^{238}U & ^{235}U decay chains and ^{40}K decay is summarized in Table 5.2. For the ^{238}U decay chain, values above and below ^{230}Th are given. It should be noted that this beta ray attenuation model represents a somewhat simplified approach because the shapes of beta spectra of single transitions may vary. Also, most of the thin enamel samples have rough surfaces of varying thickness, which makes it difficult to accurately determine the beta ray contribution.

5.6 WATER ATTENUATION FACTOR

Part of the alpha, beta and gamma energies can be absorbed by water, causing a reduction of the effective annual dose. A water attenuation factor must therefore be included in the dose rate calculation. The correction factor W_C is obtained from the following formula (Bowman, 1976),

$$W_C = (1 + H_C K/(1 - K))^{-1} \qquad (5.9)$$

where K is the water content (wt.%/100) of the enamel, dentine or sediment and H_C is a correction factor for the

TABLE 5.2. Integral beta doses (as percentage of the infinite matrix dose) for samples with densities of (a) 2.70 g/cm^3 - calcite, and (b) 2.95 g/cm^3 - hydroxyapatite/aragonite, irradiated from one side (2π geometry).

Thickness	Integral Beta Dose (%)									
(mm)	^{232}Th		^{238}U - ^{230}Th		^{230}Th - ^{206}Pb		^{235}U		^{40}K	
	a	b	a	b	a	b	a	b	a	b
0.02	42.8	42.6	48.7	48.6	44.8	44.7	43.2	43.0	49.0	48.9
0.05	40.3	40.6	47.4	47.2	43.1	42.9	40.6	40.3	47.5	47.3
0.1	38.6	38.2	45.6	45.3	40.8	40.4	37.9	37.5	45.2	44.8
0.2	35.1	34.5	42.9	42.5	37.0	36.3	34.0	33.3	41.1	40.3
0.3	32.3	31.6	40.6	40.0	33.7	32.9	30.9	30.1	37.4	36.5
0.4	29.9	29.1	38.5	37.8	31.0	30.0	28.2	27.4	34.2	33.0
0.5	27.9	27.0	27.3	35.7	28.6	27.6	26.0	25.0	31.4	30.2
0.6	26.4	25.1	34.8	33.9	26.5	25.4	23.9	22.9	28.8	27.6
0.8	23.0	22.0	31.6	30.5	23.0	22.0	20.6	19.5	24.7	23.3
1.0	20.5	19.5	28.8	27.6	20.3	19.3	17.9	16.9	21.3	20.0
1.2	18.4	17.4	26.4	25.1	18.1	17.1	15.7	14.7	18.7	17.4
1.4	16.6	15.7	24.2	23.0	16.4	15.4	14.0	13.0	16.5	15.3
1.6	15.2	14.2	22.3	21.1	14.9	13.9	12.5	11.6	14.7	13.6
2.0	12.8	11.9	19.2	18.0	12.5	11.7	10.3	9.5	12.1	11.1
2.5	10.6	9.8	16.2	15.0	10.5	9.7	8.3	7.7	9.8	8.9
3.0	9.0	8.3	13.9	12.8	8.9	8.3	7.0	6.4	8.2	7.5

energy absorption by water and has values of 1.49, 1.25 and 1.14 for alpha, beta and gamma rays respectively (Aitken, 1974). Some groups use $H_\gamma = 1.0$.

Teeth from living animals have a water content of 0.9 to 2.5% in enamel, 8 to 16% in dentine and up to 32% in cementum (Weatherell and Robinson, 1973). During fossilization, inorganic minerals present in solutions which enter the samples from the exterior will precipitate, filling in any internal voids (Badone and Farquhar, 1982). Fossilized samples can therefore be considered to have a negligible water content.

The water content of the surrounding sediment depends on the nature of the sediment (eg. clay, sand, gravel) and the degree of cementation and compaction. Since the sediment samples had dried to some extent between the time they were collected and analysed, the water content was not determined. A water content of 10 wt% (20% by volume) was therefore assumed for all sediment samples. Although this value may have a high degree of error, its effect on the ESR age is not great. For an arbitrary sample, Table 5.3 demonstrates that a sediment with a water content of 20 ± 10 wt.% (40 ± 20% by vol.) implies an uncertainty of only 3.8% in the ESR age. It should be noted that the water content may have fluctuated in the past. But as Table 5.3 demonstrates, the uncertainty of the water content will only lead to small errors in the ESR age.

TABLE 5.3. Dependence of the error in the ESR age on the uncertainty in the water content of the sediment.

For an arbitrary sample:

AD = 10 krad

U = 1 ppm in enamel

U = 100 ppm in dentine

$^{234}U/^{238}U = 1.5$

k = 0.15

Sediment has: U = 2 ppm

Th = 6 ppm

K_2O = 1.6%

Water Content (wt. %)	Uncertainty of Water Content (%)	Error in ESR Age (%)
20	±10	0.7
	±20	1.5
	±40	3.1
	±50	3.8
	±60	4.6
	±80	6.1
	±100	7.6

5.7 RADIUM AND RADON LOSS

^{226}Ra and ^{222}Rn deficiencies in fossil bones have been reported by a number of authors (eg. Charalambous and Papastefanou, 1977; Ikeya, 1982; Yokoyama et al., 1982). Due to the high geochemical mobility of radium, it can be leached out from samples by percolating water. Chemically inert radon gas can escape by diffusion. In terms of dose rates, ^{226}Ra leaching can be treated the same as ^{222}Rn loss, since the difference between the nuclides is the emission of only one alpha particle. No separate correction for the loss of ^{226}Ra has been made. The effect of 50% loss of ^{226}Ra would be comparable to that of ^{222}Rn loss; in fact it is unlikely that more than a few percent of ^{226}Ra would be lost from the relatively compact dentine, or from enamel.

In most cases, the uranium concentration in the samples is considerably higher than in the surrounding sediment. ^{222}Rn loss from dentine (and enamel, if it has a high U concentration) should therefore be incorporated in the dose rate calculation. Failure to do so can result in an overestimate of the annual dose. Charalambous and Papastefanou (1977) calculated radon loss in fossil bones to range from 30 to 65%. Since enamel and dentine have a lower porosity than bone, the dose rate calculations are based on no radon loss as well as a continuous radon loss of 50%. Radon

loss from the surrounding sediment can be neglected, since the thick sequences can be considered to behave as closed systems.

5.8 URANIUM DISEQUILIBRIUM

During fossilization, uranium is incorporated into dentine/cementum and enamel. The ^{230}Th and ^{231}Pa radionuclides are not fixed with uranium since they are insoluble in water which percolates through the sediment. Samples of Quaternary age will therefore exhibit some degree of disequilibrium, particularly with regard to ^{234}U, ^{230}Th and ^{231}Pa. Dose rate corrections must be applied to the U-decay chains to take into account any excess ^{234}U and deficient ^{230}Th and ^{231}Pa. The annual dose therefore becomes time dependent, increasing according to the growth of uranium daughter nuclides (Fig. 5.4).

For enamel and dentine, the dose rate D(t) (ie. IDR(t) and DDR(t)) can be calculated using a modified equation of Ikeya (1982 & 1985),

$$D(t) = D_{238} + D_{235} + D_{234}(r_o - 1)\exp(-\lambda_{234}t) - D_{231}\exp(-\lambda_{231}t) - D_{230}[1 - (^{230}Th/^{238}U)_t] \quad (5.10)$$

where t is the time since formation, D_{238}, D_{235}, D_{234}, D_{231} & D_{230} are the effective dose rates of the U-series decays from ^{238}U to ^{206}Pb, ^{235}U to ^{207}Pb, ^{234}U to ^{230}Th, ^{231}Pa to ^{207}Pb & ^{230}Th to ^{206}Pb respectively, and r_o is the initial $^{234}U/^{238}U$

FIG. 5.4. Increase with age of the average annual dose by the uranium series radionuclides for 1 ppm U. ^{238}U = 99.28%, ^{235}U = 0.72%, $(^{230}Th/^{234}U)_0$ = 0, $(^{231}Pa/^{235}U)_0$ = 0, and $(^{234}U/^{238}U)_0$ = 1.0.

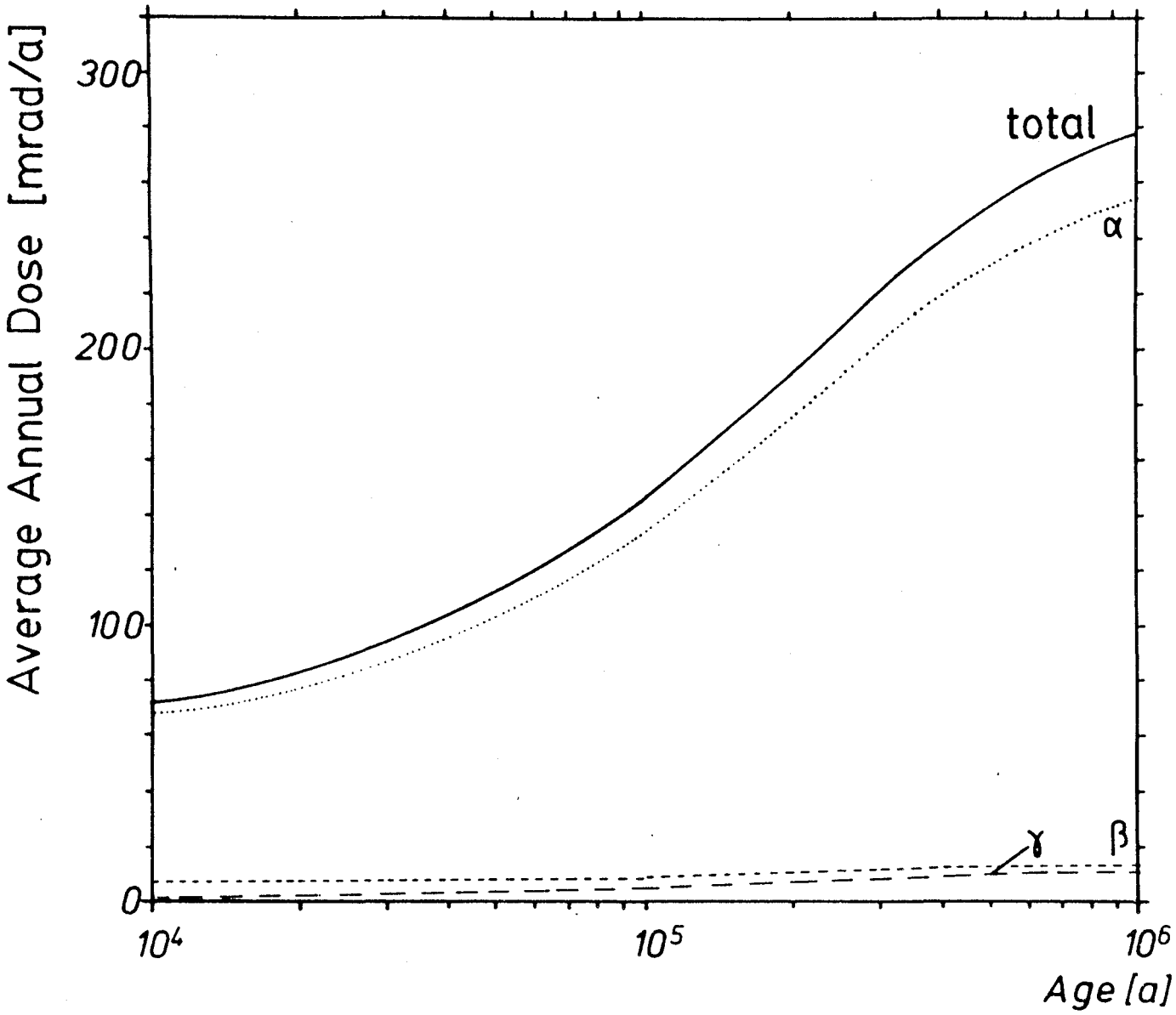
Average Annual Dose [mrad/a]
300
200
100
0
total
α
γ
β
10⁴
10⁵
10⁶
Age [a]

activity ratio. To avoid measurement of the $^{230}Th/^{238}U$ activity ratio, equation 5.10 can be rewritten as,

$$D(t) = D_{238} + D_{235} + D_{234}(r_o - 1)\exp(-\lambda_{234}t) - D_{231}\exp(-\lambda_{231}t)$$
$$-D_{230}(\exp(-\lambda_{230}t) - (r_o - 1)[\exp(-\lambda_{234}t) - \exp(-\lambda_{230}t)]\lambda_{230}/(\lambda_{230} - \lambda_{234})). \quad (5.11)$$

The first two terms of the equation are due to ^{238}U & ^{235}U alone, the third term to excess of ^{234}U, and the fourth and fifth terms to insufficient buildup of ^{231}Pa & ^{230}Th.

Equation 5.11 contains two unknowns, the initial $^{234}U/^{238}U$ activity ratio (r_o) and the time t. From the Medicine Hat area, the $^{234}U/^{238}U$ ratio of 8 bone samples ranging in age from 11,000 to >200,000 a, have an average value of 1.41±.08 (Szabo et al., 1973). An initial $^{234}U/^{238}U$ ratio of 1.41 is therefore assumed and used in all age calculations. The time t is calculated iteratively and is discussed in chapter 5.10.

5.9 URANIUM ACCUMULATION

The fossil teeth in this study have uranium concentrations ranging from 4.2 to 1,820 ppm in dentine/cementum and 0.3 to 28.8 ppm in enamel. One of the main problems in the attempt to date these samples lies in determining the nature of uranium uptake during fossilization. The two most frequently used models are based on either rapid uranium uptake shortly after deposition of the tooth or continuous, linear

uranium accumulation during the total burial history. The annual dose is strongly dependent on the model used and can result in a deviation of the ESR age by a factor of 2.

A comparison of U-series and ^{14}C ages of 8 bone samples from varied geological environments, indicates that the average time lag for U uptake is about 2,700 a (Szabo, 1980). Concordant ^{230}Th and ^{231}Pa dates obtained on several samples from the Medicine Hat area (Szabo et al., 1973) indicates that after U fixation, the bones behaved as closed systems. U-series dating of fossil teeth by McKinney (1978) also suggests early U uptake in enamel. Dentine and bone, however, gave anomalous U-series ages, suggesting open system behaviour.

A study of the radioactivity of fossil bones of various geological ages was carried out by Charalambous and Papastefanou (1977). Their results show that older Pliocene to Upper Miocene bones have throughout a higher U content than younger samples of Holocene to Pleistocene age. This suggests that U uptake may be a continuous process. It also indicates that Pleistocene samples have not reached saturation and are still able to accumulate uranium. Similar results were reported by Hennig and Grün (1983). Ikeya (1982) also noted that more comparable ESR ages for bones can be obtained if a linear uranium accumulation model is used.

In this thesis, dose rate calculations for models of both early and continuous linear uranium accumulation will be used.

5.10 EARLY URANIUM UPTAKE MODEL

For samples which accumulate uranium very early and subsequently remain as closed systems, the dose rate D(t) can be calculated using equation 5.11. The U uptake is assumed to be instantaneous in both the enamel and dentine. The total dose TD_E can be obtained by integrating D(t) from t = 0 to t = T,

$$TD_E = \int_0^T D(t)dt. \qquad (5.12)$$

TD_E can now be expressed as,

$$\begin{aligned} TD_E = {} & D_{238}T + D_{235}T + D_{234}(r_0 - 1)(1 - \exp(-\lambda_{234}T))/\lambda_{234} \\ & - D_{231}(1 - \exp(-\lambda_{231}T))/\lambda_{231} - D_{230}((1 - \exp(-\lambda_{230}T))/\lambda_{230} \\ & - (r_0 - 1)[1 - (\lambda_{230}\exp(-\lambda_{234}T) - \lambda_{234}\exp(-\lambda_{230}T))/(\lambda_{230} - \lambda_{234})]/\lambda_{230}) \end{aligned} \qquad (5.13)$$

where the symbols have the same meaning as in equation 5.10. For enamel,

$$TD_E = \left(\sum_{i=1}^{3} TD_{E(i)}\right) + EDR \cdot T \qquad (5.14)$$

where TD_{E1}, TD_{E2}, TD_{E3} and $EDR \cdot T$ correspond to the total dose fraction received from dentine layer 1, dentine layer 2, enamel and the surrounding environment respectively.

The age T (a) of the sample is derived by iterating equation 5.14 until TD_E is equal to the experimentally derived AD. The calculation is easily carried out with a

computer program (Appendix II). The program takes into account all the dose rate parameters discussed in chapter 5.

5.11 CONTINUOUS LINEAR URANIUM UPTAKE MODEL

If uranium accumulation in both dentine and enamel progressed in a continuous, linear manner, then the total dose TD_L can be expressed as (Ikeya, 1982),

$$TD_L = (C_u/T) \int_0^T TD_E(t)dt \qquad (5.15)$$

where C_u is the present uranium concentration. Incorporating C_u into D_{238}, D_{235}, D_{234}, D_{231} & D_{230} and integrating the equation gives,

$$TD_L = D_{238}T/2 + D_{235}T/2 + D_{234}(r_0 - 1)[1 - ((1 - \exp(-\lambda_{234}T))/(\lambda_{234}T))]/\lambda_{234} \qquad (5.16)$$
$$- D_{231}[1 - ((1 - \exp(-\lambda_{231}T))/(\lambda_{231}T))]/\lambda_{231} - D_{230}[[1 - ((1 - \exp(-\lambda_{230}T))/(\lambda_{230}T))]/\lambda_{230}$$
$$- (r_0 - 1)[1 - (\lambda^2_{230}(1 - \exp(-\lambda_{234}T)) - \lambda^2_{234}(1 - \exp(-\lambda_{230}T)))/(\lambda_{230}\lambda_{234}T(\lambda_{230} - \lambda_{234})))]/\lambda_{234}\}.$$

Again, the age of the enamel sample is solved by iteration of equation 5.14 6

5.12 OTHER URANIUM UPTAKE MODELS

The continuous U uptake model assumes that uranium accumulation in fossil samples progressed in a linear manner (Ikeya, 1982). However, this may not be the case. Uranium accumulation could have been rapid at first and then increased more slowly. Or perhaps an "episodic" uptake should be considered, where uranium accumulation was con-

trolled by groundwater fluctuation (Hansen and Begg, 1970). It has also been proposed that uranium absorbed in the sample during the decay of organic material, is leached out by groundwater after the decay ceases (Seitz and Taylor, 1974; Badone and Farquhar, 1982). However, the data of Charalambous and Papastefanou (1977) and Hennig and Grün (1983) suggests that the U leaching stage is not reached for Pleistocene samples.

Each model will lead to a different average annual dose, which in turn affects the estimated ESR age. At present, it is impossible to determine the mode of continuous U uptake (ie. linear, exponential, episodic, etc.). However, the linear approach is easier to model and represents the "average estimate" of the other possibilities.

A few samples with extremely high U concentrations (>20 ppm in enamel and/or >800 ppm in dentine/cementum), yield very low ESR dates compared to the estimated ages. These samples could have accumulated additional uranium at a very late stage. The late U uptake would not have contributed to the average annual dose and its incorporation in the dose rate calculation can result in a gross underestimate of the ESR age. The relative merit of the various models may become more evident when comparing the ESR dates to independently estimated ages of the samples.

CHAPTER 6

ESR AGES OF TOOTH ENAMEL FROM ALBERTA AND SASKATCHEWAN

6.1 ANALYTICAL DATA

The analytical data for all samples is given in Appendix I. The ESR ages are based on this information and were calculated using both an early and a continuous, linear U uptake model. The ESR data for each site are given in Table 6.1 and are compared to what is known of the absolute age of each site with either ^{14}C or U-series dates of bone, fission track dates of volcanic ash or paleomagnetic, stratigraphic and faunal data. Beyond the ^{14}C dating range of approximately 30,000 a, these age estimates should be considered very approximate, as is evident from the large age discrepancies between these estimates at some sites. U-series ages are based on early uranium fixation and subsequent closed system behaviour in bone. They should therefore only be compared with the early uranium uptake ESR dates. All fission track dates should be considered as minima, given the susceptibility of tracks in volcanic glass to annealing.

The faunal assemblages at the various sites can in most cases be satisfactorily correlated with faunas found elsewhere in the continent. Assignment of absolute ages to these various faunas is more difficult, since the relation of land mammal ages to the subdivision of the Pleistocene, is at present uncertain. At some sites, difficulties can also arise in determining the age of the fauna because of inter-

TABLE 6.1. ESR data for teeth samples from Alberta and Saskatchewan. All ages are given in ka. ESR dates are based on the following models:
1) Early U uptake, no radon loss.
2) Early U uptake, 50% radon loss.
3) Continuous, linear U uptake, no radon loss.
4) Continuous, linear U uptake, 50% radon loss.
Independent age information is based on:
C = carbon-14 date,
F = fauna associated with teeth,
FT = fission track of ash beds,
M = paleomagnetism,
S = stratigraphic correlation,
US = uranium series age of bone.
* = ESR age based on estimation of one of the dose rate parameters.
** = ESR age based on external dose rate only.

Sample Locality And Number	AD (krad)	ESR Age (ka) 1	2	3	4
Lindoe Bluff	(C= 11.2±0.2; US= 9.5±1.5)				
84LN1	3.98	8.1	8.2	13.8	14.0
84LN3	3.61	12.4	12.7	18.3	18.5
84LN6	4.22	12.6	12.8	19.2	19.4
84LN6al	7.74	12.1	12.2	20.5	20.6
Average		11.3±1.8	11.5±1.9	18.0±2.5	18.1±2.5
Empress Site	(F,S= <80)				
84EM2*	5.27	34	35	41	42
84EM4a	5.22	36	37	44	45
84EM4e	4.95	26	26	38	39
84EM5	4.51	39	40	42	42
84EM8	6.68	34	35	44	46
Average		33.8±4.3	34.6±4.7	41.8±2.2	42.8±2.5
Older Samples:					
84EM4d	32.4	128	139	201	215
84EM9	145.8	652	652	845	845
84EM10	84.1	363	363	525	525
Reservoir Gully	(S= 18-25; F= <175; US= 73±6 & >64)				
84RG3	138.0	205	234	353	398

(continued)

Sample Locality And Number	AD (krad)	ESR Age (ka) 1	2	3	4
Galt Island	(C= >39; FT= 430±70; F,S= 45 "Mid Wisconsin")				
84GI6**	62.2	<349	<349	<349	<349
Mitchell Bluff	a: (US= >71 & 72±6; F= 80-130 "Sangamon")				
84MI9e	19.5	38	40	61	64
84MI9i	19.3	35	37	57	60
84MI11	34.1	50	53	84	89
Average		41±7	44±7	67±12	71±13
	b: (US= >162 & >200; F= 600-1000 "Kansan")				
84MI10	693.1	130	150	246	285
Riddell Site	(M= <730; FT,S= 600-700; F= 80-130 "Sangamon")				
84RS1	43.7	99	108	169	183
Surprise Bluff	(F,S= 400-600 "Yarmouthian")				
84SB4	95.0	139	148	238	251
Island Bluff	(F,S= 600-1000 "Kansan")				
84IB7	31.6	239	242	288	291
84IB9*	35.7	269	312	269	312
Average		254±15	277±35	279±10	302±11
Low Bluff	(F,S= 600-1000 "Kansan")				
84LB1	183.0	87	99	164	187
Bow Island	(F,S= ? preglacial)				
84BOW3**	18.0	<118	<118	<118	<118
Frisch Site	(F= >1000)				
84FR2	231.7	236	262	406	445
84FR4*	236.2	267	295	457	500
84FR6*	233.0	277	303	474	513
Average		260±18	287±18	446±29	486±30
Wellsch Valley	(F= >1500; combined FT & M= 1000-1600)				
84WV5	456.0	167	181	314	340

mingling of taxa that are usually found separate in time (Stalker and Churcher, 1982). Due to these problems, as well as other problems encountered in Quaternary stratigraphy (chapter 1.2.1), the age estimates based on faunal assemblages should be regarded as very approximate.

Lindoe Bluff

At Lindoe Bluff, ^{14}C and U-series ages are available to compare with the ESR data. Given a time period of approximately 2 to 3 thousand years for uranium fixation in bone after burial, the U-series age of 9.5 ka (Szabo et al., 1973) is in good agreement with the radiocarbon date of 11.2 ka. The ESR ages (average 11.3 ± 1.8 and 11.5 ± 1.9 ka) agree very well with the other two estimates, particularly for the early U uptake model. The samples also show good agreement within the ESR results. Sample 84LN6a1 is altered. However, the resulting age is in good agreement with the non-altered samples, which suggests that the AD was not affected by alteration (which probably happened recently). Based on these dates, Lindoe Bluff can be assigned to interglacial stage 1 (Fig. 1.3).

Empress Site

The Empress Site has not been dated by any absolute dating method. However, based on the fauna and its stratigraphic position, it is believed to be a relatively young

deposit, either latest Wisconsin (stage 2) or Mid-Wisconsin (stage 3) (A.M. Stalker and C.S. Churcher, pers. comm. 1984). ESR dates obtained on five samples are consistent with stage 3, regardless of the uptake model used. Three other samples give older results. The presence of numerous dinosaur bones in the same deposit suggests that the older samples represent recycled tooth fragments from earlier interglacial deposits.

Reservoir Gully

The 18 - 20 ka age estimate for Reservoir Gully is partly based on stratigraphic position. The faunal assemblage, particularly the presence of Mammuthus sp. and Equus conversidens (Mexican ass) (Stalker and Churcher, 1982), is typical of the Late Rancholabrean (<175,000). U-series dates suggest an age of >64 ka (Szabo et al., 1973) and the ESR estimate indicates an older age (>205 ka). Perhaps the tooth fragment represents recycled material from an older deposit. Since only one sample was available, the results are inconclusive.

Galt Island

At Galt Island, again only one tooth sample was available for analysis. The sample had insufficient dentine and enamel for U analysis; hence the beta dose contribution could not be determined. However, if only the environmental dose rate is used, an upper age limit can be obtained. The <349 ka ESR date suggests that the fission track age of 430 ka

(Westgate et al., 1978) is too high. The overall faunal assemblage (14 different species; Stalker and Churcher, 1982) is characteristic of Rancholabrean age (consistent with an age of <475 ka). The estimated age of 45 ka for the site is based on the presence of a mammoth of unknown species and a radiocarbon date of 39 ka (Stalker and Churcher, 1982). However, the magnitude of the ^{14}C date suggests that it is an infinite date. The high AD (62.2 krad) indicates a somewhat older age. U-series dating on two bones samples proved unsuccessful due to extensive migration of uranium and/or daughter elements (Szabo et al., 1973).

Mitchell Bluff

The main bone horizon at Mitchell Bluff contains a diverse faunal assemblage. Of 31 identified species, 11 represent a distinct "Sangamon" (stage 5) faunal assemblage (Stalker, 1976; Stalker and Churcher, 1982). U-series ages are also available. Both the U-series and ESR dates are somewhat younger than the estimated faunal age. However, sample 84MI11 is within the estimated 80 - 130 (stage 5) range if the linear U uptake model is used. Szabo et al. (1973) obtained some discordant ^{231}Pa and ^{230}Th dates on bone, indicating open system behaviour. Hence the continuous linear U uptake model is expected to come closer to the "true" age.

One sample (84MI10) from a lower bone horizon on the same outcrop, is believed on the basis of associated fauna, to have an age of 600 - 1,000 ka (Stalker and Churcher, 1982). The ESR date of 130 to 285 ka is inconsistent with this age assignment. The tooth sample contained extremely high amounts of uranium, both in the enamel (23 ppm) and dentine (1820 ppm). It might be likely that this sample has undergone late stage uranium accumulation. More samples are needed to verify the age assignment of this unit.

Riddell Site

The associated fauna at the Riddell Site, particularly Ondatra zibathicus (muskrat) and Lagurus curtatus (sagebrush vole), is representative of Late Rancholabrean time (Skwara-Woolf, 1981). The beginning of Late Rancholabrean time in North America seems to correlate best with the beginning of ^{18}O stage 6, dated at ca. 175,000 a (Repenning, 1980). The paleoecological evidence and stratigraphic position indicates that the composite Riddell fauna is of "Sangamon" age (stage 5) (SkwaraWoolf, 1981). Another age of 600 - 700 ka is based on stratigraphic correlation with the Wascana Creek Ash near Regina, dated by fission track (Westgate et al., 1976). However, one of the above co-authors (Christiansen, pers. comm. 1984) believes that SkwaraWoolf's age estimate for the Riddell Site is more consistent with the local stratigraphy. The single tooth analysed gave an ESR age (99 to 108 ka) in

good agreement with the latter age (stage 5) estimate, using the early U uptake model. The continuous U uptake model implies a somewhat older age.

Surprise, Island and Low Bluffs

Surprise Bluff, Island Bluff and Low Bluff are three outcrops along the bank of the South Saskatchewan River. Faunal and stratigraphic dates suggests that these sites are quite old (>0.5 Ma) (Stalker and Churcher, 1982). The ESR data however, indicates much younger ages in all cases. The dose rate values for samples 84IB7 and 84IB9 are shown in Table 7.1. For the Island Bluff samples, the EDR, which has the lowest uncertainty of all dose rate calculations, is the main contributor to the dose. Hence, the ESR dates should more accurately reflect the "true" age of the sample. Using the linear U uptake model, Surprise Bluff and Island Bluff can be assigned to interglacial stages 7 and 9 respectively. The ESR age of Low Bluff is questionable since the dentine has a high U concentration, possibly of late accumulation.

Bow Island

The sediments at Bow Island are believed to represent preglacial valley deposits (Stalker and Churcher, pers. comm. 1984). There are no till beds present here. Sediments higher up in the sequence are contorted and thrusted, suggesting that at one time a glacier overrode the region but

either did not deposit any till or the till deposits have subsequently been eroded. The sample contained insufficient dentine and enamel for U analysis. The ESR age is therefore based on the environmental dose rate and should be considered an overestimate. The ESR data shows that the age of these sediments has to be younger than 118 ka and cannot possibly represent preglacial sediments.

Frisch Site

The Frisch Site is located east of Medicine Hat, several kilometers distant from the South Saskatchewan River. The site occurs in an outlier of Quaternary sediment. There are no absolute dates for this site. Current identification of the fauna by C.S. Churcher (Dept. of Zoology, University of Toronto) and stratigraphic correlation by A.M. Stalker (GSC), suggests that the deposit is older than 1,000 ka. The ESR dates are considerably younger, and there is good agreement between the ESR ages of the three samples. The ESR dates (average 446±29 & 486±30 ka, linear U uptake) suggest that the age of this site can be assigned to stage 13, much younger than the 1,000 ka estimate.

Wellsch Valley

The Wellsch Valley Site probably represents one of the oldest known Pleistocene deposits in the Prairies. Based on an Early Irvingtonian land mammal faunal assemblage (Stalker

and Churcher, 1972), paleomagnetism and fission track data, the age of the bone horizon is estimated at >1,500 ka (Fig. 6.1). The ESR data represents a gross underestimate of this age. The sample has a very high U content in enamel (29 ppm) and dentine (825 ppm), which may have accumulated at a late stage. ESR analysis on additional samples should prove useful since this is one of the few Pleistocene sites in western North America with good geochronological control.

FIG. 6.1. 10 m section of "Jaw Face", Wellsch Valley, Sask. Paleomagnetic stratigraphy is by Foster and Stalker (1976). Fission track of the volcanic ash is by Westgate et al. (1978). Irvingtonian/Rancholabrean land mammal stage boundary is after Harington (1984). SkwaraWoolf (1981) places the boundary at 475 ka, the start of ^{18}O stage 12. Ages of paleomagnetic boundaries are from Mankinen and Dalrymple (1979).

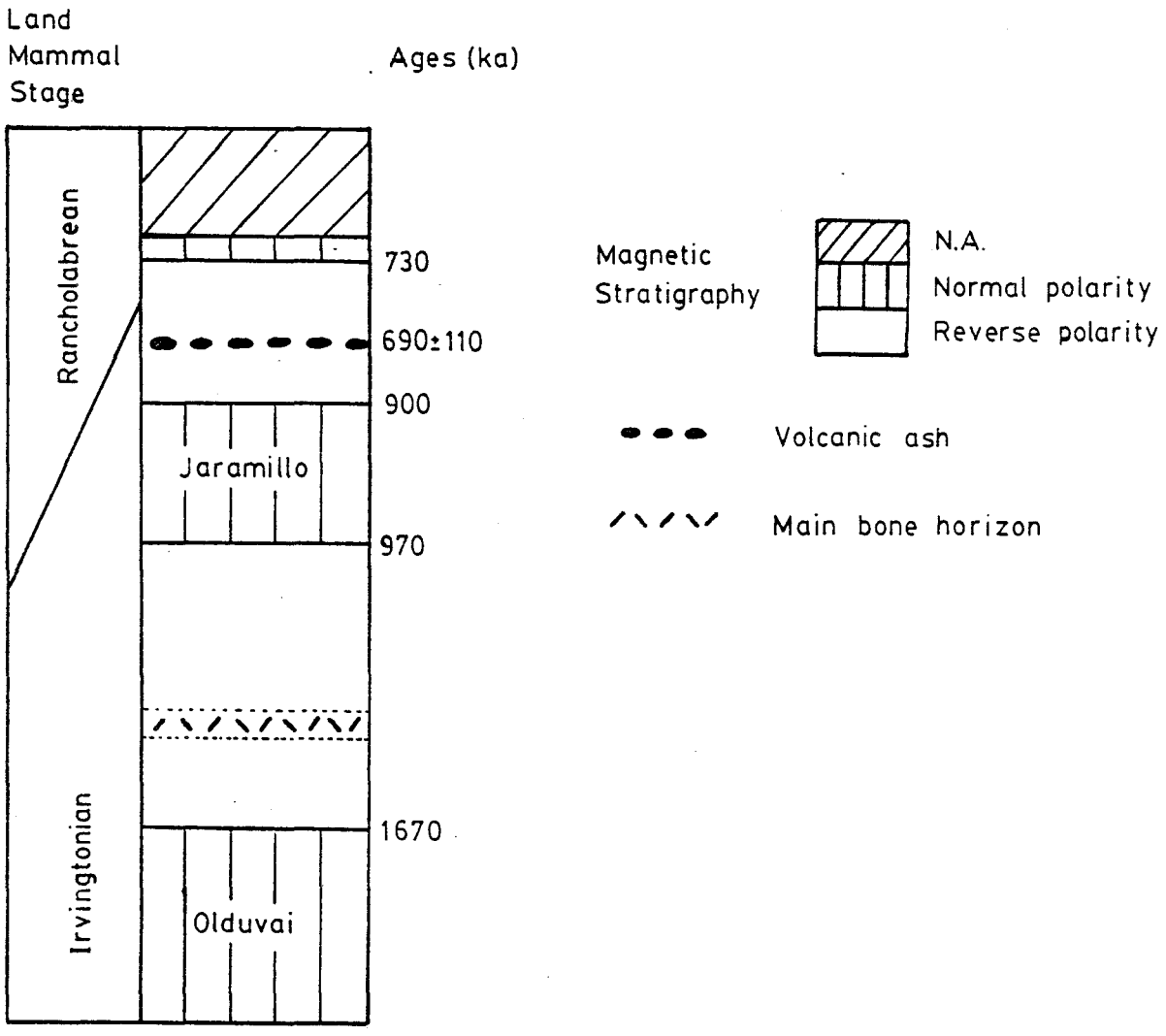
Land
Mammal
Stage
Ages (ka)
Rancholabrean
Irvingtonian
730
690±110
900
Jaramillo
970
1670
Olduvai
Magnetic
Stratigraphy
N.A.
Normal polarity
Reverse polarity
Volcanic ash
Main bone horizon

CHAPTER 7

CONCLUDING REMARKS

7.1 DISCUSSION

No errors were assigned to the ESR age estimates in Table 6.1. At present, there are still several assumed parameters in the dose rate calculation which can lead to unrealistically high and/or meaningless error estimates. In most cases, the various inputs to the calculation tend to cancel each other; some increase the dose rate, while others decrease it.

The high U content in dentine represents the major source of error in the age calculation, since it has a strong influence on the dose rate (Table 7.1). The main problem lies in the determination of the nature of U accumulation in dentine. Presently this problem cannot be solved. The fact that some fossil bones give concordant U-series ages while others discordant (Szabo et al., 1973), indicates that U uptake may have been early in some samples, while others remained open systems over their burial history. ESR studies on a mammoth tooth by Grün and Invernati (1985) produced similar conclusions. They applied a direct and linear U accumulation model on five different regions of a mammoth tooth. The ESR results demonstrated that samples from regions of the tooth not affected by U accumulation yielded good ages with both models, whereas samples of other regions give only reliable results when the "right" model is applied.

TABLE 7.1. IDR, DDR and EDR contribution of several samples, for early (E), and linear (L) U uptake models, with no radon loss.

Sample	AD	U Concentration (ppm)			Dose Rate (mrad/a)					
		Enamel	Dentine	Soil	IDR		DDR		EDR	
				U / Th/K_2O%	E	L	E	L	E	L
84LN1	3.98	3.3	109x2	2.0/7.7/1.45	48.9	24.8	362.4	182.2	81.5	81.5
84LN3	3.61	1.7	102	2.0/7.7/1.45	27.7	13.7	157.8	78.3	105.5	105.5
84EM4a	5.22	0.37	26.5	1.6/4.3/1.87	8.0	3.7	43.9	21.2	94.0	94.0
84MI11	34.1	4.81	231	2.1/6.9/1.95	114.8	59.3	450.9	229.1	119.4	119.4
84SB4	95.0	9.2	89.9	1.9/5.5/1.69	326.4	166.1	250.3	126.5	106.6	106.6
84IB7	31.6	0.67	8.4	2.0/6.0/1.77	31.0	14.1	10.8	5.1	90.5	90.5
84IB9	35.7	0.7		2.0/6.0/1.77	33.6	15.2			99.2	99.2
84FR2	231.7	7.53	171	3.4/10./2.01	322.6	161.9	503.7	252.6	156.2	156.2
84WV5	456.0	28.8	825x2	2.5/7.5/2.04	1215.6	631.6	1417.8	723.9	96.9	96.9

It therefore seems to be necessary to find some indicators for determining the model of U uptake for each sample to be dated.

Another problem involves the distribution of U in dentine. Fission track analysis by Grün and Invernati (1985) indicates that there can be a large variation in uranium concentration between the outer and inner part of teeth. High U concentrations at the outer edge of a thick dentine layer may not contribute to the dose rate, resulting in an underestimate of the ESR age. It is advisable to perform fission track mapping of dentine for more precise beta dose attenuation calculations.

The error in the determination of the AD is rather low. AD results can usually be reproduced with a deviation of <5%. The good agreement between AD's from samples collected at the same site also suggests that the AD represents the true accumulated dose of the samples. To test this hypothesis, a modern tooth was irradiated with a gamma dose of 20 krad. The AD derived from the sample was 21 krad, an uncertainty of only 5%. Similar results are reported by Grün and Invernati (1985).

Additional sources of error could arise from:

1) analytical error in determination of (U, Th and K),

2) saturation of traps with electrons,

3) competition for traps by non-paramagnetic radicals (eg. fluorine; Ikeya, 1985),

4) over/under estimate of the initial $^{234}U/^{238}U$ ratio,

5) over/under estimate of Rn loss,

6) late stage U accumulation/leaching, and

7) inclusion of teeth reworked from earlier deposits.

7.2 CONCLUSIONS

ESR dates based on early and linear U uptake models were compared to the estimated ages of several sites in southern Alberta and Saskatchewan. The wide range and uncertainty of independent age estimates at some sites causes difficulties in determining which ESR model most accurately reflects the "true" age of the sample. The ESR ages are in relatively good agreement with independent estimates at the young, well dated sites. For slightly older samples (approx. 100 ka), the linear U uptake model comes closer to the estimated age at one site (Mitchell Bluff), but for the Riddell Site, the early U uptake model agrees more favourably with the estimated age. For even older samples (Mitchell Bluff(b), Low Bluff and Wellsch Valley), the ESR models yield highly underestimated ages. However, these samples have very high U concentrations and may have experienced a late stage of U accumulation.

ESR gives ages for some sites which are younger than those determined by faunal and stratigraphic correlation. Using the linear U uptake model, Surprise Bluff, Island Bluff and the Frisch Site can be assigned to interglacial stages 7, 9 and 13 respectively. These age assignments may represent more realistic values, since the faunal and stratigraphic correlation is sometimes unclear. For example, note the discrepancies between these independent dates within the following four sites,

Reservoir Gully	-	F,S: 18-25 ka;	US: >64 & 73±6 ka
Galt Island	-	F,S: 45 ka;	FT: 430±70 ka
Mitchell Bluff(a)	-	F,S: 80-130 ka;	US: >71 & 72±6 ka
Riddell Site	-	F: 80-130 ka;	FT: 600-700 ka

Another problem associated with the faunal and stratigraphic age estimates is that they are based on the assumption that there were only four glacial-interglacial cycles during Pleistocene time. However, as is evident from Fig. 1.2, it is not clear what ages the interglacials/glacials (eg. Yarmouthian, Kansan, etc.) really represent. Use of a more modern classification based on isotope stages (Fig. 1.3) is recommended.

At some sites, the analysed sample may represent an older, recycled tooth fragment. This is particulary evident at the Empress Site, where five samples yielded similar ESR

dates in good agreement with the estimated age of the deposit and three other samples give varying older ages. The recycled nature of the older samples is supported by the presence of dinosaur bones in the same deposit. It is therefore essential to analyse and compare the data of several samples (5 or more) from each site.

Finally, it appears that the U accumulation process can vary from sample to sample and it would therefore be futile to use one general model of U uptake. A partial solution to the problem may be to analyse several samples from each site. If some of the samples display uniform AD values (as for Empress and Frisch samples), then they may prove easier to model. Samples with anomalously high U concentrations should be avoided since they yield highly underestimated ESR dates. Whenever possible, the ESR dates should be compared to ^{14}C, U-series, fission track and paleomagnetic data.

7.3 SUGGESTIONS FOR FUTURE WORK

At a number of sites, only one sample was available for analysis. For reliable and meaningful ESR age determinations it is required that several samples be analysed from each site.

Some outcrops along the bank of the South Saskatchewan River contain 3 to 4 fossiliferous horizons. Sampling along such vertical sequences will allow for a better comparison of ESR dates for samples with unquestionable sequences of ages.

More sites with established absolute ages are required to test the ESR models. Wellsch Valley probably represents the oldest known fossiliferous Pleistocene deposit in North America. The good absolute age control at this site should prove useful in testing the upper limit of ESR dating.

Determination of U concentration and distribution in dentine and enamel by fission track mapping is advised for more precise beta ray attenuation calculations. Fission track analysis may also prove useful in determining the appropriate U accumulation model.

REFERENCES

Aitken, M.J., 1974. Physics and Archaeology, 2nd Edition. Clarendon Press, Oxford, 291p.

Aitken, M.J., Clark, P.A., Gaffney, C.F. and Lovborg, L., 1985. Beta and gamma gradients. Nuclear Tracks, 10, 647-654.

Alley, N.F. and Harris, S.A., 1974. Pleistocene glacial lake sequences in the foothills, Southwestern Alberta, Canada. Can. J. Earth Sci., 11, 1220-1235.

Apers, D., Debuyst, R., DeCanniere, P., Dejehet, F. and Lombard, E., 1981. A criticism of the dating by electron paramagnetic resonance (ESR) of the stalagmitic floors of Caune de l'Arago at Tautavel. In Absolute dating and isotope analysis in prehistory - methods and limits (H. de Lumley and J. Labeyrie, eds.). Proceedings, 533-550.

Badone, E. and Farquhar, R.M., 1982. Application of neutron activation analysis to the study of element concentration and exchange in fossil bones. J. Radioanal. Chem., 69, 291-311.

Barendregt, R.W. and Stalker, A.MacS., 1978. Characteristic magnetization of some Middle Pleistocene sediments from the Medicine Hat area of Southern Alberta. GSC Paper, 78-1A, 487-488.

Bell, W.T., 1976. The assessment of the radiation dose-rate for thermoluminescence dating. Archaeometry, 18, 107-111.

Bell, W.T., 1977. Thermoluminescence dating: revised dose-rate data. Archaeometry, 19, 99-100.

Bell, W.T., 1979. Thermoluminescence dating: radiation dose-rate data. Archaeometry, 21, 243-245.

Bender, M.L., Fairbanks, R.G., Taylor, F.W., Matthews, R.K., Goddard, J.K. and Broecker, W.S., 1979. Uranium series dating of the Pleistocene reef tracts of Barbados, West Indies. Geol. Soc. Amer., 90, 577-594.

Boellstorff, J., 1978. North American Pleistocene stages reconsidered in light of probable Pliocene-Pleistocene continental glaciation. Science, 202, 305-307.

Bowman, S.G.E., 1976. Thermoluminescence dating: the evaluation of radiation dosage. D.Phil. Thesis (unpublished), Oxford University, Oxford.

Cevc, P., Schara, M. and Ravnik, C., 1972. Electron paramagnetic resonance of irradiated tooth enamel. Radiation Research, 51, 581-589.

Charalambous, S. and Papastefanou, C., 1977. On the radioactivity of fossil bones. Nuclear Instruments and Methods, 142, 581-588.

DeCanniere, P., Debuyst, R., Dejeht, F., Apers, D. and Grün, R., 1986. ESR dating: a study of ^{210}Po coated geological and synthetic samples. Nuclear Tracks, in press.

Driessens, C.F.M., 1980. The mineral in bone, dentine and tooth enamel. Bull. Soc. Chim. Belg., 89, 663-689.

Flint, R.F., 1971. Glacial And Quaternary Geology. John Wiley and Sons, Inc., New York, 892p.

Foster, J.H. and Stalker, A.MacS., 1976. Paleomagnetic stratigraphy of the Wellsch Valley site, Saskatchewan. GSC Paper, 76-1C, 191-193.

Gibbons, A.B., Megeath, J.D. and Pierce, K.L., 1984, Probability of moraine survival in a succession of glacial advances. Geology, 12, 327-330.

Gilinskaya, L.G., Shcherbakova, M.Ya. and Zanin, Yu.N., 1971. Carbon in the structure of apatite according to electron paramagnetic resonance data. Soviet Physics - Crystallography, 15, 1016-1019.

Grün, R., 1985. Beiträge zur ESR-Datierung. PhD Thesis, Geologisches Institut der Universitaet zu Koeln, 157p.

Grün, R., 1986. Beta dose attenuation in thin layers. Ancient TL, in press.

Grün, R. and Invernati, C., 1985. Uranium accumulation in teeth and its effect on ESR dating - a detailed study of a mammoth tooth. Nuclear Tracks, 10, 869-877.

Hansen, R.O. and Begg, E.L., 1970. Age of Quaternary sediments and soils in the Sacramento Area, California, by uranium and actinium series dating of vertebrate fossils. Earth and Planet. Sci. Letters, 8, 411-419.

Harington, C.R., 1984. Mammoths, bison and time in North America. In Developments in palaeontology and stratigraphy, 7 - Quaternary dating methods (W.C. Mahaney, ed.). 299-309.

Hennig, G.J. and Grün, R., 1983. ESR dating in Quaternary geology. Quat. Sci. Rev., 2, 157-238.

Ikeya, M., 1975. Dating a stalactite by electron paramagnetic resonance. Nature, 255, 48-50.

Ikeya, M., 1978. Electron spin resonance as a method of dating. Archaeometry, 20, 147-158.

Ikeya, M., 1981. Paramagnetic alanine molecular radicals in fossil shells and bones. Naturwissenschaften, 68, 474-475.

Ikeya, M., 1982. A model of linear uranium accumulation for ESR age of Heidelberg (Mauer) and Tautavel bones. Jap. J. of Applied Physics, 21, L690-L692.

Ikeya, M., 1985. Dating methods of Pleistocene deposits and their problems: IX - electron spin resonance. In Dating methods of Pleistocene deposits and their problems (N.W. Rutter, ed.). Geosci. Can. Reprint Series 2, 73-87.

Mankinen, E.A. and Dalrymple, G.B., 1979. Revised geomagnetic polarity time scale of the interval 0-5 m.y. B.P. Jour. Geophys. Res., 84, 615-626.

Martin, M.J. and Blichert-Toft, P.H., 1970. Radioactive atoms - auger-electrons, alpha, beta, gamma and x-ray data. Nuclear Data Tables, A8, 1-198.

McKinney, C.R., 1978. An evaluation of uranium series disequilibrium dating of fossil teeth. Geol. Soc. Amer. Abstracts, 10, 454.

McMorris, D.W., 1969. Trapped-electron dating: ESR-studies. Nature, 222, 870-871.

Molleson, T.I., 1981. The application of the principles of bone fossilization to relative dating problems, with particular reference to bones from the Caune de l'Arago at Tautavel. In Absolute dating and isotope analysis in prehistory - methods and limits (H. de Lumley and J. Labeyrie, eds.). Proceedings, 659-676.

Repenning, C.A., 1980. Faunal exchanges between Siberia and North America. Can. J. Anthrop., 1, 37-44.

Sato, K., 1979. Studies of an asymmetric ESR signal in x-irradiated human tooth enamel. Calcified Tissue Int., 29, 95-99.

Seitz, M.G. and Taylor, R.E., 1974. Uranium variations in dated fossil bone series from Olduvai Gorge, Tanzania. Archaeometry, 16, 129-135.

Shackleton, N.J. and Opdyke, N.D., 1973. Oxygen isotope and paleomagnetic stratigraphy of equatorial Pacific core V28-238: oxygen isotope temperatures and ice volumes on a 10^5 year and 10^6 year scale. Quat. Res., 3, 39-55.

Shackleton, N.J. and Opdyke, N.D., 1976. Oxygen isotope and paleomagnetic stratigraphy of equatorial Pacific core V28-239. Late Pliocene to Latest Pleistocene. In Quaternary paleoceanography and paleoclimatology (R.M. Cline and J.D. Hays, eds.). Geol. Soc. Amer. Mem., 145, 449-464.

SkwaraWoolf, T., 1981. Biostratigraphy and paleoecology of Pleistocene deposits (Riddell Member, Floral Formation, Late Rancholabrean), Saskatoon, Canada. Can. J. Earth Sci., 18, 311-322.

Stalker, A.MacS., 1963. Quaternary stratigraphy in Southern Alberta. GSC Paper, 62-34, 52p.

Stalker, A.MacS., 1969. Quaternary stratigraphy in Southern Alberta; report II: sections near Medicine Hat. GSC Paper, 69-26, 28p.

Stalker, A.MacS., 1972. Southern Alberta. In Quaternary geology and geomorphology between Winnipeg and the Rocky Mountains (N.W. Rutter and E.A. Christiansen, eds.). 24th International Geological Congress (Montreal) Guidebook, Field Excursion C-22, 62-79.

Stalker, A.MacS., 1976. Quaternary stratigraphy of the Southwestern Canadian Prairies. In Quaternary stratigraphy of North America (W.C. Mahaney, ed.). Dowden, Hutchinson & Ross, Stroudsburg, Pa., 381-407.

Stalker, A.MacS. and Churcher, C.S., 1972. Glacial stratigraphy of the Southwestern Canadian Prairies; the Laurentide record. 24th International Geological Congress (Montreal), Section 12, 110-119.

Stalker, A.MacS. and Churcher, C.S., 1982. Ice age deposits and animals from the southwestern part of the Great Plains of Canada. GSC Misc. Report, 31.

Stalker, A.MacS. and Harrison, J.E., 1977. Quaternary glaciation of the Waterton-Castle River region of Alberta. Bull. of Can. Petroleum Geology, 25, 882-906.

Szabo, B.J., Stalker, A.MacS. and Churcher, C.S., 1973. Uranium-series ages of some Quaternary deposits near Medicine Hat, Alberta, Canada. Can. J. Earth Sci., 10, 1464-1469.

Szabo, B.J., 1980. Results and assessment of uranium-series dating of vertebrate fossils from Quaternary alluviums in Colorado. Arctic and Alpine Res., 12, 95-100.

Tochilin, E. and Goldstein, N., 1966. Dose rate spectral measurements from pulsed x-ray generators. Health Phys., 12, 1705-1713.

Weatherell, J.A. and Robinson, C., 1973. The inorganic composition of teeth. In Biological mineralization (I. Zipkin, ed.). John Wiley and Sons, New York, 43-74.

Westgate, J.A., 1972. The Cypress Hills. In Quaternary geology and geomorphology between Winnipeg and the Rocky Mountains (N.W. Rutter and E.A. Christiansen, eds.).

24th International Geological Congress (Montreal) Guidebook, Field Excursion C-22, 50-62.

Westgate, J.A., Christiansen, E.A. and Boellstorff, J.D., 1977. Wascana Creek ash (Middle Pleistocene) in Southern Saskatchewan: characterization, source, fission track age, paleomagnetism, and stratigraphic significance. Can. J. Earth Sci., 14, 357-374.

Westgate, J.A., Briggs, N.D., Stalker, A.MacS. and Churcher, C.S., 1978. Fission-track age of glass from tephra beds associated with Quaternary vertebrate assemblages in the Southern Canadian plains. Geol. Soc. Amer. Abstracts, 10, 514-515.

Wintle, A.G., 1977. Thermoluminescence dating of minerals - traps for the unwary. J. Electrostatics, 3, 281-288.

Yokoyama, Y., Nguyen, H.V., Quaegebeur, J.P. and Poupeau, G., 1982. Some problems encountered in the evaluation of annual dose-rates in electron spin resonance dating of fossil bones. PACT, 6, 103-115.

Zeller, E.J., Levy, P.W. and Mattern, P.L., 1967. Geological dating by electron spin resonance. In Proceedings of the symposium on radioactive dating and methods of low level counting. IAEA, Vienna, 531-540.

APPENDIX I

TABLE I-1. Analytical data for samples used in this study. ( ) = Estimated value based on comparison with other sample.

Sample Number	Av. Enamel Thickness (mm)		AD (krad)	U Concentration (ppm)				Th Conc. Sediment (ppm)	K_2O Conc. Sediment (%)
	Uncleaned	Cleaned		Enamel	Dentine1	Dentine2	Sediment		
84LN1	0.9	0.7	3.98	3.3	109	109	2.0	7.7	1.45
84LN3	1.1	0.9	3.61	1.7	102		2.0	7.7	1.45
84LN6	1.1	0.9	4.22	5.69	88.4		2.0	7.7	1.45
84LN6alt	1.1	0.9	7.74	24.8	88.4		2.0	7.7	1.45
84EM2	0.8	0.6	5.27	0.55	(20)		1.6	4.3	1.87
84EM4a	1.2	1.0	5.22	0.37	26.5		1.6	4.3	1.87
84EM4d	1.0	0.8	32.4	1.5	27.1		1.6	4.3	1.87
84EM4e	1.0	0.8	4.95	0.9	30.6	30.6	1.6	4.3	1.87
84EM5	0.9	0.7	4.51	0.3	4.2		1.6	4.3	1.87
84EM8	0.9	0.7	6.68	1.29	36.9		1.6	4.3	1.87
84EM9	1.0	0.8	145.8	1.92			1.6	4.3	1.87
84EM10	2.0	1.4	84.1	2.7			1.6	4.3	1.87
84RG3	1.1	0.9	138.0	2.8	178		2.1	5.1	1.78
84GI6	1.0	0.8	62.2	na	na		2.8	9.1	2.07
84MI9e	1.2	1.0	19.5	2.68	206		2.1	6.9	1.95
84MI9i	1.0	0.8	19.3	2.43	206		2.1	6.9	1.95
84MI11	1.0	0.8	34.1	4.8	231		2.1	6.9	1.95
84MI10	1.0	0.8	693.1	22.8	1820		1.8	5.4	1.60
84RS1	1.2	1.0	43.7	3.42	130		1.0	2.9	1.43
84SB4	0.8	0.6	95.0	9.2	89.9		1.9	5.5	1.69
84IB7	2.4	1.8	31.6	0.67	8.4		2.0	6.0	1.77
84IB9	2.6	2.0	35.7	(0.7)			2.0	6.0	1.77
84LB1	2.2	1.6	183.0	0.6	887	887	1.9	4.2	1.27
84BOW3	0.9	0.7	18.0	na	na		4.8	5.0	1.10
84FR2	0.9	0.7	231.7	7.53	171		3.4	10.0	2.01
84FR4	1.2	1.0	236.2	6.73	(170)		3.4	10.0	2.01
84RF6	1.5	1.3	233.0	(7)	(170)		3.4	10.0	2.01
84WV5	3.0	2.0	456.0	28.8	825	825	2.5	7.5	2.04

APPENDIX II

COMPUTER PROGRAM (APPLE II BASIC)

FOR ESR ENAMEL DATING

```
10  REM    *** ESR ENAMEL DATING ***
20  HOME : CLEAR : PRINT
30  PRINT "******** ESR AGE DETERMINATION ******** ": PRINT : PRINT
40  PRINT "GIVE ALL PERCENTAGE VALUES"
50  PRINT "IN THE FORM 0.XX": PRINT : PRINT
60  REM  *** INPUT DATA ***
70  INPUT "SAMPLE NAME? ";NM$: PRINT
80  INPUT "NUMBER OF DENTINE LAYERS? (0,1 or 2)? ";D2
90  INPUT "AD (KRAD)? ";A$:A =  VAL (A$)
100  IF A <  = 0 THEN  PRINT : PRINT "AD MUST BE GREATTER THAN ZERO.": PRINT
     : PRINT : GOTO 90
110  INPUT "U (PPM) SAMPLE? ";B$:B =  VAL (B$)
120  IF D2 = 0 THEN 160
130  INPUT "U (PPM) DENTINE-1? ";C$:C =  VAL (C$)
140  IF D2 = 1 THEN 160
150  INPUT "U (PPM) DENTINE-2? ";D$:D =  VAL (D$)
160  INPUT "U (PPM) SEDIMENT? ";E$:E =  VAL (E$)
170  IF E = 0 THEN 210
180  INPUT "Th (PPM) SEDIMENT? ";F$:F =  VAL (F$)
190  INPUT "K2O (%) SEDIMENT? ";GK$:GK =  VAL (GK$):G = GK * 0.83015
200  IF E > 0 THEN 220
210  INPUT "EXTERNAL GAMMA RADIATION (MRAD/A)? ";S$:S =  VAL (S$)
220  INPUT "INITIAL 234U/238U RATIO OF SAMPLE? ";U$:U =  VAL (U$)
230  IF U < 1 THEN  LET U = 1
240  INPUT "K-VALUE? ";Y$:Y =  VAL (Y$)
250  IF Y <  = 0 THEN  LET Y = 0.15
260  INPUT "WATER CONTENT (WT.%) OF SAMPLE? ";V$:V =  VAL (V$)
270  IF C = 0 THEN 290
280  INPUT "                        DENTINE? ";X$:X =  VAL (X$)
290  IF E = 0 THEN 310
300  INPUT "                        SEDIMENT? ";W$:W =  VAL (W$)
310  INPUT "RADON LOSS (%)? ";Z$:Z =  VAL (Z$)
320  LET C1 = 2.841E - 6:C2 = 9.217E - 6:C3 = 2.133E - 5
330  IF C = 0 AND E = 0 THEN 940
340  REM  *** CALCULATE BETA ATTENUATION ***
350  PRINT : PRINT
360  PRINT "SAMPLE SYMMETRY FOR THE CALCULATION OF  BETA RAY ATTENUATION
      OF THIN SAMPLES"
370  PRINT : PRINT
380  PRINT "       A-SIDE  / SAMPLE /  B-SIDE"
390  PRINT "     ----------/--------/----------"
400  PRINT "     DENTINE-1 / ENAMEL / DENTINE-2"
410  PRINT "     DENTINE-1 / ENAMEL / SEDIMENT"
420  PRINT "     SEDIMENT  / ENAMEL / SEDIMENT"
430  PRINT : PRINT
440  INPUT "DENSITY OF SAMPLE? ";D1$:D1 =  VAL (D1$)
450  IF D1 <  = 0 THEN  LET D1 = 2.95
460  INPUT "INITIAL SAMPLE THICKNESS (MICRON)? ";TT$:TT =  VAL (TT$)
470  LET TT = TT / 1000
480  INPUT "REMOVED THICKNESS A-SIDE (MICRON)? ";AA$:AA =  VAL (AA$)
490  LET AA = AA / 1000
```

```
500  INPUT "REMOVED THICKNESS B-SIDE (MICRON)? ":BB$:BB =  VAL (BB$)
510  LET BB = BB / 1000
520  IF AA + BB < TT THEN 570
530  PRINT : PRINT
540  PRINT : PRINT "THE THICKNESS REMOVED IS GREATER THAN"
550  PRINT "THE TOTAL THICKNESS OF THE SAMPLE."
560  PRINT "CHECK YOUR INPUTS AND REENTER.": PRINT : PRINT : GOTO 460
570  HOME : PRINT : PRINT : PRINT "*** CALCULATING BETA-RAY ATTENUATION
     ***"
580  IF G = 0 THEN 1270
590 AB = 1:MM = .1619: GOSUB 820:R3 = R1:R4 = R2: GOSUB 860
600  IF C = 0 THEN  LET M1 = R3
610  IF D = 0 THEN  LET M2 = R4
620  LET L = M1 + M2:R3 = 0:R4 = 0
630  FOR NN = 1 TO 8: READ AB,MM: GOSUB 820: NEXT NN: GOSUB 860: GOSUB 8
     90:M = M1:P = M2:H = M5
640  FOR NN = 1 TO 24: READ AB,MM: GOSUB 820: NEXT NN: GOSUB 860: GOSUB
     890:N = M1:Q = M2:I = M5
650  FOR NN = 1 TO 16: READ AB,MM: GOSUB 820: NEXT NN: GOSUB 860: GOSUB
     890:O = M1:R = M2:J = M5
660  IF F = 0 OR D > 0 THEN 940
670  FOR NN = 1 TO 27: READ AB,MM: GOSUB 820: NEXT NN: GOSUB 860
680  IF C = 0 THEN  LET M1 = R3
690  IF D = 0 THEN  LET M2 = R4
700  LET K = M1 + M2
710  GOTO 940
720  DATA  .0001, .0002, .0009, .0012, .0064, .0035, .0454, .0114, .0001
     , .0495, .9364, .3020, .006, .1928, .0048, .1528
730  DATA  .0008, .0115, .0014, .0493, .0001, .056, .0697, .0738, .0716,
      .0821, .0054, .0919, .0014, .1158, .0172, .1229
740  DATA  .0159, .1286, .0135, .1385, .0139, .1556, .0055, .1728, .0309
     , .1785, .0682, .1899, .0664, .1957, .0049, .2057
750  DATA  .0148, .2229, .0049, .2402, .0426, .2459, .1768, .4448, .0023
     , .0013, .2782, .1401, .0492, .0016, .0178, .0002
760  DATA  .0001, .0055, .0059, .0112, .0006, .0121, .031, .02, .0247, .
     0231, .0095, .0007, .0005, .0183, .0089, .0534
770  DATA  .0044, .1127, .3612, .1703, .0004, .0584, .0003, .0525, .418,
      .1793, .0109, .0001, .0418, .0009, .0738, .0026
780  DATA  .01, .001, .005, .0421, .0071, .0471, .0061, .0642, .0181, .1
     167, .0082, .1209, .0289, .135
790  DATA  .1082, .1428, .0612, .2246, .0124, .2343, .0323, .2731, .0014
     , .0073, .0513, .0264, .023, .0572, .0006, .04
800  DATA  .0001, .0568, .003, .0649, .0021, .0798, .0188, .1912, .3234,
      .2957, .0024, .1221, .0266, .1581, .0311, .1914
810  DATA  .0861, .2311, .0419, .0012, .0135, .0001, .0464, .0014
820  LET MM = .33 / MM * D1 / 2.7
830  LET R1 = .5 / (MM * (TT - AA - BB)) * ( EXP ( - MM * AA) -  EXP ( -
     MM * (TT - BB))) * AB
840  LET R2 = .5 / (MM * (TT - AA - BB)) * ( EXP ( - MM * BB) -  EXP ( -
     MM * (TT - AA))) * AB
850  LET R3 = R3 + R1:R4 = R4 + R2: RETURN
```

```
860  LET R3 =  INT (R3 * 10000 + .5) / 10000
870  LET R4 =  INT (R4 * 10000 + .5) / 10000
880  LET M1 = 0:M2 = 0:M3 = 0:M4 = 0:M5 = 0: RETURN
890  IF C > 0 THEN  LET M1 = R3
900  IF D > 0 THEN  LET M2 = R4
910  IF C = 0 THEN  LET M3 = R3
920  IF D = 0 THEN  LET M4 = R4
930  LET M5 = M3 + M4:R3 = 0:R4 = 0: RETURN
940  REM  *** PRINTOUT OF INPUT VALUES ***
950  PR# 1: PRINT : PRINT : PRINT  TAB( 10);NM$: PRINT
960  PRINT "AD (krad)         = ";A
970  PRINT "U (ppm) SAMPLE    = ";B
980  IF C = 0 THEN 1020
990  PRINT "U (ppm) DENTINE-1 = ";C
1000  IF D = 0 THEN 1020
1010  PRINT "U (ppm) DENTINE-2 = ";D
1020  IF E = 0 THEN 1060
1030  PRINT "U (ppm) SEDIMENT  = ";E
1040  PRINT "Th (ppm) SEDIMENT = ";F
1050  PRINT "K20 (%) SEDIMENT  = ";GK
1060  IF C = 0 AND E = 0 THEN 1260
1070  PRINT "EFFECTIVE BETA CONTRIBUTION"
1080  PRINT "    INITIAL SAMPLE THICKNESS (MICRON)       = ";TT * 1000
1090  PRINT "    REMOVED THICKNESS A-SIDE (MICRON)       = ";AA * 1000
1100  PRINT "    REMOVED THICKNESS B-SIDE (MICRON)       = ";BB * 1000
1110  PRINT "    DENSITY OF THE SAMPLE (g/cm3)           = ";D1
1120  IF E = 0 OR D > 0 THEN 1180
1130  PRINT "    SEDIMENT (238U-230Th)   = ";H
1140  PRINT "             (230Th-206Pb)  = ";I
1150  PRINT "             (235U)         = ";J
1160  PRINT "             (232Th)        = ";K
1170  PRINT "             (40K)          = ";L
1180  IF C = 0 THEN 1260
1190  PRINT "    DENTINE-1 (238U-230Th)  = ";M
1200  PRINT "              (230Th-206Pb) = ";N
1210  PRINT "              (235U)        = ";O
1220  IF D = 0 THEN 1260
1230  PRINT "    DENTINE-2 (238U-230Th)  = ";P
1240  PRINT "              (230Th-206Pb) = ";Q
1250  PRINT "              (235U)        = ";R
1260  IF S = 0 THEN 1280
1270  PRINT "EXTERNAL GAMMA RADIATION (MRAD/A) = ";S
1280  PRINT "INITIAL 234U/238U RATIO OF SAMPLE = ";U
1290  PRINT "K-VALUE = ";Y
1300  PRINT "WATER CONTENT (WT.%) OF SAMPLE   = ";V
1310  IF C = 0 THEN 1330
1320  PRINT "                         DENTINE  = ";X
1330  IF E = 0 THEN 1350
1340  PRINT "                         SEDIMENT = ";W
1350  IF Z = 0 THEN 1370
1360  PRINT "RADON LOSS (%) = ";Z
```

```
1370  PRINT : PRINT
1380  REM  *** CALCULATE WATER ATTENUATION ***
1390  LET W1 = 1 + 1.49 * V / (1 - V)
1400  LET W2 = 1 + 1.25 * V / (1 - V)
1410  LET W3 = 1 + 1.25 * X / (1 - X)
1420  LET W4 = 1 + 1.25 * W / (1 - W)
1430  LET W5 = 1 + 1.14 * W / (1 - W)
1440  REM  *** CALCULATE ENVIRONMENTAL DOSE RATE ***
1450  LET A1 = (E * 11.81 + F * 4.98 + G * 24.92 + S) / W5
1460  LET A2 = (E * (H * 5.51 + I * 8.81 + J * 0.35) + F * K * 2.89 + G *
      L * 83.03) / W4
1470  REM  *** CALCULATE EFFECTIVE INTERNAL BETA DOSE ***
1480  LET B1 = 1 - (H + M + P)
1490  LET B2 = 1 - (I + N + Q)
1500  LET B3 = 1 - (J + O + R)
1510  REM  *** CALCULATE INTERNAL & DENTINE DOSE RATES ***
1520  LET S1 = B * (Y * 267.6 / W1 + (B1 * 5.51 + B2 * 8.81) / W2)
1530  LET S2 = B * (U - 1) * (Y * 29.71) / W1
1540  LET S3 = B * (Y * 12.16 / W1 + B3 * 0.35 / W2)
1550  LET E1 = C * (M * 5.51 + N * (8.81 - RN * RB)) / W3
1560  LET E3 = C * O * 0.35 / W3
1570  LET F1 = D * (P * 5.51 + Q * (8.81 - RN * RB)) / W3
1580  LET F3 = C * R * 0.35 / W3
1590  LET DA = S1 + S3:DJ = E1 + E3 + F1 + F3:DB = S2:DD = A1 + A2
1600  LET DI = B * (Y * 211.77 / W1 + B2 * 8.81 / W2)
1610  LET DF = C * N * (8.81 - RN * RB) / W3
1620  LET DG = D * Q * (8.81 - RN * RB) / W3
1630  LET DC = DF + DG
1640  LET DE = B * (Y * 10.89 / W1 + B3 * 0.31 / W2)
1645  LET DK = C * O * 0.31 / W3 + D * R * 0.31 / W3
1650  REM  *** CALCULATE AGE - DIRECT U UPTAKE ***
1660  LET TH = A * 1E6 / (DD + .0000001):TL = A * 1E6 / (DA + DB + DJ +
      DD + .0000001):T = (TH + TL) / 2
1670  LET TB = (1 -  EXP ( - C1 * T)) / C1
1680  LET TC = (1 -  EXP ( - C2 * T)) / C2
1690  LET TD = (U - 1) * (1 - (C2 *  EXP ( - C1 * T) - C1 *  EXP ( - C2 *
      T)) / (C2 - C1)) / C1
1700  LET TE = (1 -  EXP ( - C3 * T)) / C3
1710  LET X1 = (DA * T + DB * TB - DI * (TC - TD) - DE * TE) / 1E6
1712  LET X2 = (DJ * T - DC * (TC - TD) - DK * TE) / 1E6
1714  LET X3 = DD * T / 1E6
1716  LET AD = X1 + X2 + X3
1720  IF AD > (A) THEN  LET TH = T:T = (TH + TL) / 2
1730  IF AD < (A) THEN  LET TL = T:T = (TH + TL) / 2
1740  IF (TH / TL - 1) > 0.001 THEN 1670
1750  IF T > 100000 THEN  LET T =  INT (T * .001 + .5):T = T / .001: GOTO
      1790
1760  IF T > 10000 THEN  LET T =  INT (T * .01 + .5):T = T / .01: GOTO 1
      790
1770  IF T > 1000 THEN  LET T =  INT (T * .1 + .5):T = T / .1: GOTO 1790
```

```
1780  LET T =  INT (T)
1790  IF M7 = 0 THEN  PRINT "AGE (a) FOR DIRECT U-UPTAKE MODEL =
                ";T
1800  IF M7 = 1 THEN  PRINT "AGE (a) FOR DIRECT U-UPTAKE MODEL (";RN * 1
      00;"% RN LOSS) =      ";T
1802  PRINT "   EDR (mrad/a) = ";X3 / T * 1E6
1804  PRINT "   DDR (mrad/a) = ";X2 / T * 1E6
1806  PRINT "   IDR (mrad/a) = ";X1 / T * 1E6
1810  REM  *** CALCULATE AGE - LINEAR U UPTAKE ***
1820  LET TH = 2 * TH:TL = T:T = (TH + TL) / 2
1830  LET TB = (1 - (1 -  EXP ( - C1 * T)) / (C1 * T)) / C1
1840  LET TC = (1 - (1 -  EXP ( - C2 * T)) / (C2 * T)) / C2
1850  LET TD = (U - 1) * (1 - (C2 ^ 2 * (1 -  EXP ( - C1 * T)) - C1 ^ 2 *
      (1 -  EXP ( - C2 * T))) / (C1 * C2 * T * (C2 - C1))) / C1
1860  LET TE = (1 - (1 -  EXP ( - C3 * T)) / (C3 * T)) / C3
1870  LET X1 = (DA * T / 2 + DB * TB - DI * (TC - TD) - DE * TE) / 1E6
1872  LET X2 = (DJ * T / 2 - DC * (TC - TD) - DK * TE) / 1E6
1874  LET X3 = DD * T / 1E6
1876  LET AD = X1 + X2 + X3
1880  IF AD > (A) THEN  LET TH = T:T = (TH + TL) / 2
1890  IF AD < (A) THEN  LET TL = T:T = (TH + TL) / 2
1900  IF (TH / TL - 1) > 0.001 THEN 1830
1910  IF T > 100000 THEN  LET T =  INT (T * .001 + .5):T = T / .001: GOTO
      1950
1920  IF T > 10000 THEN  LET T =  INT (T * .01 + .5):T = T / .01: GOTO 1
      950
1930  IF T > 1000 THEN  LET T =  INT (T * .1 + .5):T = T / .1: GOTO 1950

1940  LET T =  INT (T)
1950  IF M7 = 0 THEN  PRINT "AGE (a) FOR LINEAR U-UPTAKE MODEL =
                ";T
1960  IF M7 = 1 THEN  PRINT "AGE (a) FOR LINEAR U-UPTAKE MODEL (";RN * 1
      00;"% RN LOSS) =      ";T
1962  PRINT "   EDR (mrad/a) = ";X3 / T * 1E6
1964  PRINT "   DDR (mrad/a) = ";X2 / T * 1E6
1966  PRINT "   IDR (mrad/a) = ";X1 / T * 1E6
1970  IF M7 = 1 OR Z = 0 THEN 2000
1980  LET RA = Y * 152.88 / W1 + B2 * 8.7 / W2:RB = 8.7
1990  IF Z > 0 THEN  LET RN = Z:M7 = 1: GOTO 1520
2000  PRINT : PRINT : PRINT : PRINT : PRINT : PRINT : PR# 0
2010  PRINT "DO YOU WANT TO CONTINUE (Y OR N)?"
2020  GET CO$: IF CO$ = "Y" THEN 10
2030  END
```

Sample of Output:

```
          84IB7

AD (krad)            = 31.6
U (ppm) SAMPLE       = .67
U (ppm) DENTINE-1    = 8.4
U (ppm) SEDIMENT     = 2
Th (ppm) SEDIMENT    = 6
K2O (%) SEDIMENT     = 1.77
EFFECTIVE BETA CONTRIBUTION
     INITIAL SAMPLE THICKNESS (MICRON)          = 2400
     REMOVED THICKNESS A-SIDE (MICRON)          = 300
     REMOVED THICKNESS B-SIDE (MICRON)          = 300
     DENSITY OF THE SAMPLE (g/cm3)              = 2.95
     SEDIMENT (238U-230Th)     = .1353
              (230Th-206Pb)    = .0763
              (235U)           = .0555
              (232Th)          = .08
              (40K)            = .0628
     DENTINE-1 (238U-230Th)    = .1353
               (230Th-206Pb)   = .0763
               (235U)          = .0555
INITIAL 234U/238U RATIO OF SAMPLE = 1.41
K-VALUE = .15
WATER CONTENT (WT.%) OF SAMPLE    = 0
                        DENTINE   = 0
                        SEDIMENT  = .1
RADON LOSS (%) = .5


AGE (a) FOR DIRECT U-UPTAKE MODEL =                          239000
   EDR (mrad/a) = 90.3504745
   DDR (mrad/a) = 10.8269153
   IDR (mrad/a) = 31.0163979
AGE (a) FOR LINEAR U-UPTAKE MODEL =                          288000
   EDR (mrad/a) = 90.5119361
   DDR (mrad/a) = 5.11562415
   IDR (mrad/a) = 14.1108543
AGE (a) FOR DIRECT U-UPTAKE MODEL (50% RN LOSS) =            242000
   EDR (mrad/a) = 90.6440924
   DDR (mrad/a) = 8.67972403
   IDR (mrad/a) = 31.2560443
AGE (a) FOR LINEAR U-UPTAKE MODEL (50% RN LOSS) =            291000
   EDR (mrad/a) = 90.3456476
   DDR (mrad/a) = 4.16386954
   IDR (mrad/a) = 14.1225761
```